T.R.
BOLU ABANT İZZET BAYSAL UNIVERSITY
INSTITUTE OF GRADUATE STUDIES
Department of Chemistry

IMPACT OF TEMPERATURE AND LANTHANIDE ION DOPING ON THE FABRICATION OF NANO SIZED ZINC BORATE MATERIALS

MASTER OF SCIENCE

BÜŞRA ELBASAN

ACADEMIC SUPERVISOR
Prof. Dr. Ayşe MORKAN

BOLU, OCAK - 2024

APPROVAL OF THE THESIS

IMPACT OF TEMPERATURE AND LANTHANIDE ION DOPING ON THE FABRICATION OF NANO SIZED ZINC BORATE MATERIALS submitted by **Büşra ELBASAN** and defended before the Examining Committe Members listed below in partial fulfillment of the requirements for the degree of **Master of Science** in **Department of Chemistry, Institute of Graduate Studies of Bolu Abant Izzet Baysal University in 03.01.2024** by

Examining Committee Members	**Signature**
Supervisor Prof. Dr. Ayşe MORKAN Bolu Abant İzzet Baysal University	.....
Member Prof. Dr. F. Devrim ÖZDEMİRHAN Bolu Abant İzzet Baysal University	.....
Member Prof. Dr. Mecit AKSU Düzce University	.....

Prof. Dr. İbrahim KÜRTÜL

Director of Instıtute of Graduate Studies

ETHICAL DECLARATION

In this thesis dissertation that was properly prepared according to the Thesis Writing Rules of Bolu Abant İzzet Baysal University of the Institute of Graduates Studies, I hereby declare that;

- All data, information, and documents presented in the thesis were obtained in accordance with the academic and ethical rules,
- All data, documents, assessments, and results were presented in accordance with the scientific ethical and moral rules,
- All works that were benefitted in the thesis were appropriately cited,
- No alteration was made in the data used,
- Study presented in this thesis is original,

Otherwise, I declare that I accept the loss of all my rights in case any contradiction that may arise against me.

The similarity rate obtained by using the Turnitin program, a plagiarism detection software is within the limits approved by the University Senate.

_____

Büşra ELBASAN

ABSTRACT

IMPACT OF TEMPERATURE AND LANTHANIDE ION DOPING ON THE FABRICATION OF NANO SIZED ZINC BORATE MATERIALS
MSC THESIS
BÜŞRA ELBASAN
BOLU ABANT IZZET BAYSAL UNIVERSITY
INSTITUTE OF GRADUATE STUDIES
DEPARTMENT OF CHEMISTRY
(SUPERVISOR: PROF.DR. AYŞE MORKAN)
BOLU, JANUARY 2024
xiv + 89

In this present study, nanosized zinc orthoborate materials were successfully synthesized using various rare earth elements (Dy^{3+}, Eu^{3+}, Sm^{3+} and Tb^{3+}) with starting materials, zinc (II) nitrate hexahydrate, boric acid and glycine fuel via Solution Combustion Synthesis (SCS) method. The doped zinc orthoborates were synthesized in different lanthanide ion concentrations (0.005, 0.01, 0.02, 0.25 mol) and the products obtained were analyzed using XRD method for the determination of the structural properties. FTIR analysis was performed for the band variation studies. Aditionally, the optical properties were examined by UV-VIS spectroscopy.The effect of different lantanide elements and temperatures (400-900^{o}C) on the structural properties of synthesized zinc orthoborates were studied using XRD characterization. The alpha-zinc orthoborates was obtained at the lower themperature (400-500^{o}C) while the beta form formed at higher temperature (≥700^{o}C) in the formed of triclinic and monoclinic crystal structure, respectively. Analyzing the FTIR data, the bending of BO_3 vibrations at 695-720 cm^{-1}, symmetric stretching BO_3 vibrations at 1010-1065 cm^{-1} and asymmetric stretching BO_3 vibrations at 1220-1245 cm-^{1} were determined as the characteristic bands of zinc orthoborates.Optical properties of the products were examined by UV-VIS spectroscopy. The absorbance and reflectance spectra were identified between 200-900 nm. According to the UV-VIS spectra, the bands were detected in the ultraviolet region in the range of 200-400 nm. The optical band gap energies were determined by using UV-VIS absorbance values by taking the intercept of the curve in the x-axis of Tauc plot. It can be seen that the band gap energies found were between 5,14 and 5,40. These values vary depending on the concentration of the lanthanide ion and temperature

KEYWORDS: Zinc orthoborate, lanthanide ion (Tb, Sm, Eu, Dy) doped zinc orthoborates , nanosized particle, XRD, FTIR, UV-Vis

ÖZET

SICAKLIK VE LANTANİT İYON KATKISININ,NANO BOYUTLU ÇİNKO BORAT MALZEMELERİN ÜRETİMİNE ETKİSİ
YÜKSEK LİSANS TEZİ
BÜŞRA ELBASAN
BOLU ABANT İZZET BAYSAL ÜNİVERSİTESİ
LİSANSÜSTÜ EĞİTİM ENSTİTÜSÜ
KİMYA ANABİLİM DALI
(TEZ DANIŞMANI: PROF. DR. AYŞE MORKAN)
BOLU, OCAK - 2024
xiv + 89

Bu çalışmada, nano boyutlu çinko ortaboratlar, çözeltide yanma sentezi yöntemi (SCS) ile başarıyla sentezlendi. Kullanılan malzemeler çinko(II) nitrat hekzahidrat ve borik asit ile çeşitli nadir toprak elementleridir (Dy^{3+}, Eu^{3+}, Sm^{3+} ve Tb^{3+}). Sentezlenen çinko ortoboratların yapısal özellikleri, XRD karakterizasyonu ile analiz edildi, FTIR analizi ve UV-VIS spektroskopisi yapıldı. Farklı lantanit elementlerin ve sıcaklığın (400-900^{o}C) sentezlenen çinko ortoboratların yapısal özellikleri üzerindeki etkisi, XRD karakterizasyonu kullanılarak,analiz edildi. Alfa-çinko ortoboratları daha düşük sıcaklıkta (400-500^{o}C) triklinik kristal yapıda elde edilirken, daha yüksek sıcaklıkta (≥700^{o}C) monoklinik kristal yapıda oluşmuştur.

FTIR verileri incelendiğinde çinko ortoboratların karakteristik bantları BO_3 titreşimleri esnemesi 695-720 cm^{-1} de belirlenirken, simetrik gerilmeleri 1010-1065 cm^{-1} de, simetrik olmayan esnemeler 1220-1245 cm^{-1} de görülmüştür. Ürünlerin optik özellikleri UV-VIS spektroskopisi ile incelendi. Absorbans ve yansıma spektrumları 200-900 nm arasında belirlendi. UV-VIS spektrumlarına göre 200-400 nm aralığında ultraviyole bölgede bantlar tespit edilmiştir. Tauc grafiğinin x eksenindeki eğrinin kesişimi alınarak UV-VIS absorbans değerleri kullanılarak optik bant aralığı enerjileri belirlendi. Bulunan bant aralığı enerjilerinin 5,14 ile 5,40 arasında olduğu görülmektedir. Bu değerler lantanit iyonunun konsantrasyonuna ve sıcaklığa bağlı olarak değişir.

ANAHTAR KELİMELER: Çinko ortoborat, lantanit iyonu (Tb, Sm, Eu, Dy) katkılı çinko ortoboratlar, nano boyutlu partikül , XRD, FTIR, UV-Vis

TABLE OF CONTENTS

LIST OF FIGURES

Page

LIST OF TABLES

Page

LIST OF PICTURES

Page

LIST OF ABBREVIATIONS AND SYMBOLS

GLY	**:** Glycine
FT-IR	**:** Fourier Transform Infrared
XRD	**:** X-Ray Diffraction
UV-VIS	**:** Ultraviolet-Visible
SCS	**:** Solution Combustion Synthesis
ICDD	**:** International Center for Diffraction Data
DRS	**:** Diffuse Reflectance Spectroscopy
ZB	**:**Zinc Orthoborate
LREE	**:**Light-Rare Earth Element
HREE	**:**Heavy-Rare Earth Element

ACKNOWLEDGEMENTS

I would like to express my deepest gratitude thanks to my supervisor, **Prof. Dr. AYŞE MORKAN** for her great guidance, honest advice, valuable criticism, continuous encouragements and insight throughout my master's studies.

I would like to send my deepest appreciation to Liska FADLIYANI for her assistance and support during my research.

I would also like to express my sincere gratitude to my family and my friends for their love, encouragement, and support during my thesis.

1. INTRODUCTION

1.1. Boron

Boron is the 5th element in the periodic table.The symbol for boron is the capital letter b (B).Boron is also metalloid-element..The chemical properties of boron are resemblance to those of carbon and silicon , but boron is more electron deficient than both carbon and silicon.Boron has the property of being the 2nd most abundant element on the earth among the group 13 elements,the first element is aluminum.(1).Boron was successfully isolated by chemist Sir Humphry Davy and French chemists Joseph Louis Gay-Lussac and Louis Jaques Thenard in 1808.They named this newly discovered element 'bore'.(2,3,4,5)

Figure 1.1. Chemists who discovered the element boron (a) Chemist Joseph Louis Gay-Lussac (1778-1850), (b) Chemist Louis Jacques Thenard (1777-1857), (c)Chemist Humphry Davy (1778-1829).

The electron configuration is Boron $1s^2$ $2s^2$ $2p^1$.Boron shows more metal properties than nonmetal this is boron has three electrons in its outer shell. The compound called borax, is usually combined with boron sodium and oxygen in an aqueous medium. Borax may appear hard brittle dark brown and shiny like metal or it may appear as shiny black crystals.(6,7)

Figure 1.2. Borax from Kramer Borate deposits

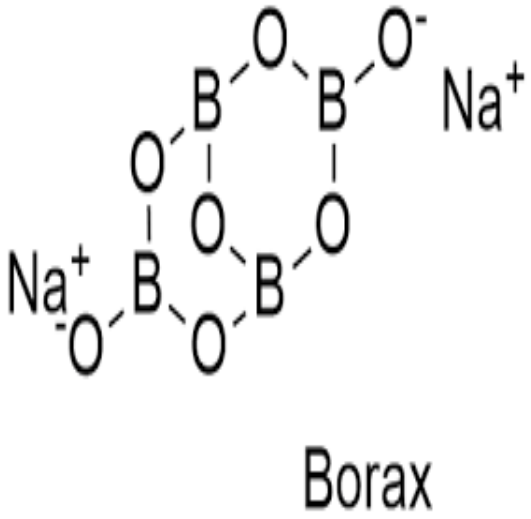

Figure 1.3. Structure Borax

1.1.1 Atomic Structure, Chemical and Physical Properties of Boron

The atomic structure properties of boron are as follows, respectively.

Ionic Radius is 0,23 Å

Number of Electrons are 5

Number of Neutrons are 6

Number of Protons are 5

Atomic Diameter is 1,17 Å

Atomic Volume is 4,6 cm3/mol

Crystal Structure is Rhombohedral

The chemicaly properties of boron are as follows, respectively.

Electrochemical Equivalent is 0,1344g/amp-hr

Electronegativity (Pauling)is 2.04

Fusion Heat is50,2 kJ/mol

First Ionization potentıal is 8,298 Second: 25,154 Third: 37,93

Valence electron potential (-eV)is 190(8)

The physically properties of boron are as follows, respectively.

Atomic-Mass is 10,811	Boiling-Point is 4.275K – 4.002°C – 7.236°F;
Condutivity: Electrical is 1,0E -12 106/cm	Thermal-Expansion Coefficient is 0,0000083 cm/cm/°C (0°C)
Density is 2,34 g/cc at 300k	Appearance: Yellow-brown non-metal crystal.
Elastic Module Bulk: 320/GPa	Atomization Enthalpy is 573,2 kJ/mol @ 25°C
Fusion Enthalpy is 22,18 kJ/mol	Molar Volume is 4,68 cm3/mol
Vaporisation Enthalpy is 480 kJ/mol	Specific Temperature is 1,02J/g
Boiling Temperature is 489,7kJ/mol	Physical Condition is (20°C & 1atm): Solid
Melting Point is 2573K 2300°C 4172°F	Vapour pressure is 0,348Pa@2300°C

All information https://www.etimaden.gov.tr/en/boron-element taken fromt his page.

Additionally naturally, the element boron had two stable isotopes these are; ^{10}B and other ^{11}B also each isotope has a nuclear spin.(9,10) This had showed particularly valuable in NMR spectroscopy, specially for ^{11}B. The big distiction in neutron absorption cross- section of the two isotopes is also no-stable and this had led to the development of a applicable separated process on an industrial area.(11,12,13) First experiment on boron ion exchange separation was performed by Makisima and his friends in 1959.(14)

1.1.2 Structures of Crystalline Boron

Borates are classified according to their structural anionic connections, for example chains, sheet and frame structures.(15) Compounds contained monomeric trigonal BO_3 units are acknowledged as rare-earth orthoborates M_3BO_3 for example $CaSnIV(BO_3)^2$ and $Mg_3(BO_3)^2$.(16)

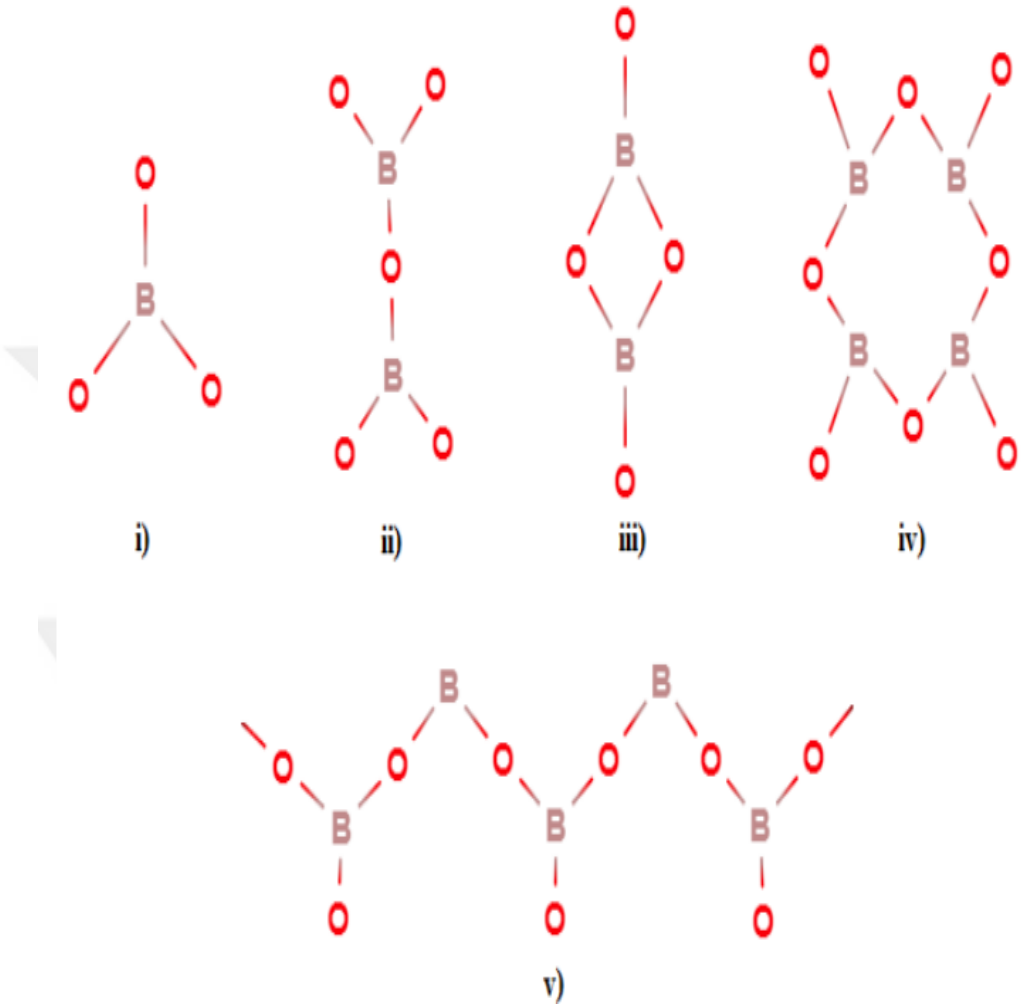

Figure 1.4. Example of borate structure i)Structure of Orthoborates ii) Structure of Pyroborates, iii)Structure of Metaborates

1.2 History of Borates

In 300 announcement, China borax in its mineral form (also known as tinkal) first saw used as a glaze.(17) A few crude borax traveled westward, and was supposedly mentioned by the alchemist Jabir Ibn Hayyan around 700 announcement. Some glaze was brought by Marcopolo in the 13th century to the Italy in the 17th Georgius Agricola said that borax used as a flux in metallurgy.(18,19)

Borates are designed as salts or ester of boric acid.(20) This compounds containing the radical B_2O_3.(Bates and Jackson 1987) A lot of minerals contains boric oxide, but the three most common and known in the world are : borax, ulexite and colemanite.(21)

1.2.1 Sources and Types of Boron Minerals

Boron is an element found in rocks, water and soil on Earth. boron up to <10 ppm is found in the earth's soils. The countries with rich soils in the possession of boron elements are as follows; they are the Western part of the United States and some regions of Mediterranean to Kazakhtan .(22,23)

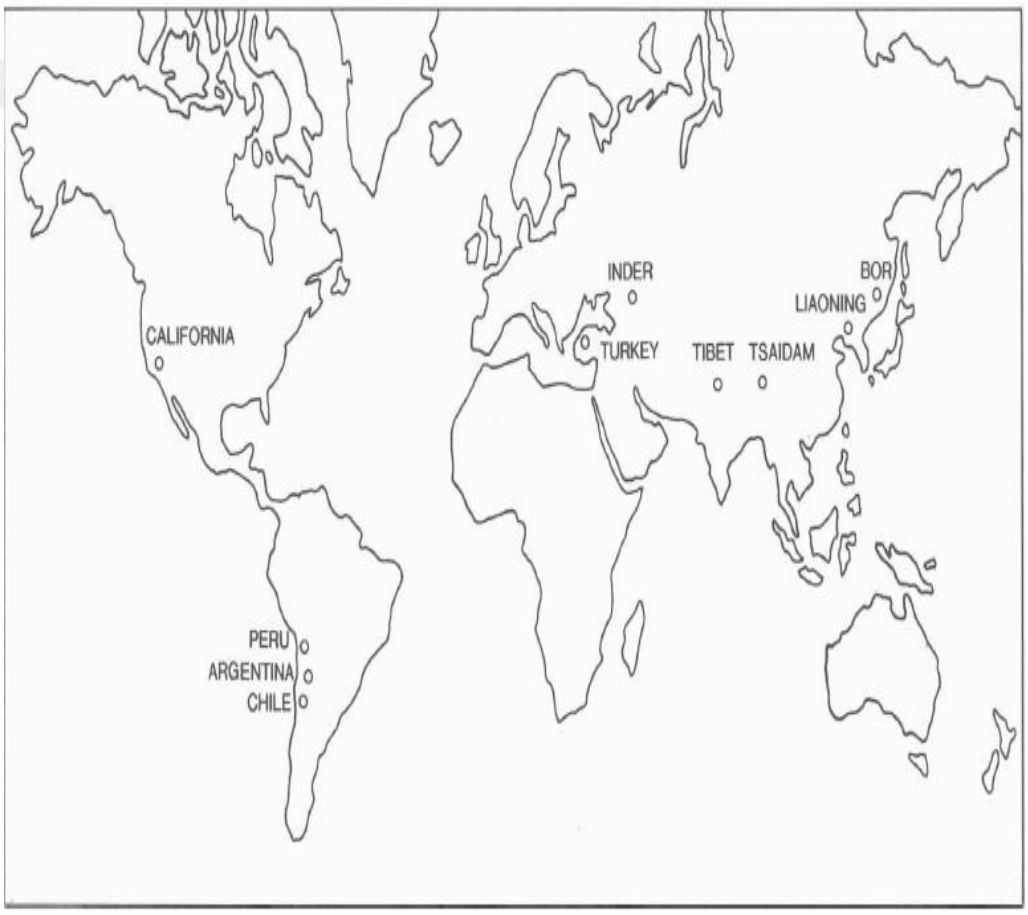

Figure 1.5. Sources of borates

As presented in Figure 1.5, shows the countries where %90 of borax, ulexite and colemanite are produced. Borax and kernite are extracted from these countries in America and ulexite, colemanite and borax are produced in Turkey.(24,25,26)

Table 1.1. The regional distribution of Turkish boron reserves (Reference Eti Mining Company)

Location	Proven Reserve	Possible Reseve	Probable Reserve	Total Reserve
Emet	266.561.602	-	1.416.000.000	1.682.561.602
Kestelek	6.994.525	-	-	6.994.525
Bigadiç	363.534.560	-	259.924.150	623.458.710
Kırka	171.971.373	377.299.000	201.350.000	750.620.373
Total Reserve	809.062.060	377.299.000	1.877.274.150	3.063.635.210

There are more than 150 boron minerals, the most important (common) of which are; ulexite ($NaCaB_5O_9 \cdot 8H_2O$), borax ($Na_2B_4O_7 \cdot 10H_2O$), kernite ($Na_2B_4O_7.4H_2O$). and colemanite ($Ca_2B_6O_{11} \cdot 5H_2O$), (27) Other common boron minerals are shown in Table 1.2.

Table 1.2. Commonly used boron minerals worldwide

Mineral	Formula	B_2O_3 (%)	Regions of mineral
Kernite (Rasortie)	$Na_2B_4O_7.4H_2O$	51.0	Kırka, USA, and Argentina
Pandermite (Priceite)	$CaB_{10}O_{19}.7H_2O$	49.8	Sultancayır and Bigadic
Ulexite (Boronatrocalcite)	$NaCa\ B_5O_9.8H_2O$	43.0	Kırka, Bigadic, Emet, and Argentina
Colemanite	$Ca_2B_6O_{11}.5H_2O$	50.8	Emet, Bigadic, Kucukler, and USA
Probertite (Kramerite)	$NaCaB_5O_9.5H_2O$	49.6	Kestelek, Emet, and USA
Szaibelyite (Ascharite)	$MgBO_2.2OH$	41.4	Russia
Boraxs (Tincal)	$Na_2B_4O_7.10H_2O$	36.6	Kırka, Emet, Bigadic, and USA
Boracite (Stassfurite)	$Mg_6B_{14}O_{26}C_{12}$	62.2	Germany
Hydroboracite	$CaMgB_6O_{11}.6H_2O$	50.5	Emet

Source: Culver et al., 1994; Lyday, 2000; and Roskill, 1999.

1.3 Uses of Boron

Borates have had a wide range uses for centuries. About 4000 years ago, the Babylonians used borax brought from the far east as a flux for working gold on the other hand borax existed by the ancient Egyptians in their mummifications process and in their lives as a medical product (28). In Figure 1.6, we can see the percentages given according to the areas of use of borates

These days, borax and boric acid are used to soften water because they dissolve easily in water it is also used in electronic instruments in the production of metal and steel in soaps, cleaning materials, glass industry, textile dyes.Borates have also been used as flame retardants in the polymer used to coat the electrical cable. In additional, boron compounds; are expected to be capable and used as jet and rocket fuels in the near future such as diborane (B_2H_6), pentaborane (B_5H_9), decaborane ($B_{10}H_{14}$) and alkali borons (29,30)

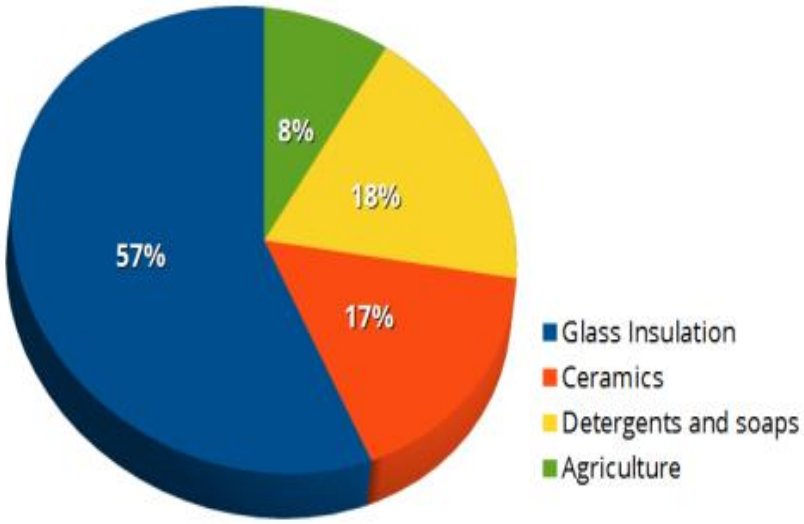

Figure 1.5. World borate end uses (after Helvacı, [21])

1.4 Metal Borates

Borates have seen great importance in recent years in terms of application. Some of these metal bonded borates are, magnesium borate, calcium borate beryllium borate, zinc borate aluminum borate, , nickel borate, copper borate, zinc borate, strontium borate, lead borate, barium borate, lithium borate and (31)

Metal orthoborates general formula of $M_3B_2O_6$ (M is the metal such as Zn, Ca, Sr, Ni, Mg, Mn, Ba, Cd, Co, etc)

Only oxygenated metal borates are often found in mineral forms and artificial forms, those are often used in today's industry.(32) The principles of the bonds in crystalline metal borates are as follows, respectively. Firstly, The protons present in aqueous borates first convert the free O_2 ions into free OH ions. Secondly, the remaining protons are used by the oxygens in the trihedral and tetrahedral planes in the borate ion. The added protons then convert the free OH ions into water. Thirdly, it can be replaced by multiple anions of the complex borate by the addition of a single edge group. Finally, Others that can exist in the presence of anions are isolated $B(OH)_3$ groups or polymers.(33)

1.4.1 Zinc Borates

Zinc borate is generally used in flame retardants, antibacterial and addition materials, as an insect and fungal repellent.(34) Zinc borates could be isolated as crystalline material of different shape with different chemical compositions and structures. One of them is crystal zinc borate with the unsupported formula $2ZnO\ 3B_2O_3\ 3.5H_2O$. hydration water at temperatures up to 290 ^oC (35) This thermal steady makes it engaging as a fire retardant additive for plastics and rubbers that require high processing temperatures.(36)

A series of different crystal shapes (like Figure 1.7) of zinc borate (ZB) have been developed and are being used. $3ZnO.2B_2O_3.3.5H_2O$, $2ZnO.3B_2O3.3H_2O$ and anhydrous ZB $2ZNOA_3B_2O_3$ known to be most commonly used zinc borate and has thermal stability at around 290-300 ^oC, which ensures the processability of the polymer and the thermal stability of anhydrous borate up to 400 ^oC.(36,37)

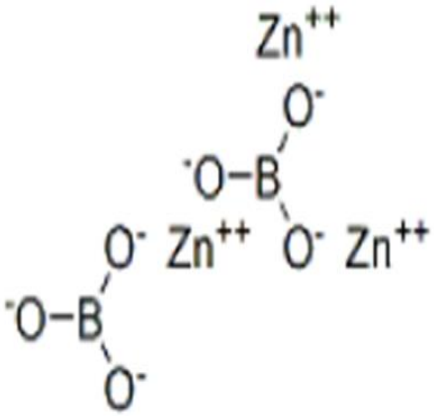

Figure 1.6. Structure of zinc borate

1.4.2 α Zinc Borate and β Zinc Borate

Borates have attracted a lot of attention because important practical applications have been studied in second harmonic generation zinc-containing borates due to their back demand values as catalysis and optical materials. For example, β-BaB_2O_4, LiB_3O_5, and $YCa_4(BO_3)_3O$ are all well-known not linear optical (NLO) crystals.(38)

At least three compounds have been proposed in the binary system of ZnB_4O_7, $Zn_3B_2O_6$, and $Zn_4O(BO_2)^6$. The crystalline structure of $Zn_3B_2O_6$ obtained at the higher temperature are known as β-form of $Zn_3B_2O_6$.(39,40) It was determined to be in a non-centripetal group *Ic* by Garcia-blanco and Fayos, who were the first to detect it, which was later set aright by Baur and Tillmanns in a non-centripetal group (*I*2/*c).*

When XRD analyses of alpha and beta zinc orthoborates were performed (Figure 1.8) The difference between the diffraction peaks and densities of alpha zinc orthoborate from the beta form is clearly seen.(41)

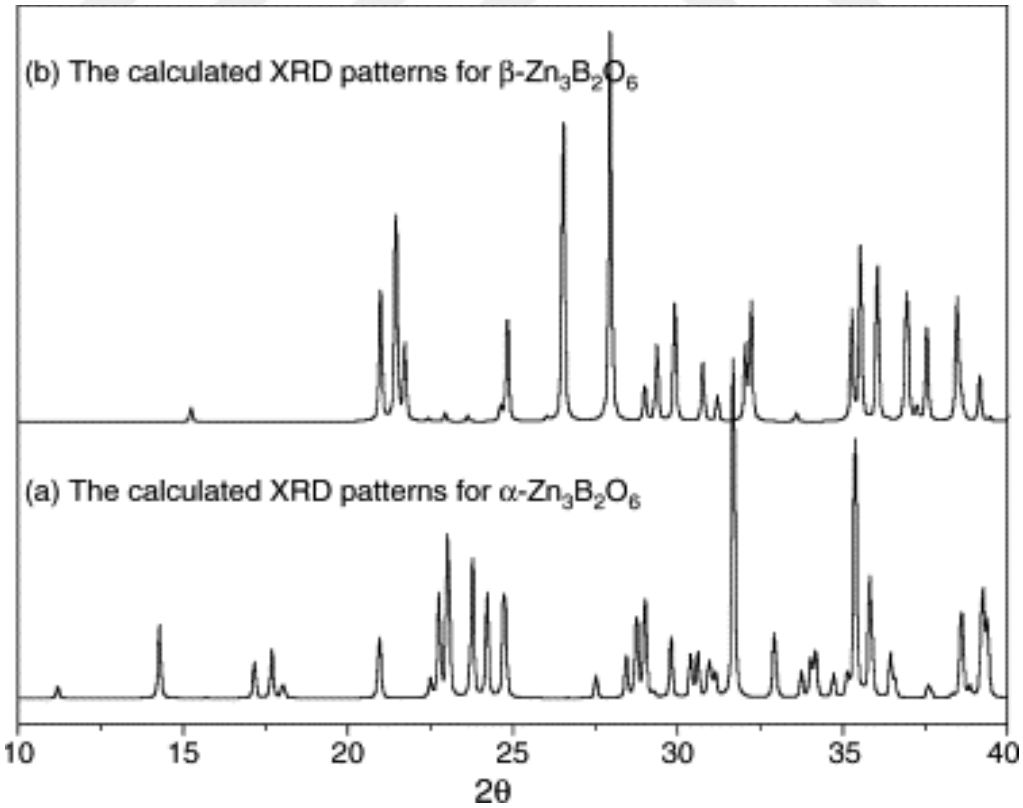

Figure 1.7. X-ray diffraction profiles for (a) α-$Zn_3B_2O_6$ and (b) β-$Zn_3B_2O_6$.

1.4.3 Rare Earth Elements and Zinc Orthoborates

The definition of rare earth elements is older than lanthanide elements.19. they have called it rare for a century to distinguish it from other elements.(42) Rare earth elements also include 15 lanthanide elements and yttrium.these elements are holmium (Ho), lanthanum (La), cerium (Ce),), ytterbium (Yb)praseodymium (Pr), neodymium (Nd), promethium (Pm), gadolinium (Gd), samarium (Sm), europium (Eu), erbium (Er), terbium (Tb), dysprosium (Dy), erbium (Er), thulium (Tm), and lutetium (Lu).

Lanthanide elements are divides into two groups among themselves: heavy rare earth elements (HREEs). light rare earth elements (LREEs) and

LREEs : lanthanum through europium

HRREs: gadolinium through lutetium

Lightest rare earth elements are known to be yttrium but it is classified with heavy rare earth elements because it is physically and chemically similar (43). In latest years, doped nano-particles have been of interest due to their optical properties and potential application areas.

In a study conducted in June 2004, the Ce^{3+} ion was used. The Ce^{3+} ion often acts as an important activator. It has one $4f^1$ electron configuration and 5d lowest excited orbital.For this reasan, the phenomenın of non-radiative multiphonon relaxation was not detected. Furthermore, to determine the novel luminescence properties of the nano-particles, the Al^{3+} was selected. It was found that the relationship between Ce^{3+} energy levels and Al^{3+} energy levels is suitable for energy transfer(44)

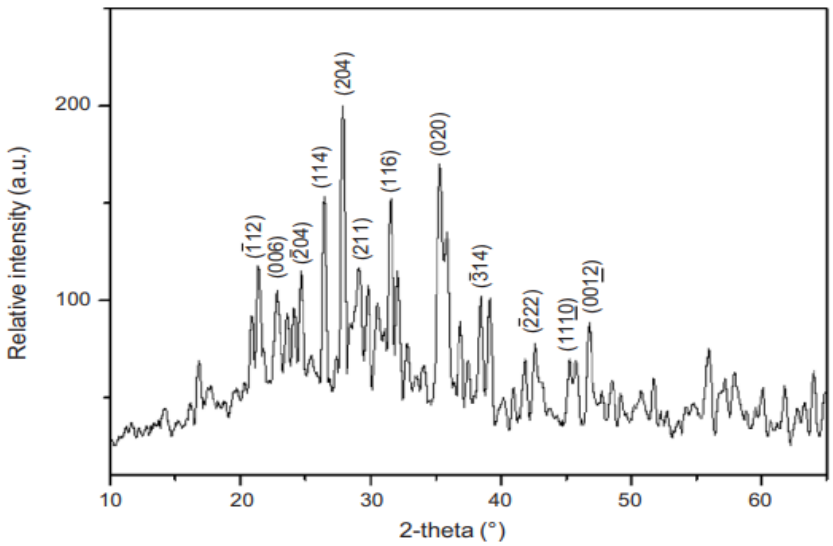

Figure 1.8. XRD pattern of the doped samples (heat treated at 700 °C).

1.5 Methods of Synthesizing Borates

The methods of synthesizing are borates divided into three according to their methods.These are solid state method,solid gas method and finally solution combustion method.(45)Additionally the solution combustion method was used in this study.

1.5.1 Solution Combustion Method

In recent years,this method has become very popular in the preparation of nano-sized materials.The reason for this can be shown as effective and low cost. (https://doi.org/10.1016/j.cossms.2008.12.002)

It is a rapid and spontaneous reaction between a fuel and an oxidant in addition to the presence of metal cations in the envoriment.This reaction called redox reaction.(46)

The final products obtained by this method have high phase purity and higher surface area, as well as narrow particle size distribution, while having superior powder properties such as optimum agglomeration and better sintering properties.(https://doi.org/10.1016/j.pcrysgrow.2018.03.001)

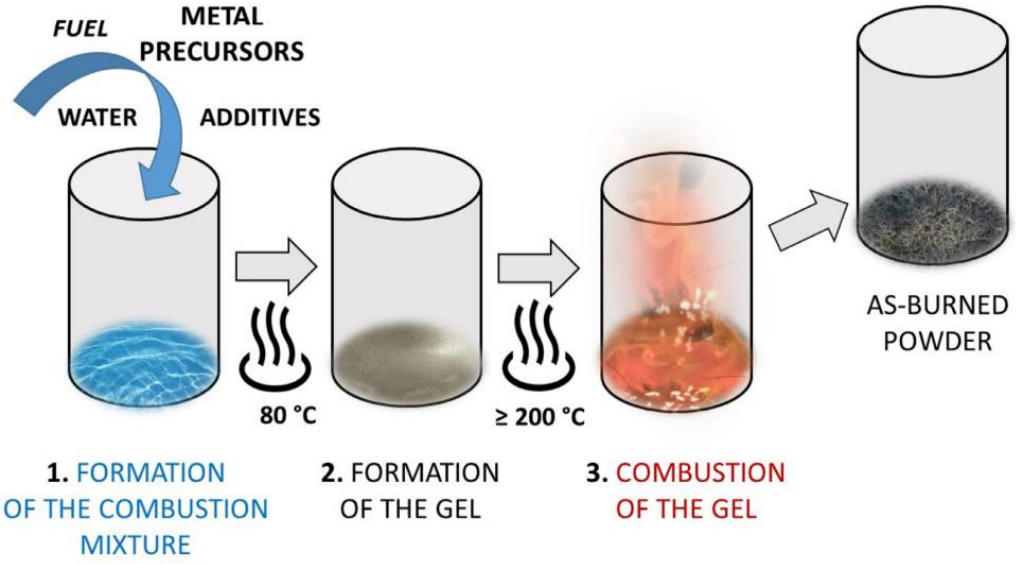

Figure 1.10 Description of SCS Method (Adapted from Mater. Tod: Proc., 4, F. Deganello, Nanomaterials for environmental and energy applications prepared by solution combustion based-methodologies: role of the fuel, Pages 5507–5516,)

2. AIM AND SCOPE OF THE STUDY

The aim of this study is to synthesize lanthanide ion doped zinc orthoborate nanoparticles by (SCS) solution combustion synthesis method. $Zn_3B_2O_6$ was synthesized using Dy^{3+}, Sm^{3+}, Tb^{3+}, and Eu^{3+} as doping materials along with glycine as fuel. The concentrations of the rare earth metals are 0.005,0.010, 0.020 and 0.025 mol, respectively.

Rare earth metal ion doped zinc orthoborate powder materials synthesized by the SCS method are heated at 100 degree intervals between 400-900°C. XRD technique was used to determine whether the crystal structure of the Dy, Sm, Eu and Tb doped zinc orthoborates produced in this study was triclinic α or monoclinic β zinc borate forms.

The Debye-Scherrer equation was used to calculate the sizes of the resulting zinc orthoborate nanoparticles.

Then, FTIR spectroscopy analysis was performed to determine the vibrational movements of the synthesized zinc orthoborates.

Finally, the optical properties were examined by taking into account the absorbance and reflection spectra obtained from the UV-VIS study.

3. MATERIALS AND METHODS

3.1 CHEMICALS

The following chemicals were used in the synthesis of products:

$Zn(NO_3)_2.6H_2O$, Zinc nitrate hexahydrate : Merck (pure 99.0%)

H_3BO_3, Boric acid : Merck, 99.00%

$C_2H_5NO_2$, Glycine : Merck, 99.70%

$Dy(NO_3)_3.5H_2O$,Dysprosium(III)nitratepentahydrate :Aldrich(pure 99.5%)

$Tb(NO_3)_3.5H_2O$, Terbium(III) nitrate pentahydrate :Sigma-Aldrich,99.9%

Europium nitrate pentahydrate, $Eu(NO_3)_3.5H_2O$:FlukaChemika,98.5%

$Sm(NO_3)_3.6H_2O$,Samarium (III) Nitrate Hexahydrate :Aldrich(pure 99.5%)

KBr, Potassium Bromide , for IR Spectroscopy : Merck, 99.90%

It was dried for 2 hours at 180°C before using.

3.2 INSTRUMENTS

3.2.1 Fourier Transform Infrared Spectrophotometer

The Perkin Elmer Fourier Transform Infrared (FTIR) spectrophotometer was used to record the bond variation of obtained products in the region of 4000-400 cm^{-1}. The Infrared spectra was recorded by preparing the pellets that are contains of 0.1500:0.0010 (wt/wt) of KBr: product ratio.

Picture 3.1. FTIR Instrument

3.2.2 UV- VIS Spectrometer

UV-VIS Spectroscopy Perkin Elmer Lambda 35 at range of wavelength 200-900 nm. The acquire spectra were plotted by used Data Processor WinLab program.

Picture 3.2. UV-VIS Instrument

3.2.3 X-ray Powder Diffractometer

To study the structural properties of the compounds, CuKa (30-40kV, 1020ma, λ=1.54056 Ǻ) radiation Rigacuminiflex and multiflex X-ray powder diffractometer were using and the obtained data were compared with ICDD data card**.**

Picture 3.3. XRD Instrument

3.2.4 Furnace

Nuve MF 120 furnace was used to heat the digested compounds at 400 degrees up to 900 ^{o}C.

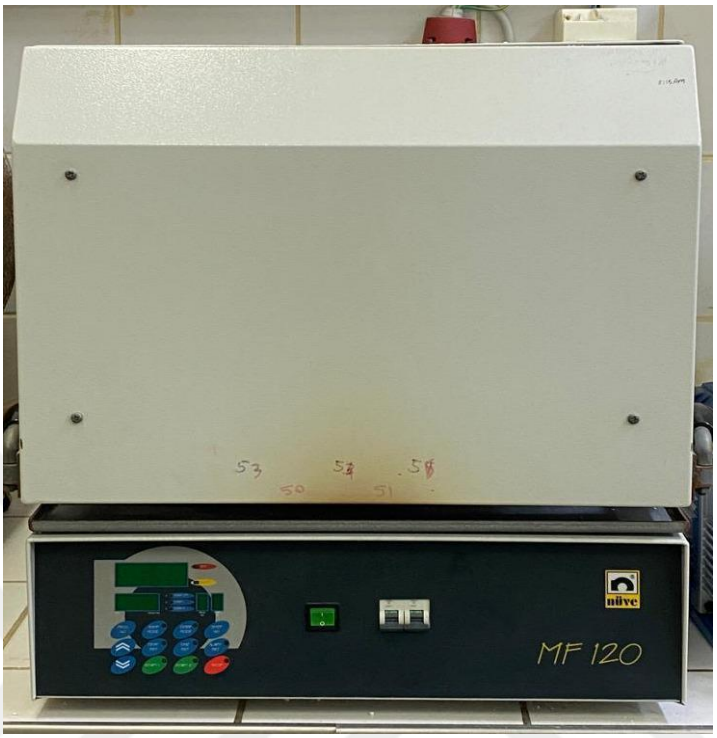

Picture 3.4. Furnance Instrument

3.2.5 Hot Plate

VELP magnetic stirrer was used to mix the starting materials into a homogeneous solutions and actualized the combustion process of as-synthesized zinc othoborates at 370^{o}C.

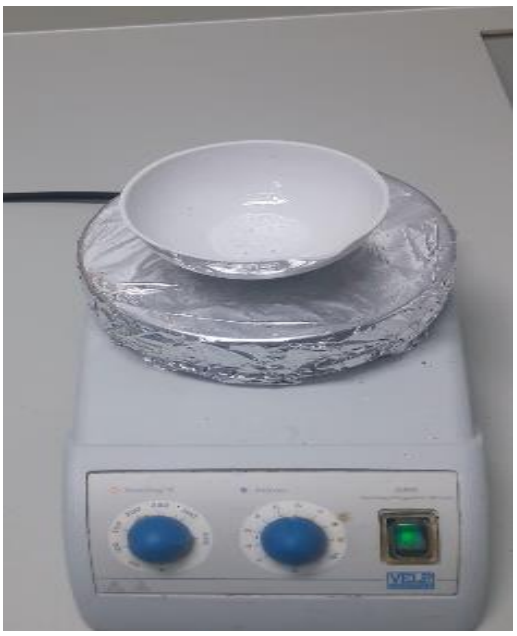

Picture 3.5. Hot Plate Instrument

3.3 The Synthesis of Zinc Orthoborates

Firstly, the preparation of zinc orthoborates has been successfully carried out by the solution combustion method. The combustion process was done directrly on hot plate at 370 ^{o}C. Starting materials Zn $(NO_3)_2.6H_2O$, H_3BO_3 and glycine was dissolved into sufficient amount of water. The as-prepared powder products was then annealed at 400-900^{o}C for an hours in 100^{o}C interval to get rid of oranic compounds and gaining higher crystallinity products.

The reaction is expected as follows;

$$9\ Zn(NO_3)_3 + 6H_3BO_3 + 10\ H_2NH_2COOH \rightarrow 3Zn_3B_2O_6$$

3.3.2 Synthesis of Zinc Orthoborates with Lanthanide Elements (Tb, Dy, Sm,Eu)

Lanthanide doped Zinc orthoborates was also fabricated by the similar procedure as undoped zinc orthoborates. Different quantity of lanthanide elements were added such as 0.005 ,0.01 , 0.02 and is 0.025 mol.

The chemical reactions of the different dopes are presented are as follows;

- **Dysprosium (Dy)**

$$\mathbf{9Zn(NO_3)_3 + Dy(NO_3)_3.5H_2O + 6H_3BO_3 + 10\ Glycine \rightarrow 3Zn_3DyB_2O_6}$$

- **Europium (Eu)**

$$\mathbf{9Zn(NO_3)_3 + Eu(NO_3)_3.5H_2O + 6H_3BO_3 + 10\ Glycine \rightarrow 3Zn_3EuB_2O_6}$$

- **Samarium (Sm)**

$$\mathbf{9Zn(NO_3)_3 + Sm(NO_3)_3.6H_2O + 6H_3BO_3 + 10\ Glycine \rightarrow 3Zn_3SmB_2O_6}$$

- **Terbium (Tb)**

$$\mathbf{9Zn(NO_3)_3 + Tb(NO_3)_3.5H_2O + 6H_3BO_3 + 10\ Glycine \rightarrow 3Zn_3TbB_2O_6}$$

4. RESULTS AND DISCUSSION

4.1 Synthesis of Zinc Orthoborates and Doped Lanthanide Elements

The investigations in the synthesis of undoped zinc borates and the lanthanide element doped (Dy,Sm,Eu and Tb) zinc orthoborate was prepared by direct combustion process of solution combustion synthesis method. To obtain a high crystalline single phase prowder products, the heating temperatures was applied from 400 °C to 900 °C. The fuel effect on the physical properties of the zinc orthoborates was observed during the synthesis process as follow;

➢ **Undoped Zinc Orthoborates**

Syntheszed with glycine as fuel, the colorless precursor gel of zinc orthoborates was observed at 370°C. During the evaporation process, small amount of gas was noticed and a fluffy light brown product was obtained after the gel allowed to heated for 7-8 minutes at the same degree.

➢ **Tb doped Zinc Orthoborates**

The colorless gel was observed at 370 ^{o}C and a small amount of gas developed. After the combustion process completed, a fluffy light brown product was obtained. It took around 8-10 minutes to complete the process after the gel formed. This procedure was applied in the same way for concentrations of 0.005, 0.01, 0.02 and 0.025. There is no significant difference in combustion time upon the concentrations differences.

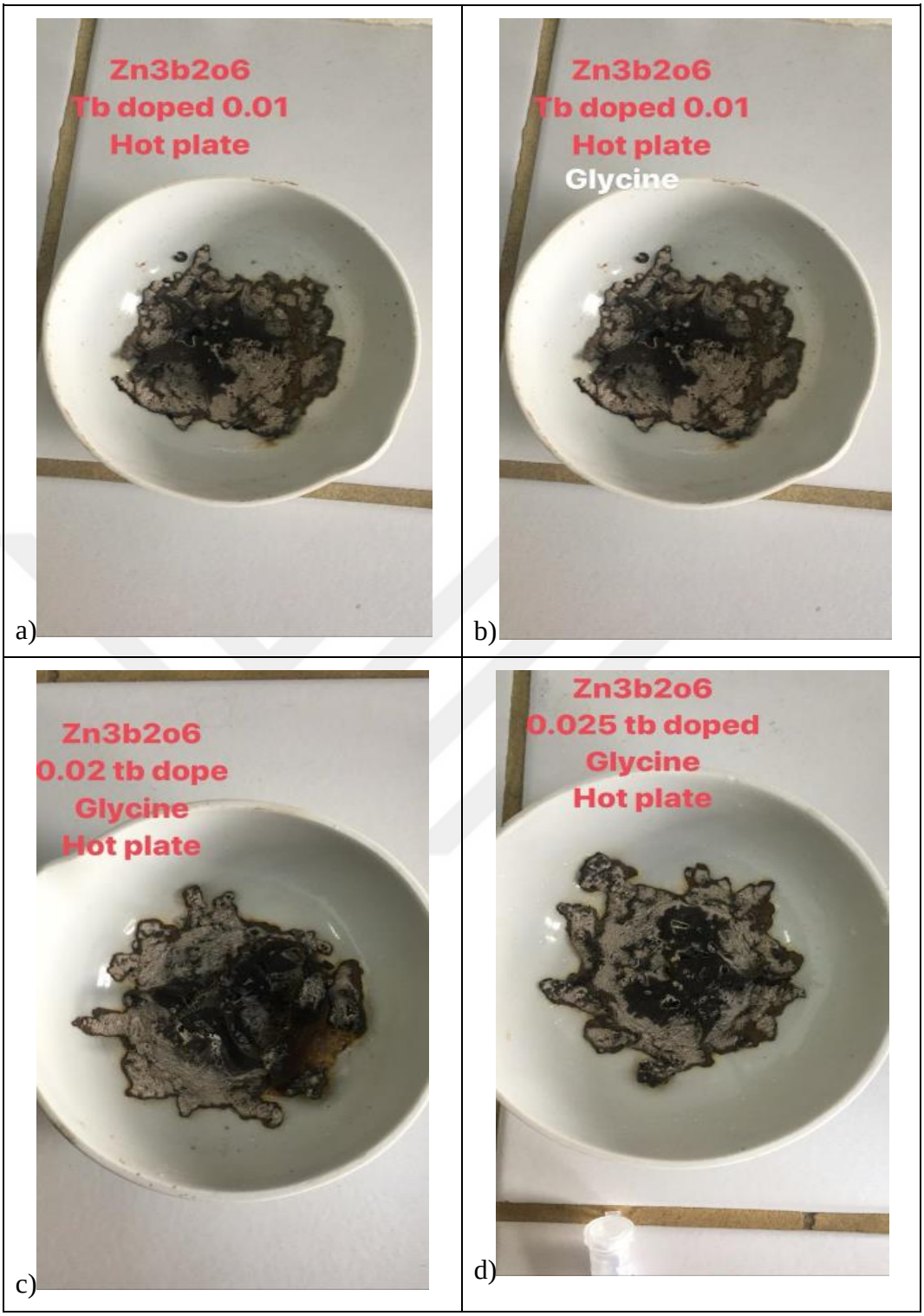

Picture 4.1. Synthesis Tb Doped Zinc Orthoborates with Different Concentration a)0.005Tb, b)0.01Tb, c) 0.02 Tb, d)0.025Tb

➢ **Dy doped Zinc Orthoborates**

A small amount of yellowish gas was observed during the evaporation process and the colorless gel was observed at 370°C was obtained. A fluffy light brown powder products product was obtained after heating for 8-10 minutes on a hotplate at the same temperature. This procedure was applied in the same way for concentrations of 0.005, 0.01, 0.02 and 0.025. It has not been observed that there is a minute difference between concentrations in the combustion process.

Picture 4.2. Synthesis Dy Doped Zinc Orthoborates with Different Concentration a) 0.005 Dy, b) 0.01 Dy, c) 0.02 Dy, d) 0.025 Dy

➢ **Sm doped Zinc Orthoborates**

The colorless gel was observed at 370 ° C and a small amount of yellowish gas developed. After the combustion process finished, a fluffy light brown product was acquired. Similar procedure was carried out fort he other conventrations and the is no dictinc change are observed.

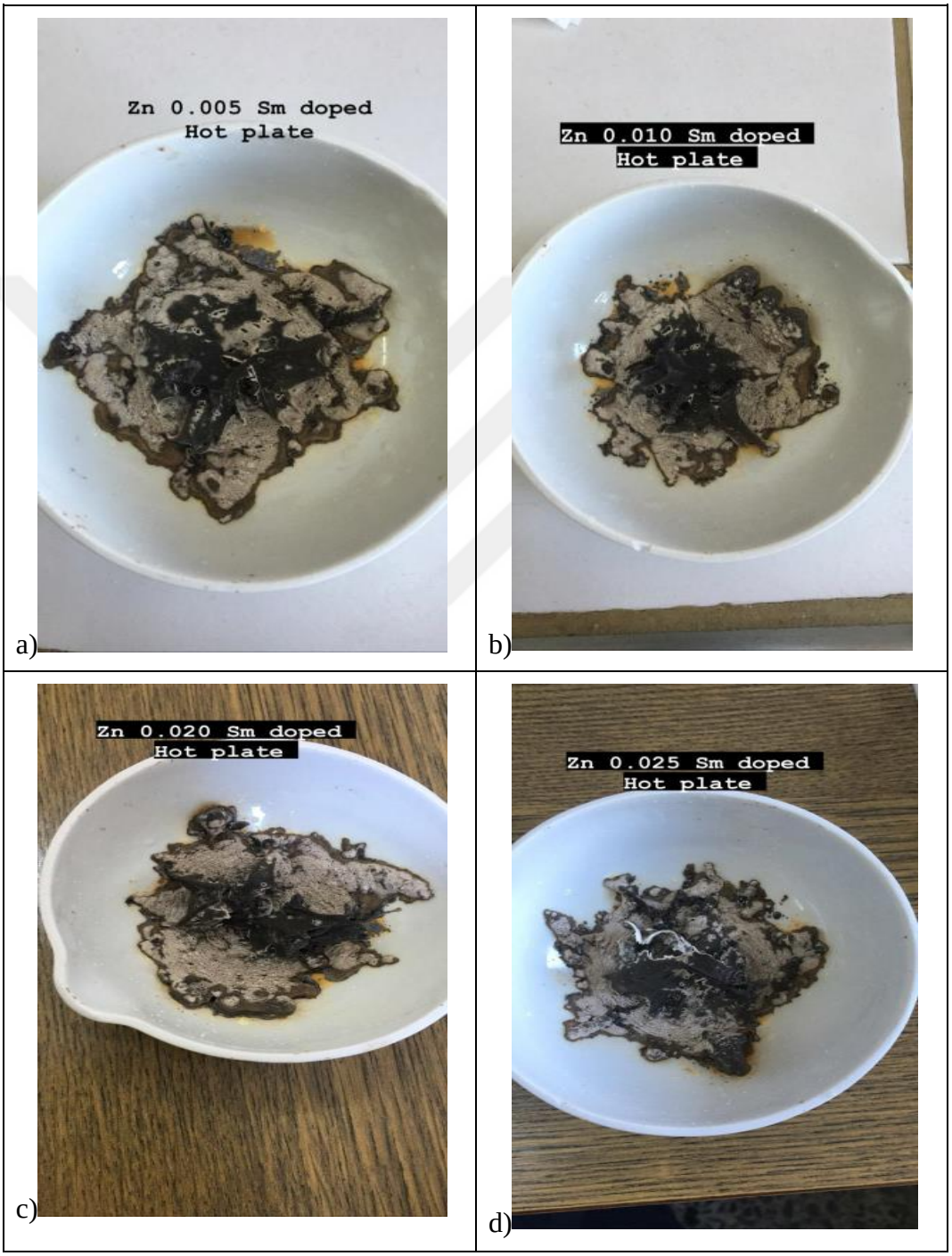

Picture 4.3. Synthesis Sm Doped Zinc Orthoborates with Different Concentration
a)0,005 Sm b)0,01 Sm c) 0,02 Sm d)0,025 Sm

➢ **Eu doped Zinc Orthoborates**

The colorless gel was observed at 370 ° C and a small amount of yellowish gas evaporated. A fluffy light brown product was obtained after 8-10 minutes of combustion process. This procedure was applied similarly for concentrations of 0.005, 0.01, 0.02 and 0.025 mol of Europium (III).

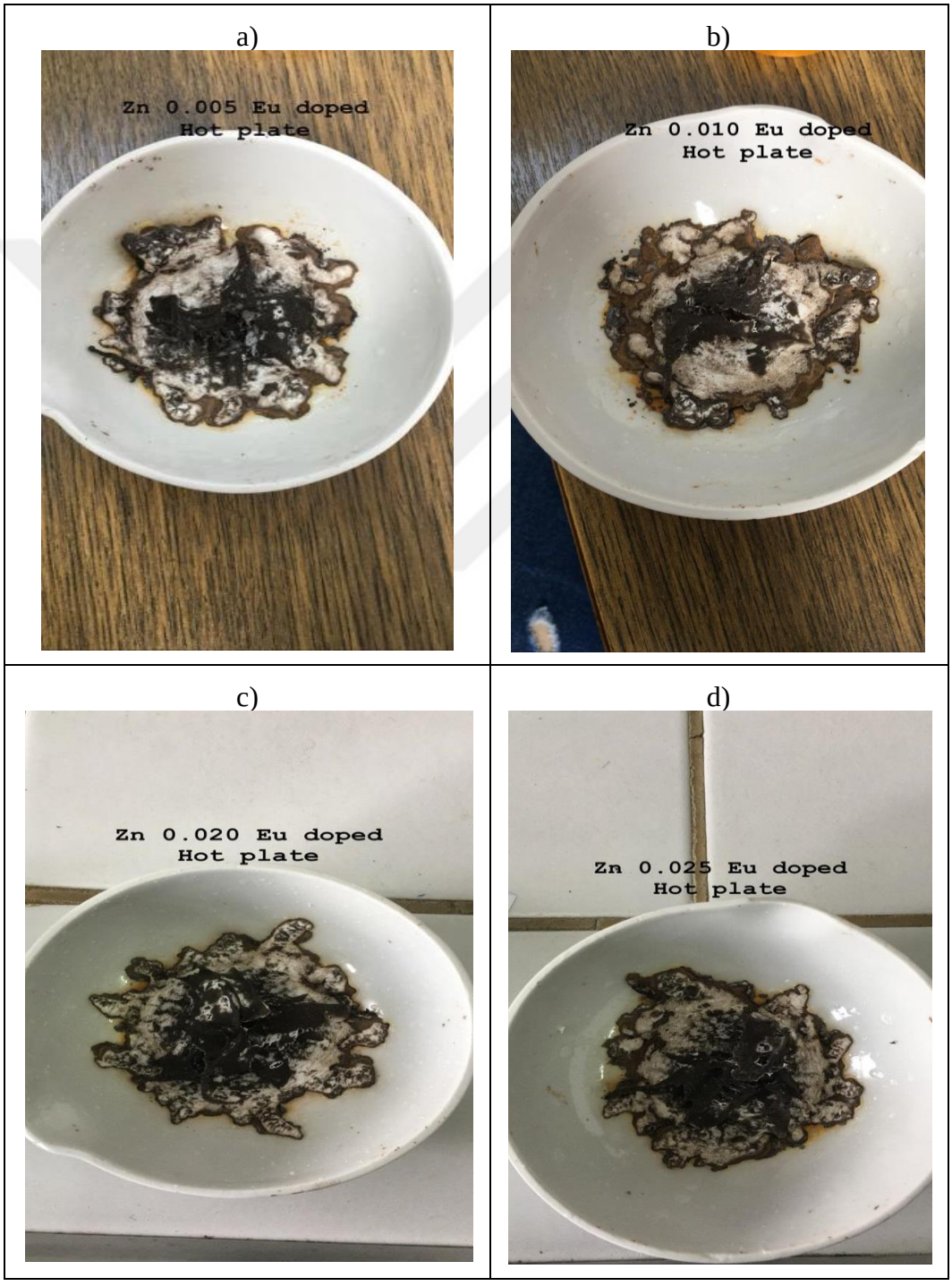

Picture 4.4. Synthesis of Eu Doped Zinc Orthoborates with Different Concentration a)0.005 Eu b)0.01 Eu c) 0.02 Eu d)0.025 Eu

4.1.2 Heating of Zinc Orthoborates and Doped Lanthanide Elements

The result of heated zinc orthoborates are showed in section 4.1, The zinc orthoborate are synthesized in different concentrations and with different lanthanide elements., starting at 400 ^{o}C,the heating process was done for 1 hour at temperatures up to 900^{o}C. In this part, it has been observed that all heated zinc orthoborates change their color from brown to white as the temperature rises. In the picture 4.5-4.6 given below.

<table>
<tr>
<td>a) 400^{o}C
 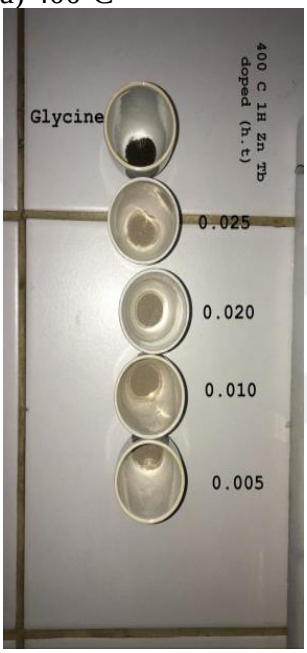
</td>
<td>b) 500^{o}C
 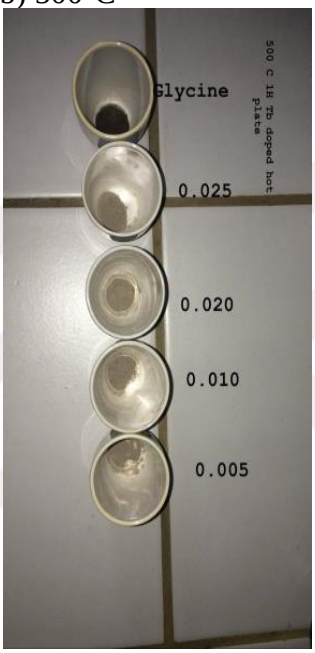
</td>
<td>c) 600^{o}C
 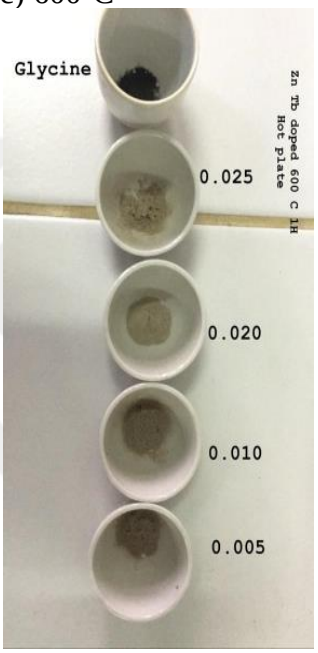
</td>
</tr>
<tr>
<td> 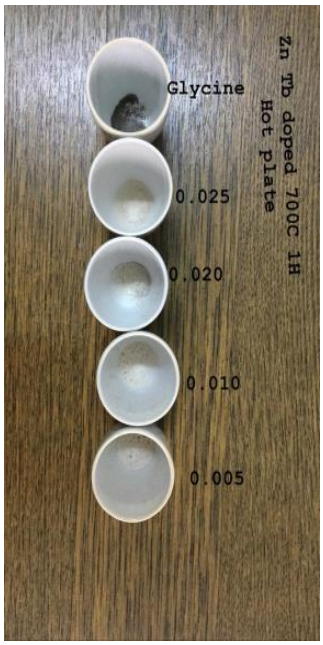

d) 700^{o}C</td>
<td> 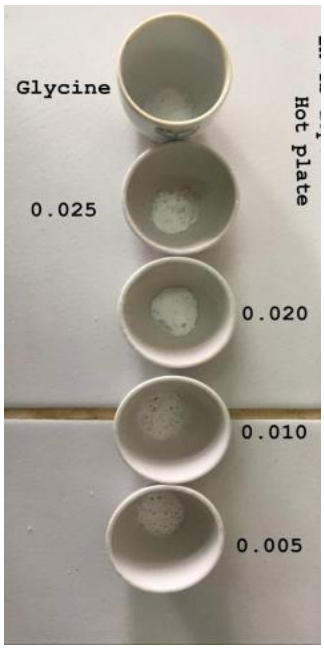

e) 800^{o}C</td>
<td> 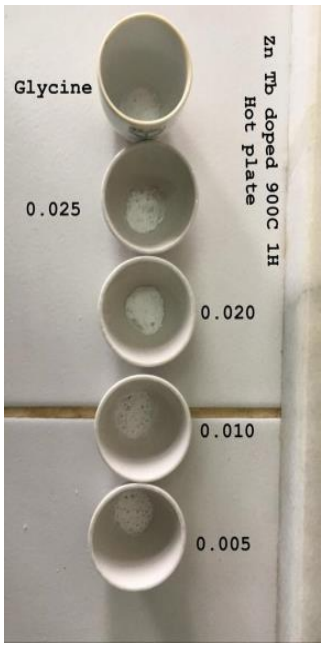

f) 900^{o}C</td>
</tr>
</table>

Picture 4.5. Heating of Tb doped Zinc Orthoborates (400ºC. to 900ºC 1 hour.)

a) 400ºC

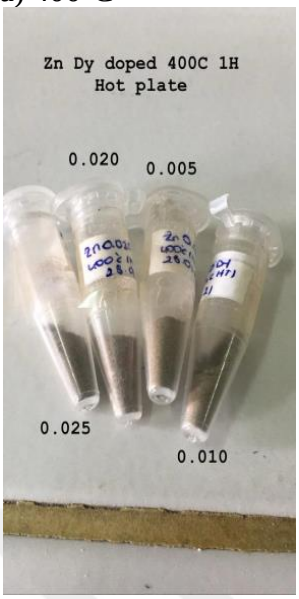

b) 500ºC

c) 600ºC

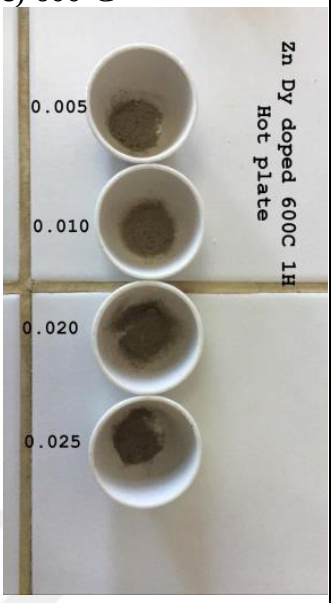

d) 700ºC

e) 800ºC

f) 900ºC

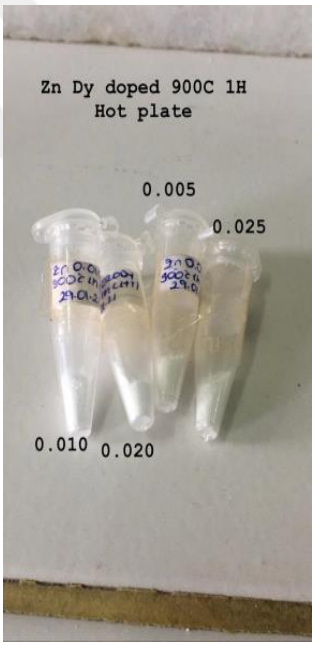

Picture 4.6. Heating of Dy doped Zinc Orthoborates (400ºC. to 900ºC 1 hour.)

4.2 FT-IR Spectroscopy Studies

In the examination of tb doped zinc orthoborate by infrared spectroscopy, it was observed that it gave a broad and strong peak in the gap of 2800-3600.(47) The values that appear in this range indicate the existence of the -OH group. On the other hand, vibrations in the area of ν_3 = 1100–1400 cm^{-1} are assigned to B–O asymmetric stretch of BO_3 group is triangular. The band at ν_2 = 700–900 cm^{-1} is contributed to out-of-plane bending whereas the one at ν_1 = 900–1000 cm^{-1} belongs to the B–O symmetric stretch. The band at around 600 cm^{-1} is appointed to stretching vibration of Zn–O. The BO_3 groups are the fundamental structural units in the zinc orthoborate crystal structure (48,49)

The difference in the synthesis of zinc borate with glycine as fuel and the synthesis of Tb metal at different concentrations by doping is as shown in figure 4.1 below. Figure 4.2 to figure 4.5 shown one hour heating diffrent temperatures.

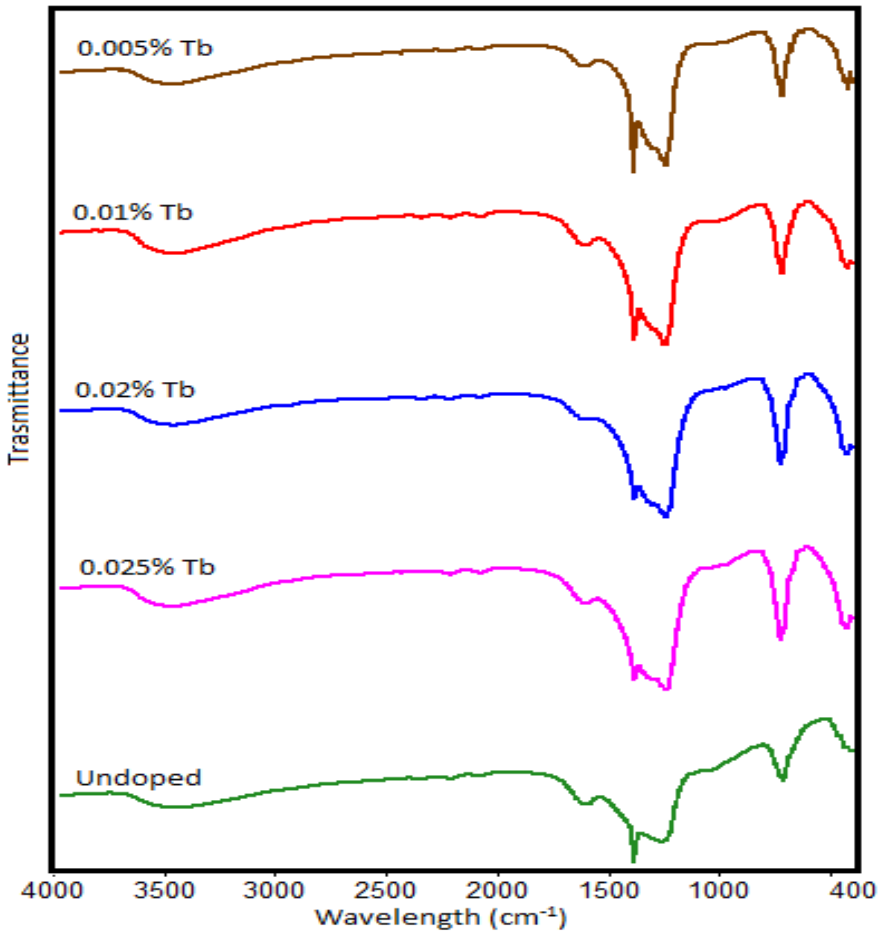

Figure 4.1. FT-IR Spectra of Synthesis Un doped and Tb doped $Zn_3B_2O_6$ at different concentrations.

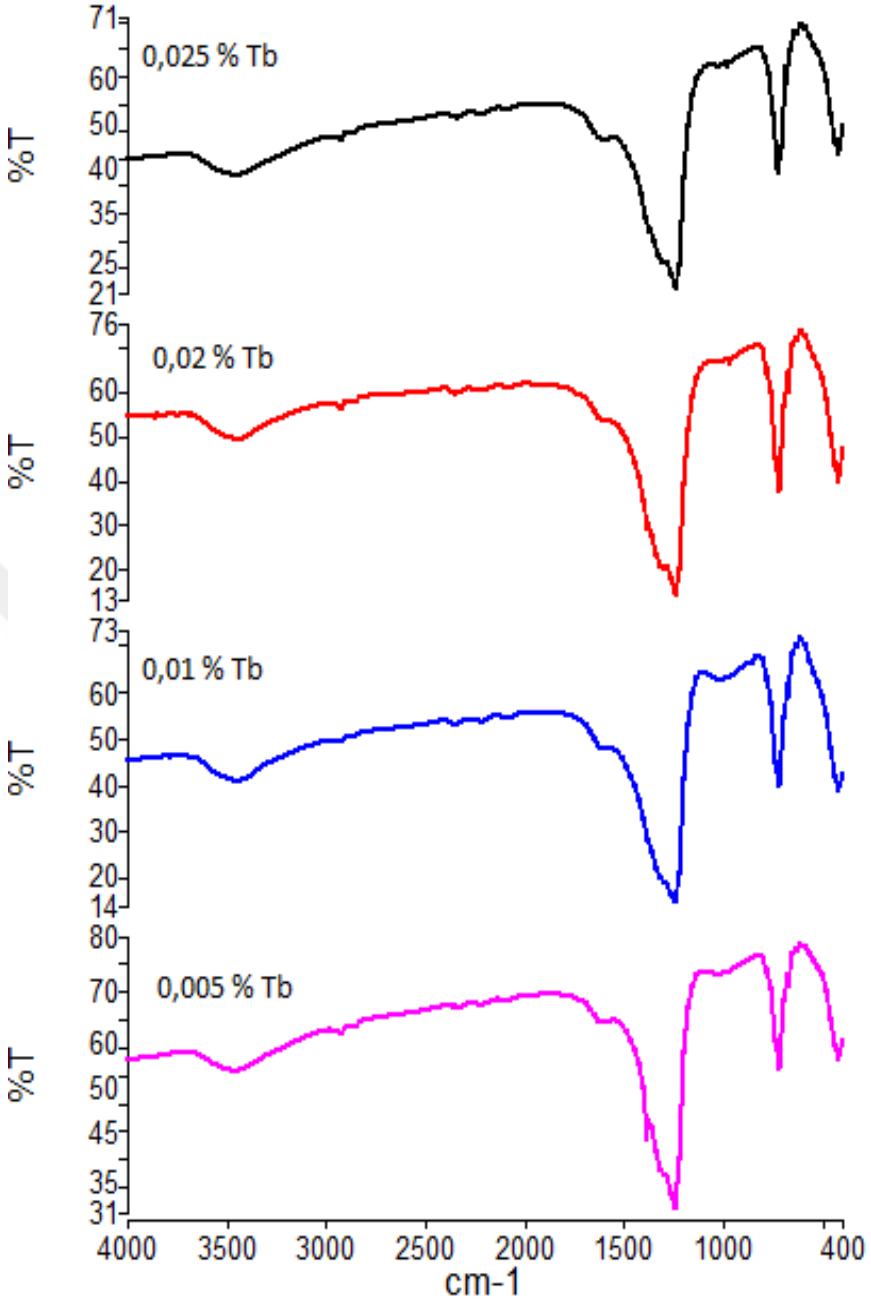

Figure 4.2. FT-IR Spectra of one hour at heating 400 °C Tb doped $Zn_3B_2O_6$ at different concentrations.

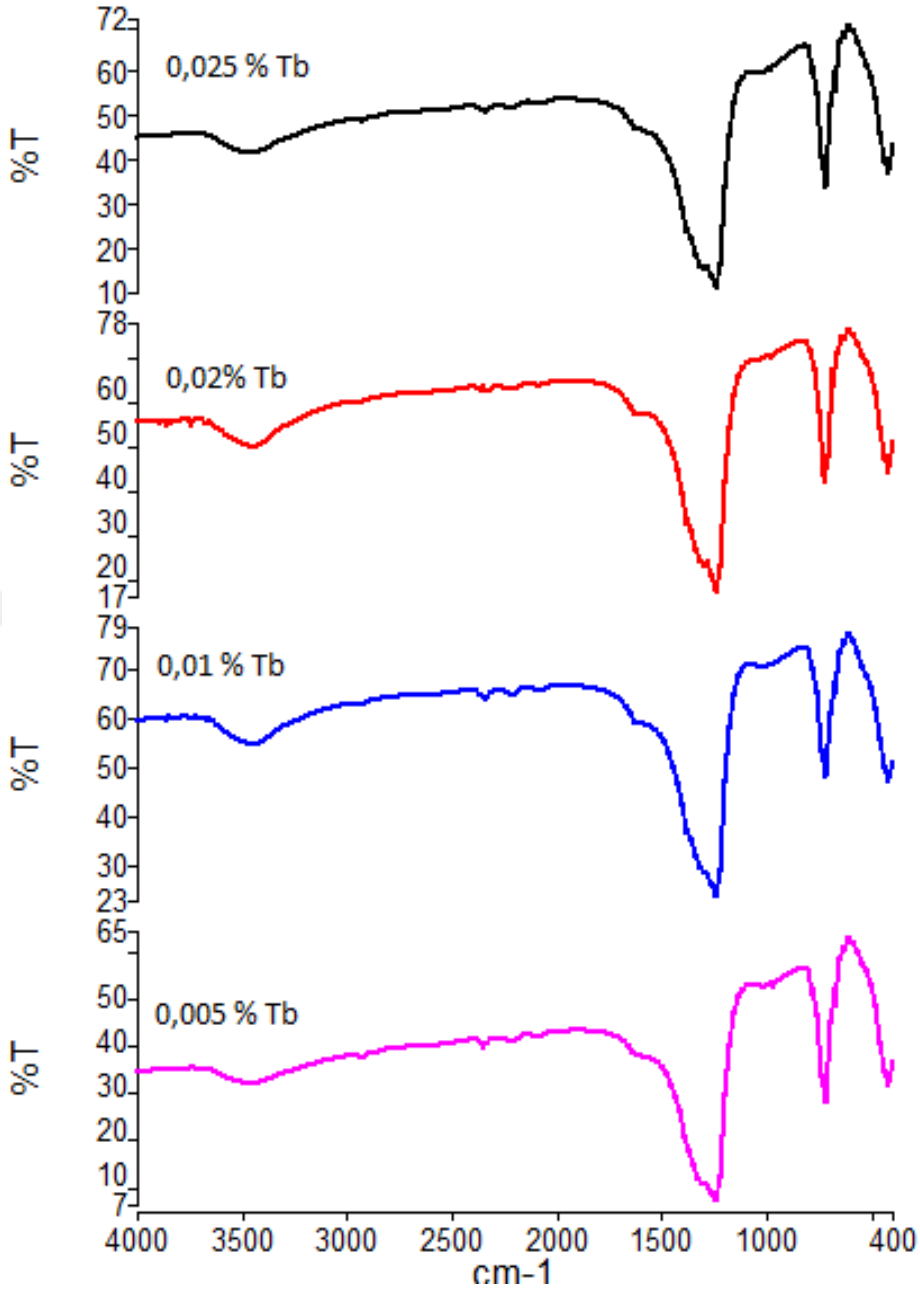

Figure 4.3. FT-IR Spectra of one hour at heating 500 ^{o}C Tb doped $Zn_3B_2O_6$ at different concentrations

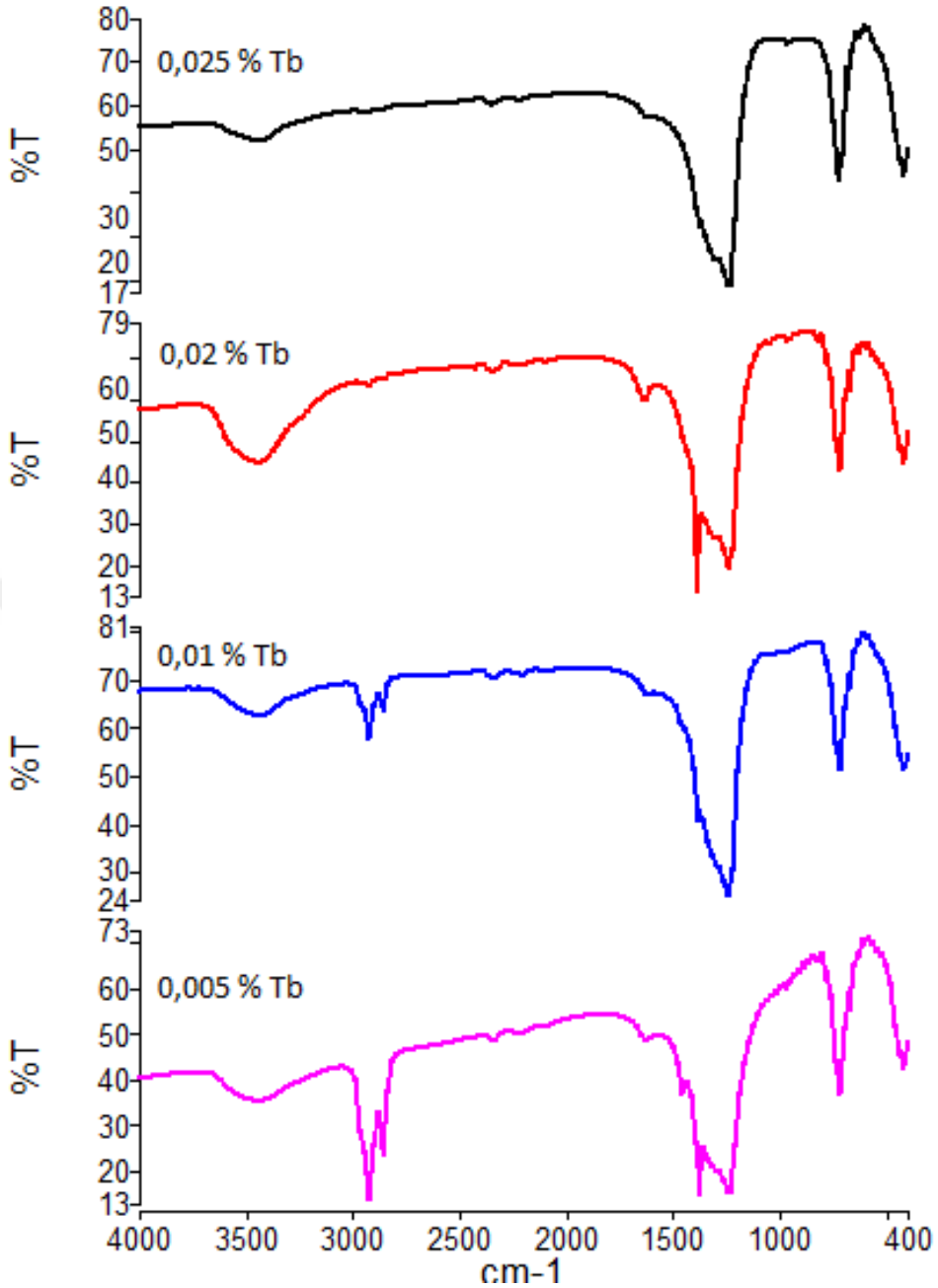

Figure 4.4. FT-IR Spectra of one hour at heating 600 °C Tb doped $Zn_3B_2O_6$ at different concentrations

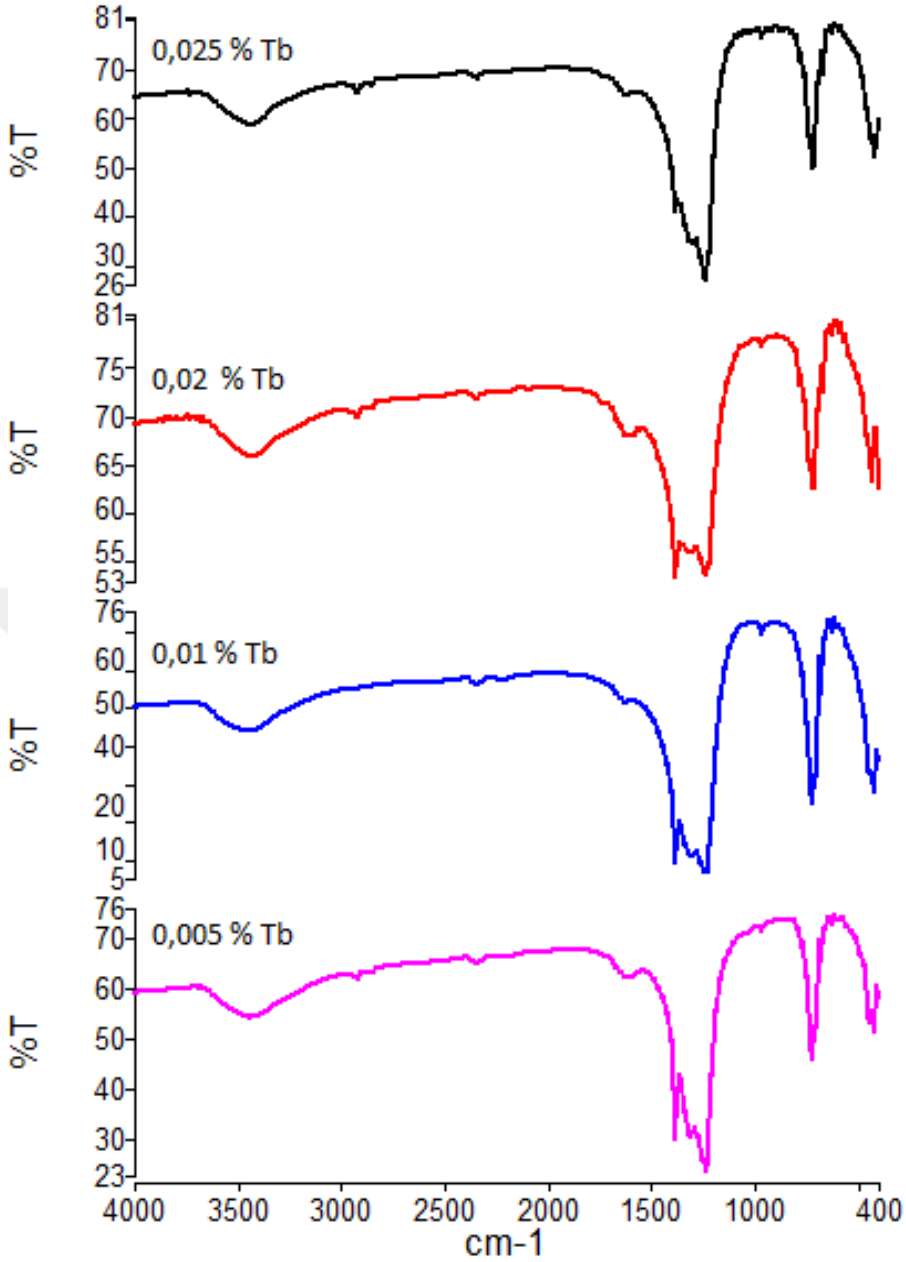

Figure 4.5. FT-IR Spectra of one hour at heating 700 °C Tb doped $Zn_3B_2O_6$ at different concentrations

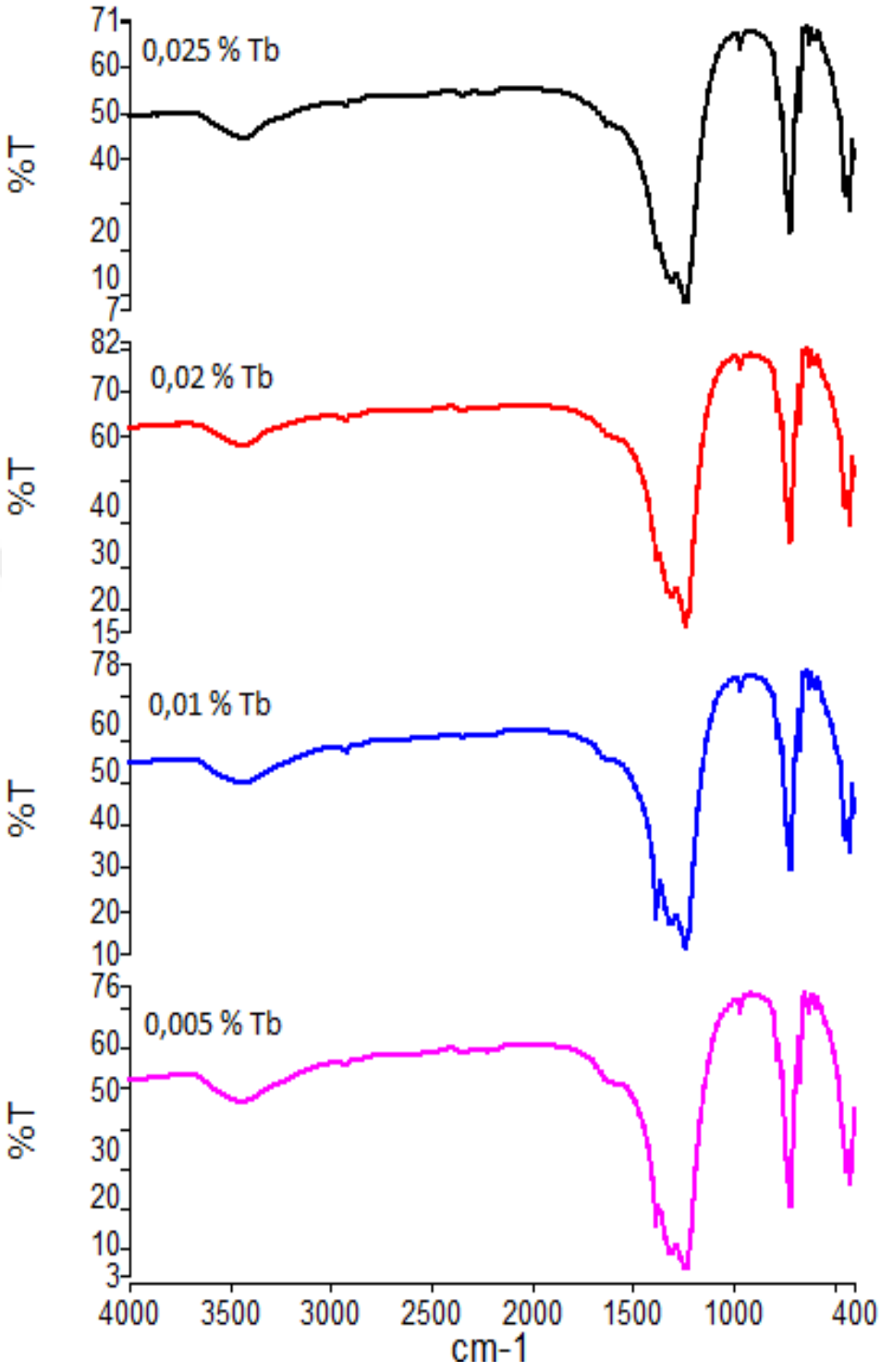

Figure 4.6. FT-IR Spectra of one hour at heating 800 °C Tb doped $Zn_3B_2O_6$ at different concentrations

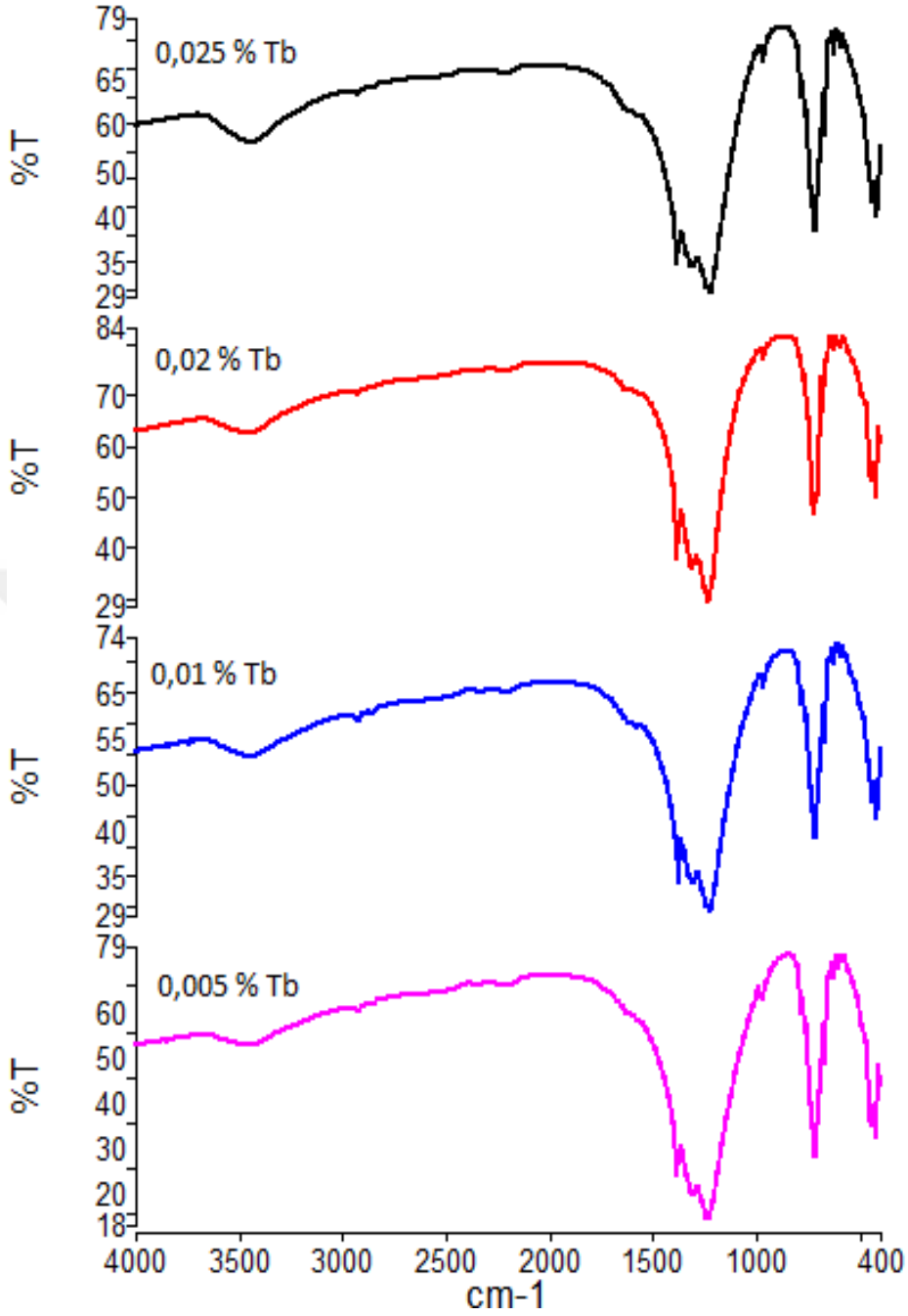

Figure 4.7. FT-IR Spectra of one hour at heating 900 °C Tb doped $Zn_3B_2O_6$ at different concentrations

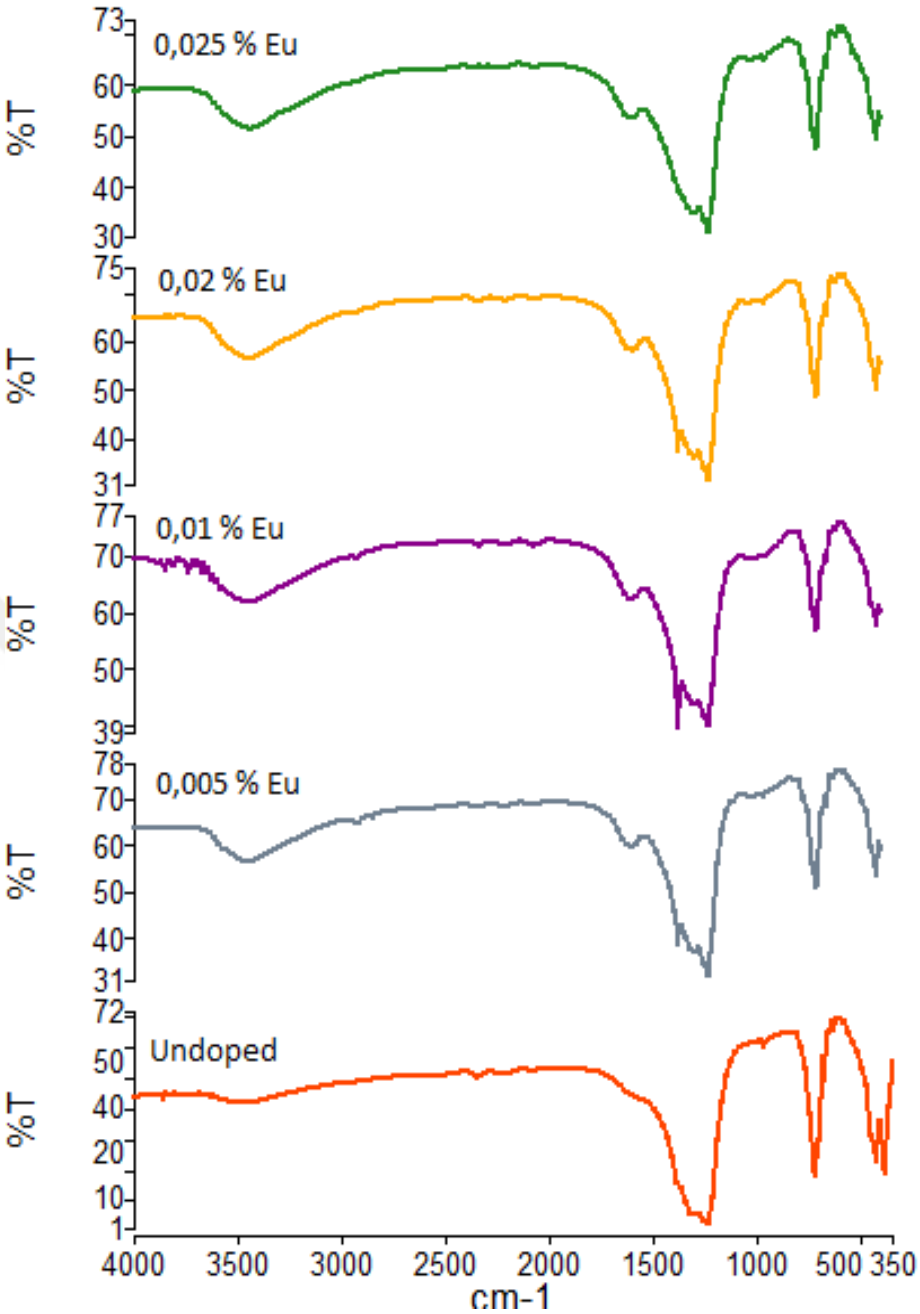

Figure 4.8. FT-IR Spectra of Synthesis Un doped and Eu doped $Zn_3B_2O_6$ at different concentrations.

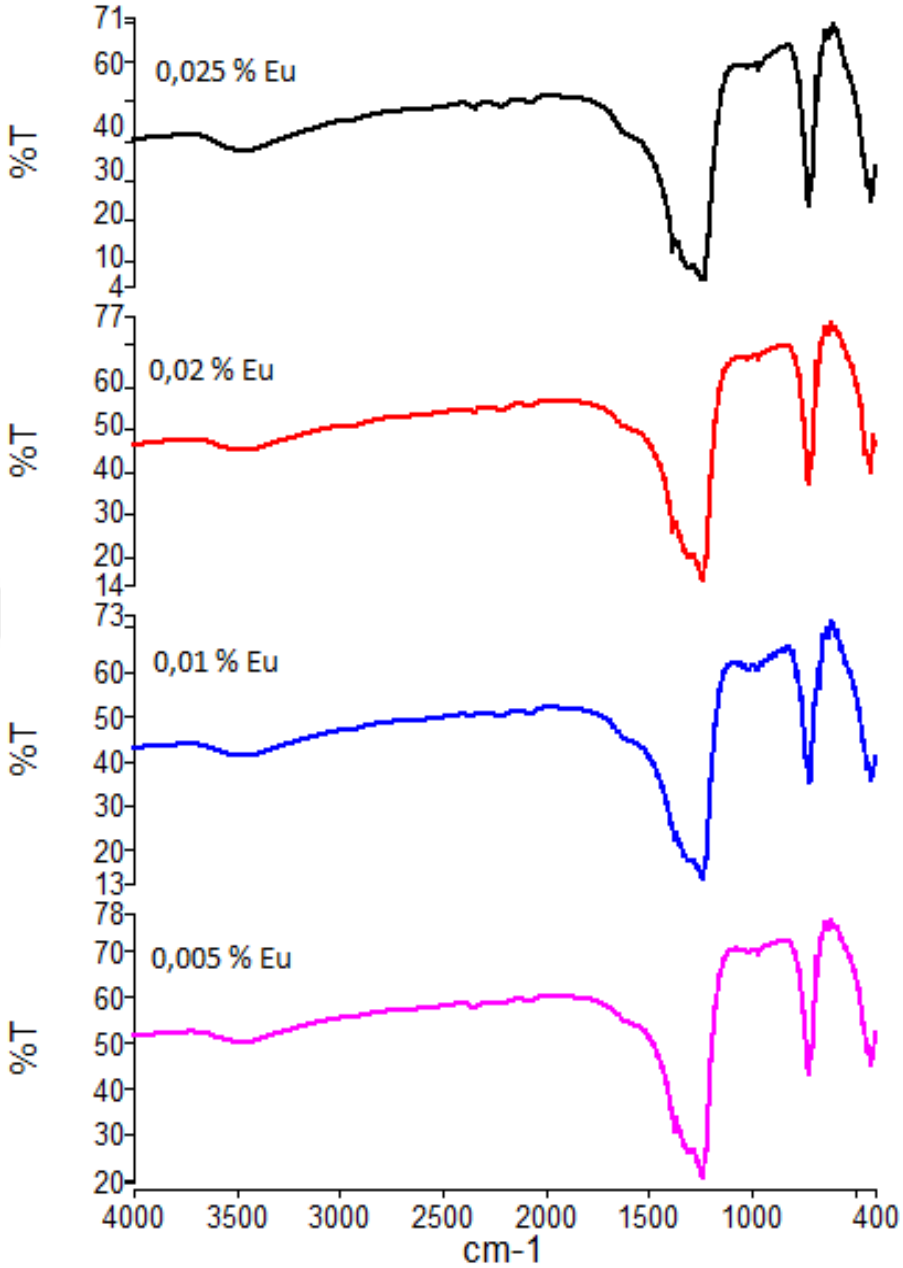

Figure 4.9. FT-IR Spectra of one hour at heating 400 ºC Eu doped $Zn_3B_2O_6$ at different concentrations

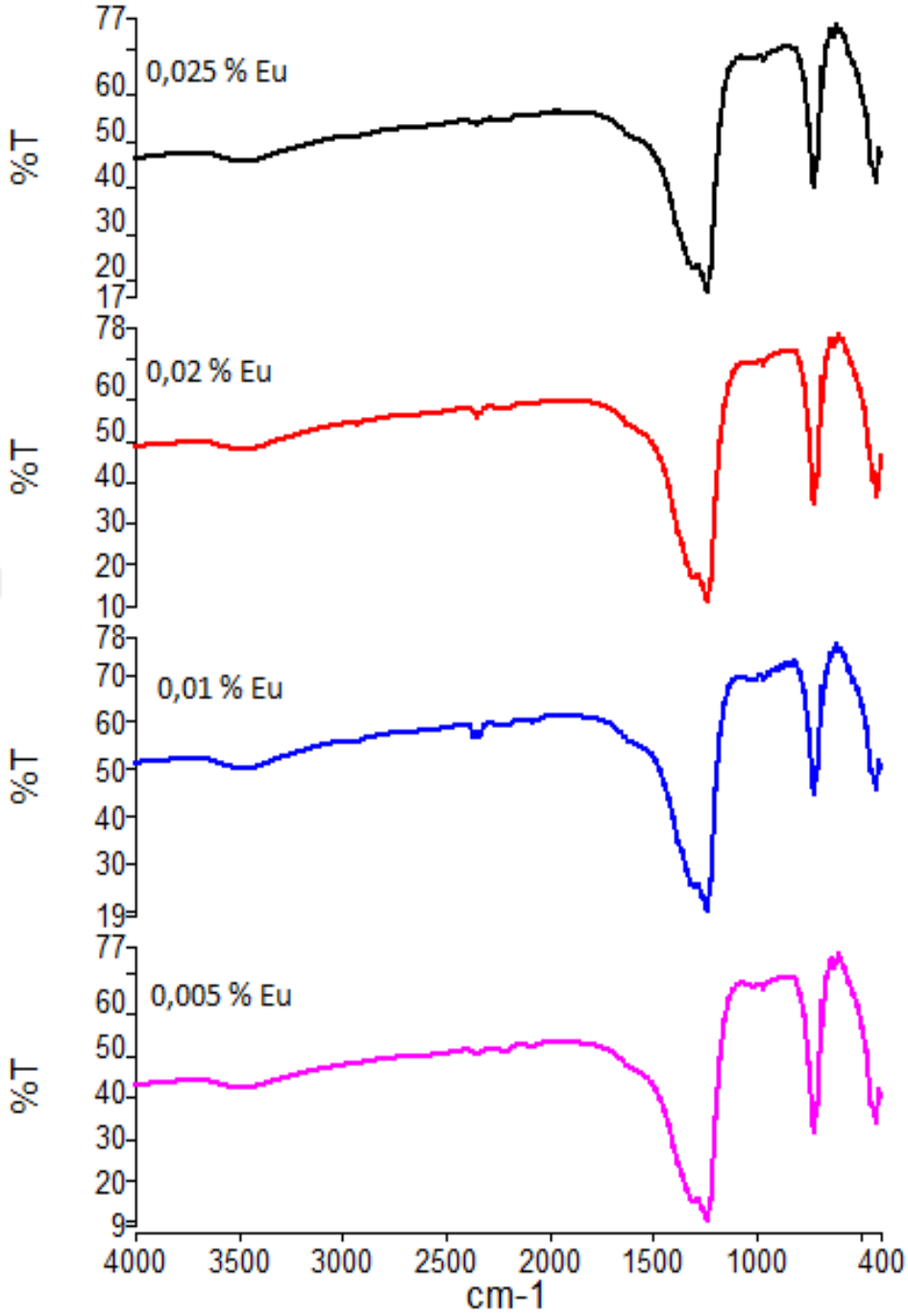

Figure 4.10. FT-IR Spectra of one hour at heating 500 ºC Eu doped $Zn_3B_2O_6$ at different concentrations

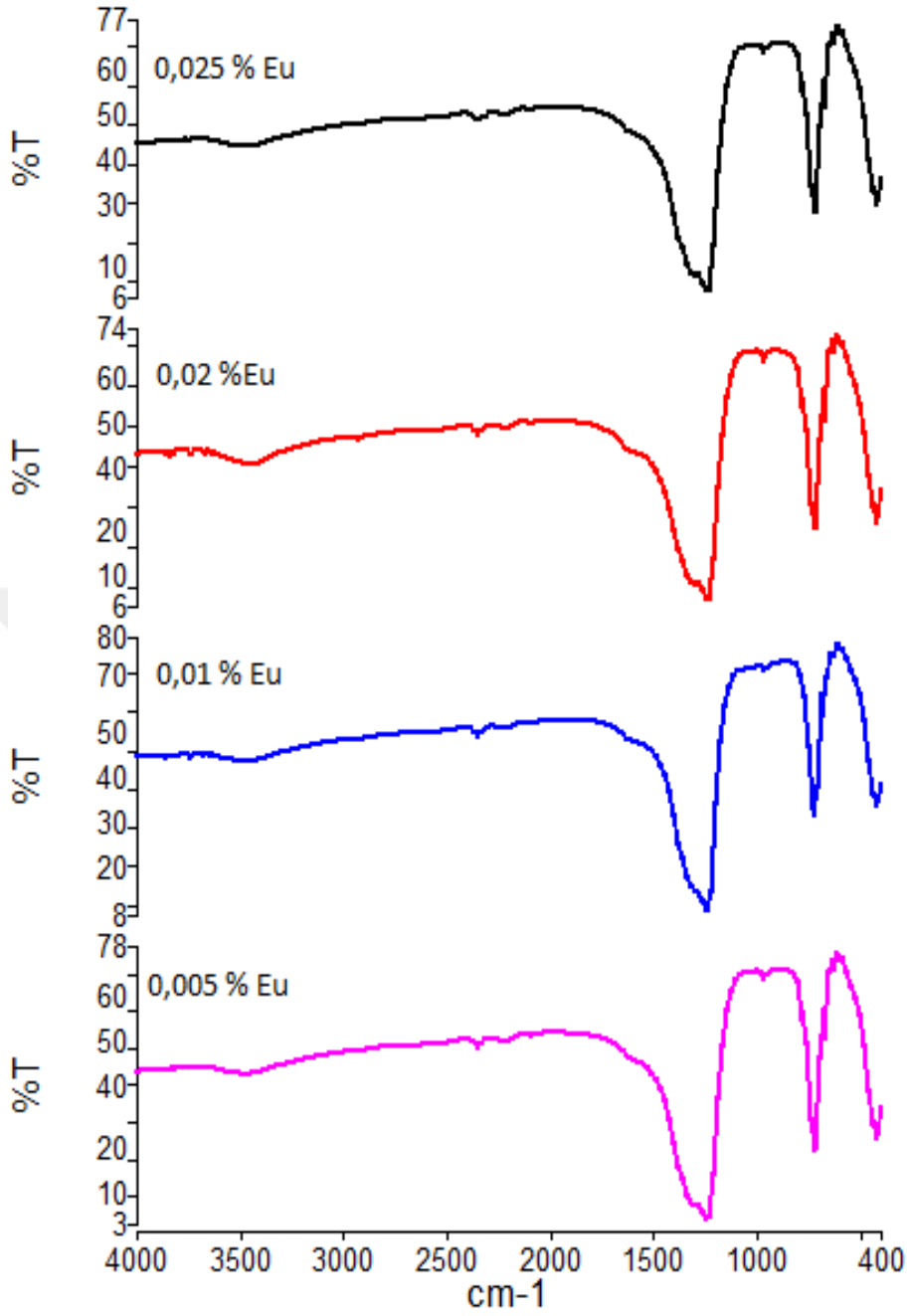

Figure 4.11. FT-IR Spectra of one hour at heating 600 ºC Eu doped $Zn_3B_2O_6$ at different concentrations

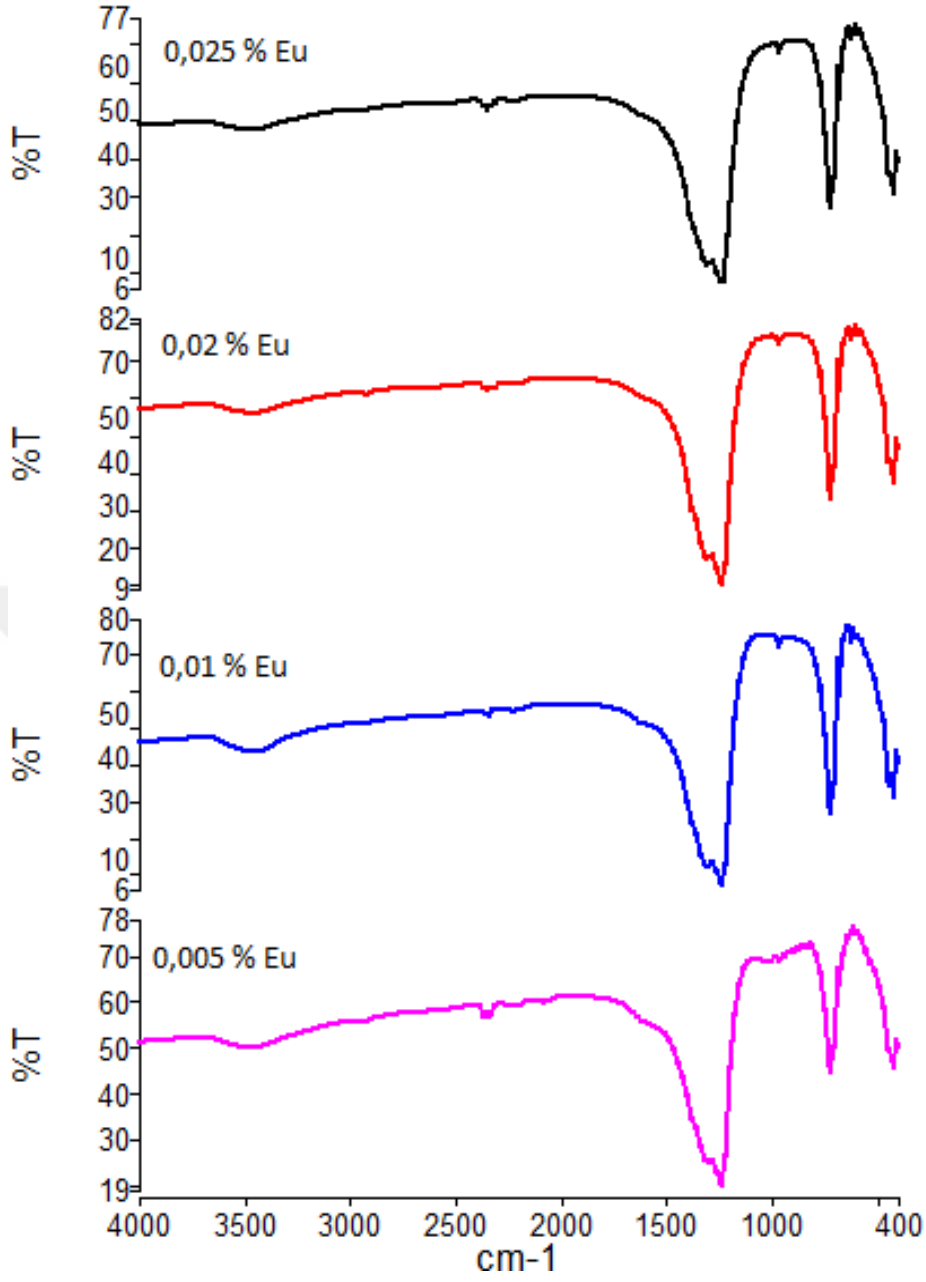

Figure 4.12. FT-IR Spectra of one hour at heating 700 ºC Eu doped $Zn_3B_2O_6$ at different concentrations

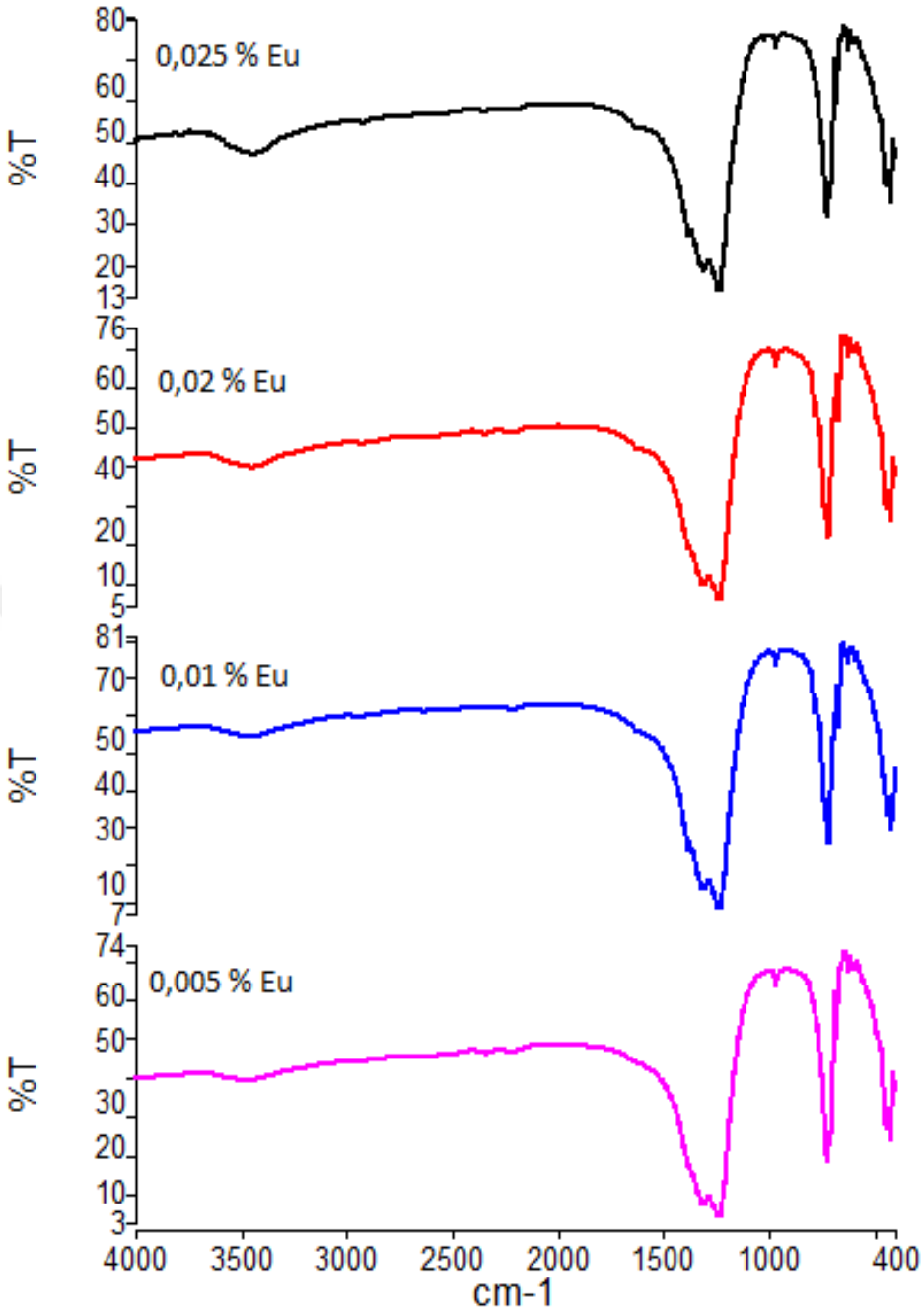

Figure 4.13. FT-IR Spectra of one hour at heating 800 °C Eu doped $Zn_3B_2O_6$ at different concentrations

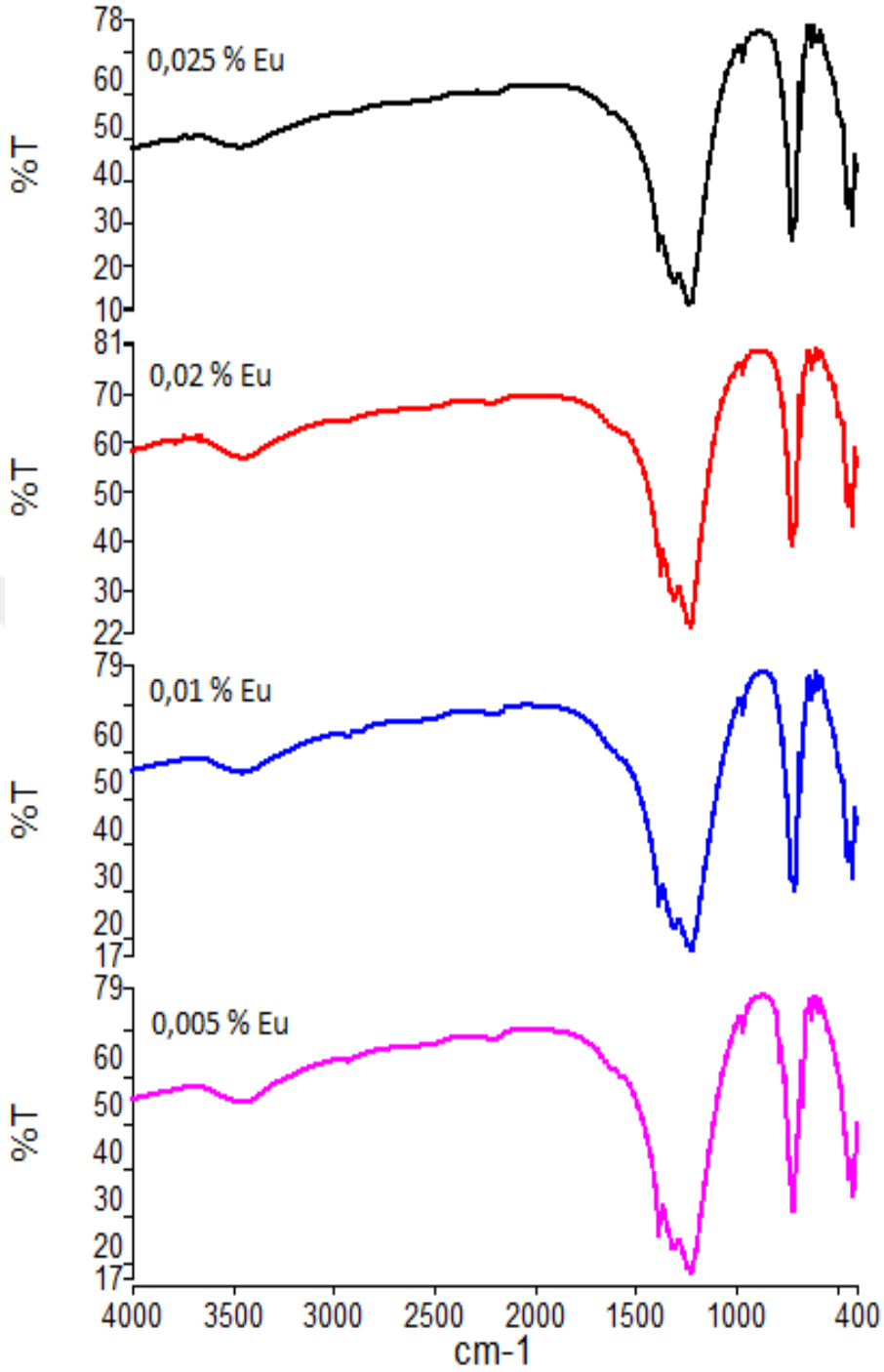

Figure 4.14. FT-IR Spectra of one hour at heating 900 °C Eu doped $Zn_3B_2O_6$ at different concentrations

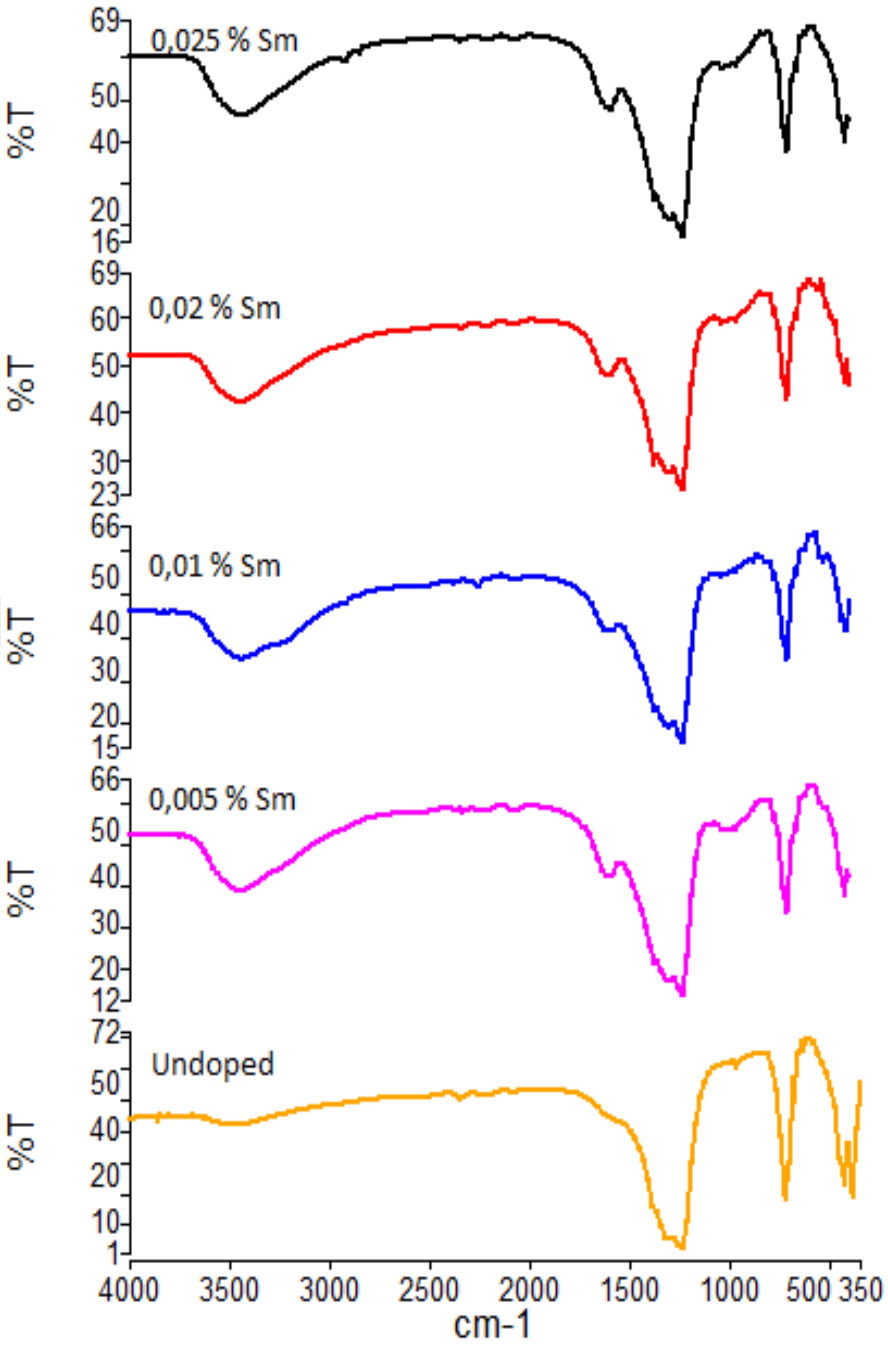

Figure 4.15. FT-IR Spectra of Synthesis Un doped and Sm doped $Zn_3B_2O_6$ at different concentrations

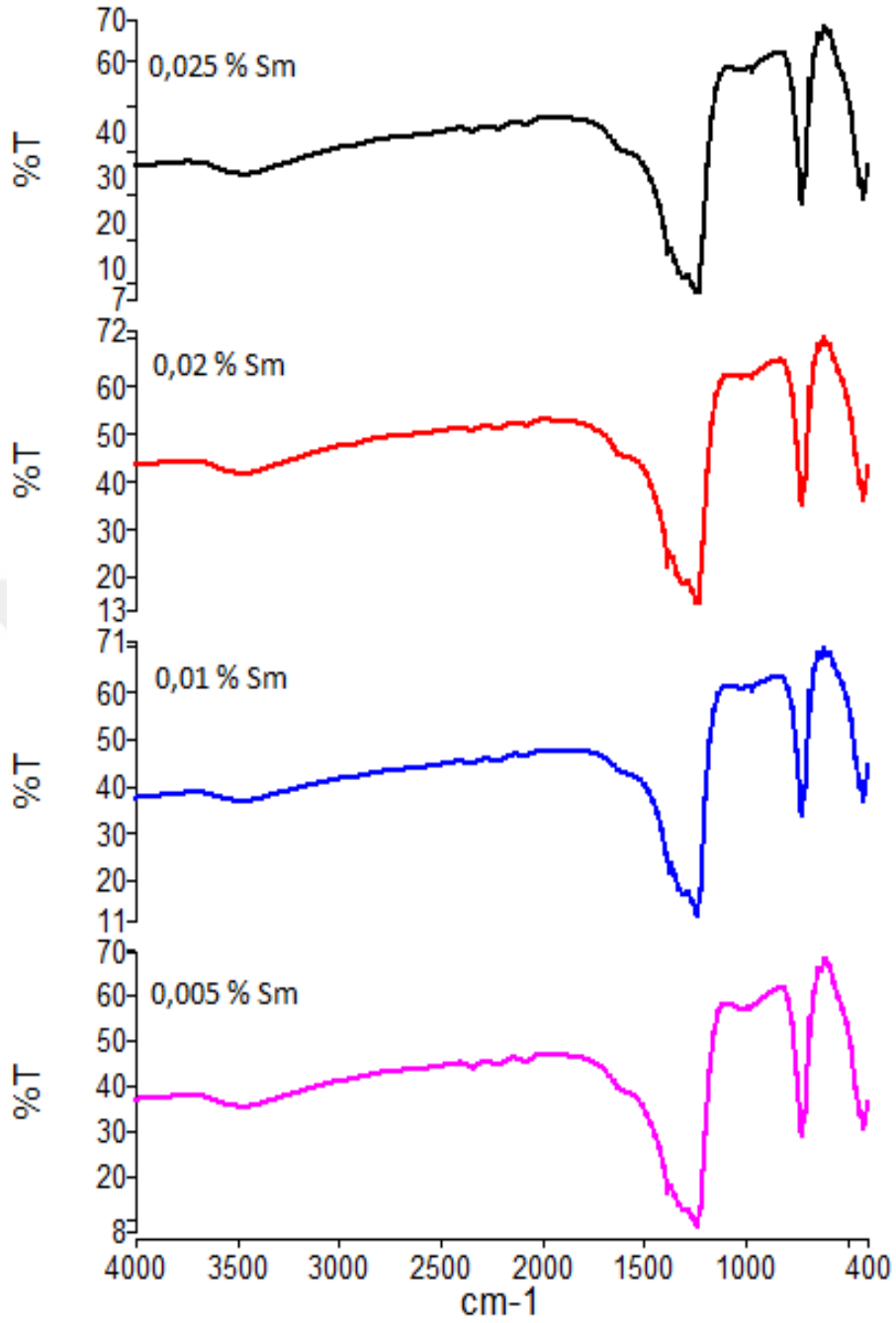

Figure 4.16. FT-IR Spectra of one hour at heating 400 °C Sm doped $Zn_3B_2O_6$ at different concentrations

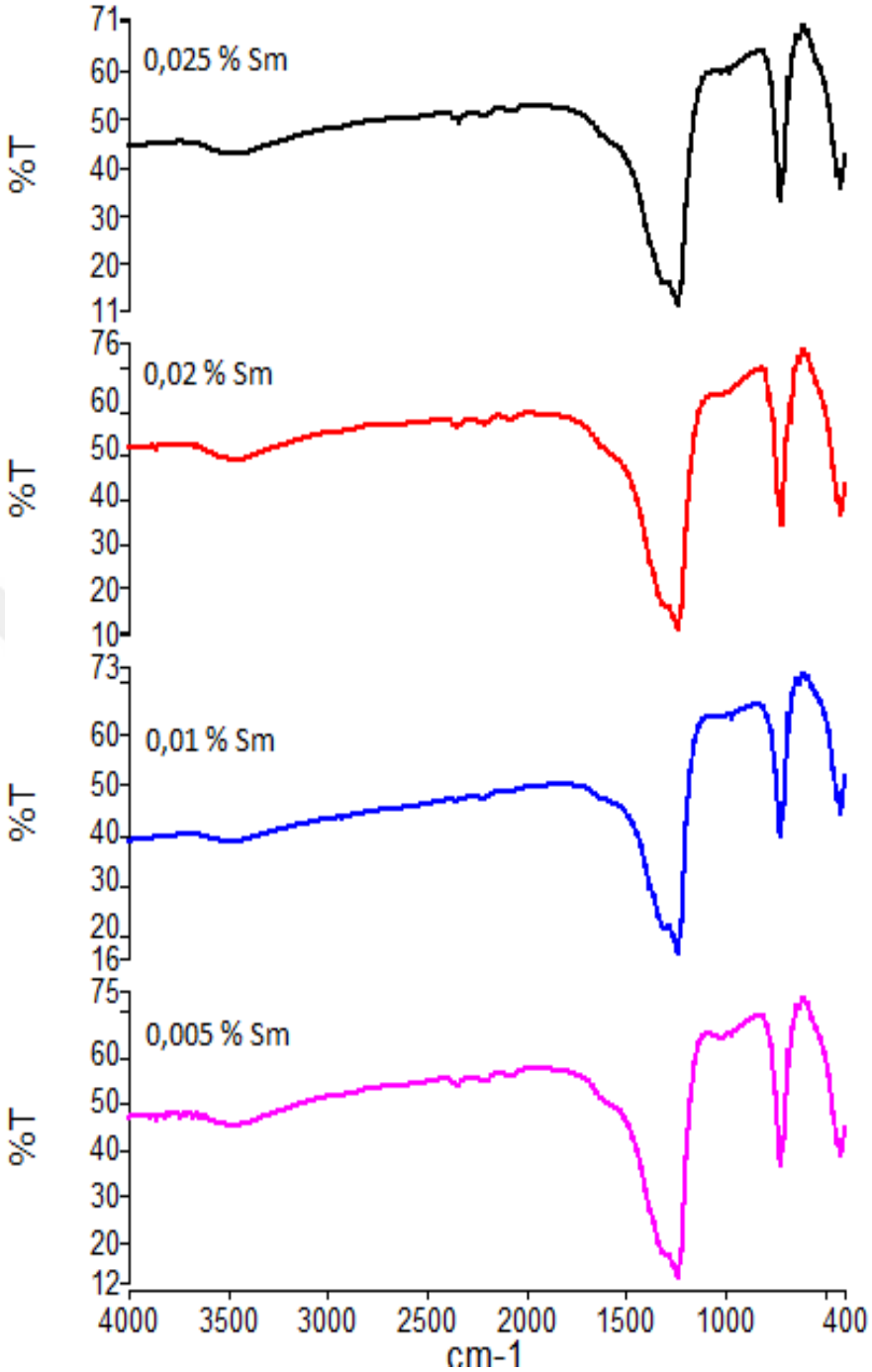

Figure 4.17. FT-IR Spectra of one hour at heating 500 °C Sm doped $Zn_3B_2O_6$ at different concentrations

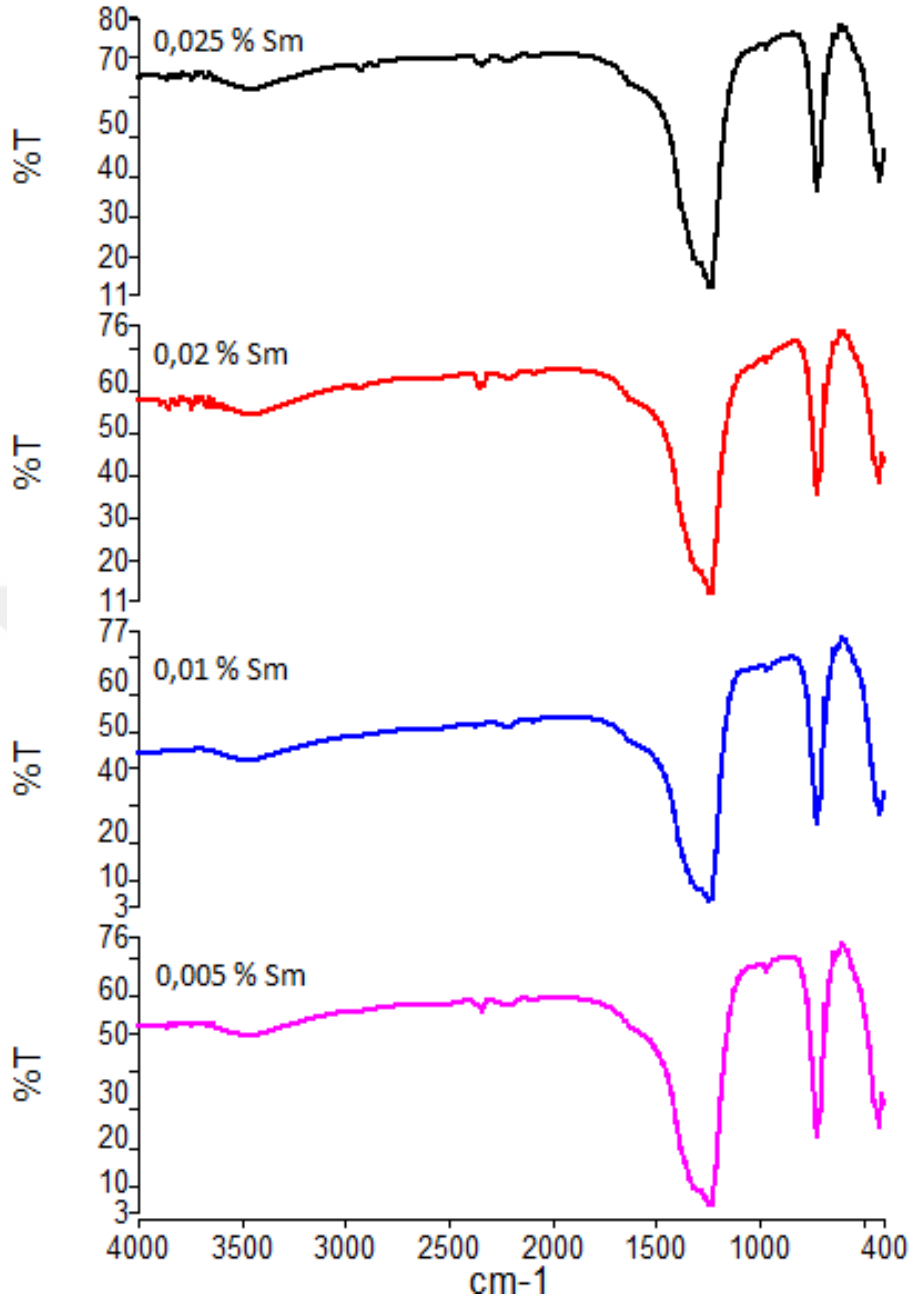

Figure 4.18. FT-IR Spectra of one hour at heating 600 ºC Sm doped $Zn_3B_2O_6$ at different concentrations

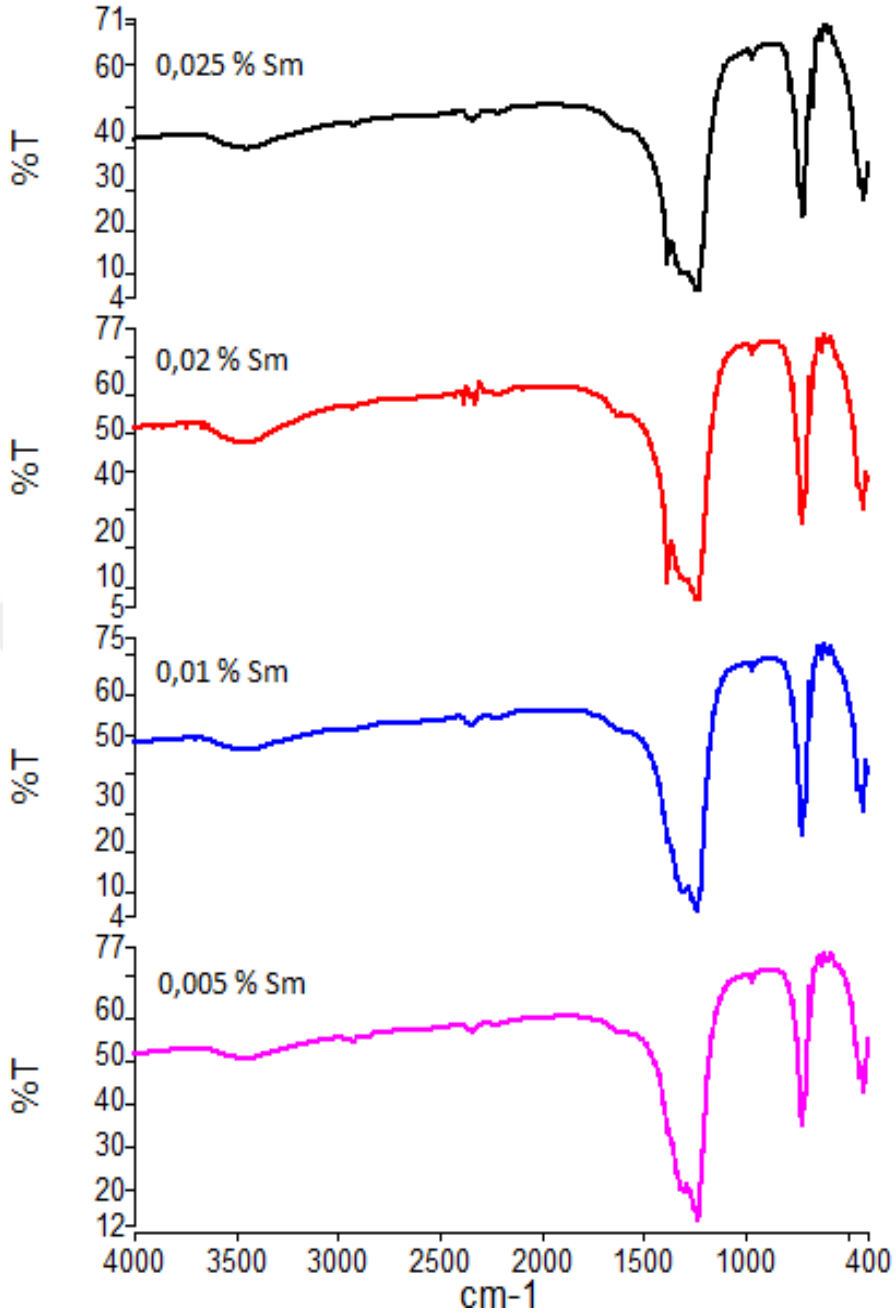

Figure 4.19. FT-IR Spectra of one hour at heating 700 °C Sm doped $Zn_3B_2O_6$ at different concentrations

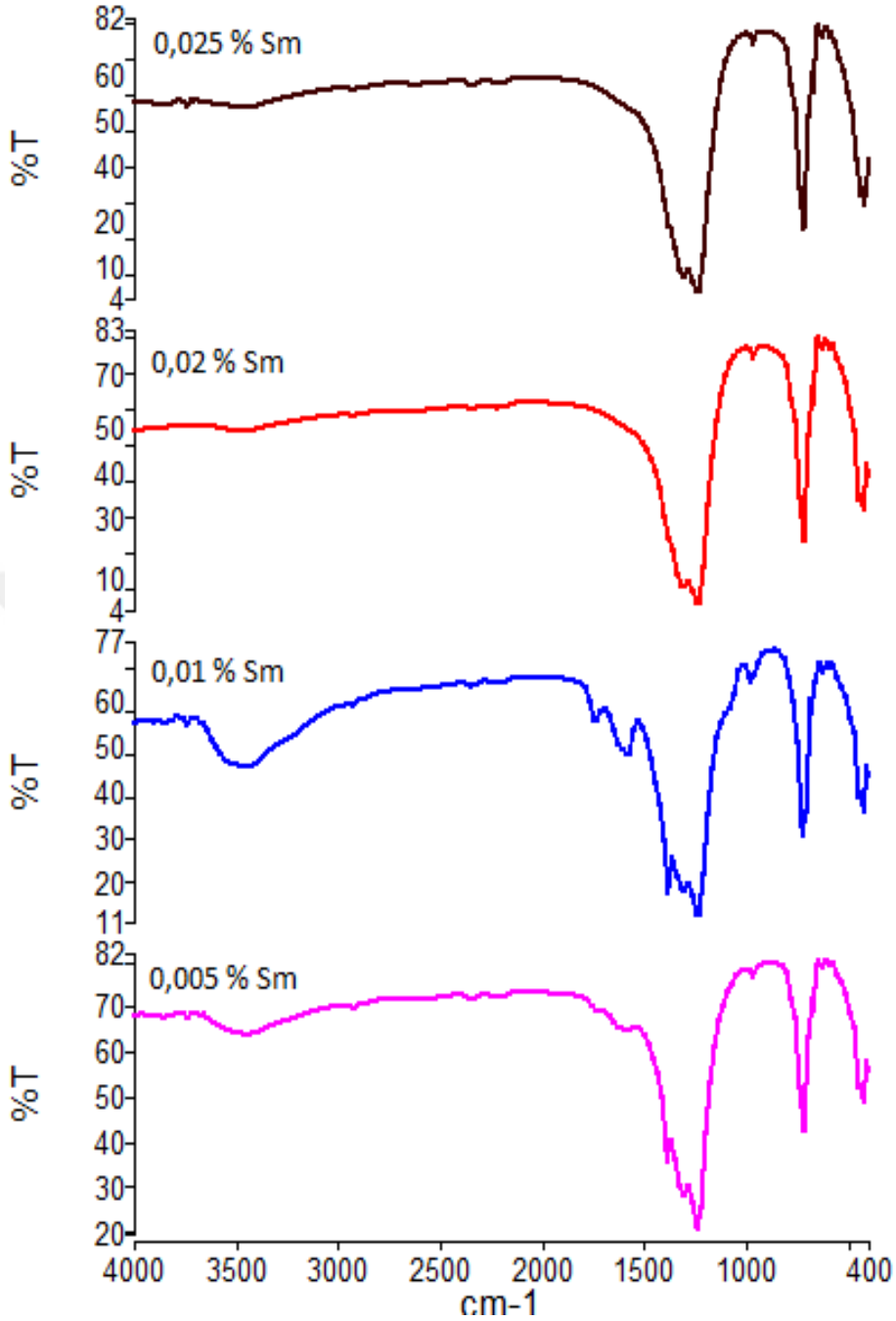

Figure 4.20. FT-IR Spectra of one hour at heating 800 °C Sm doped $Zn_3B_2O_6$ at different concentrations

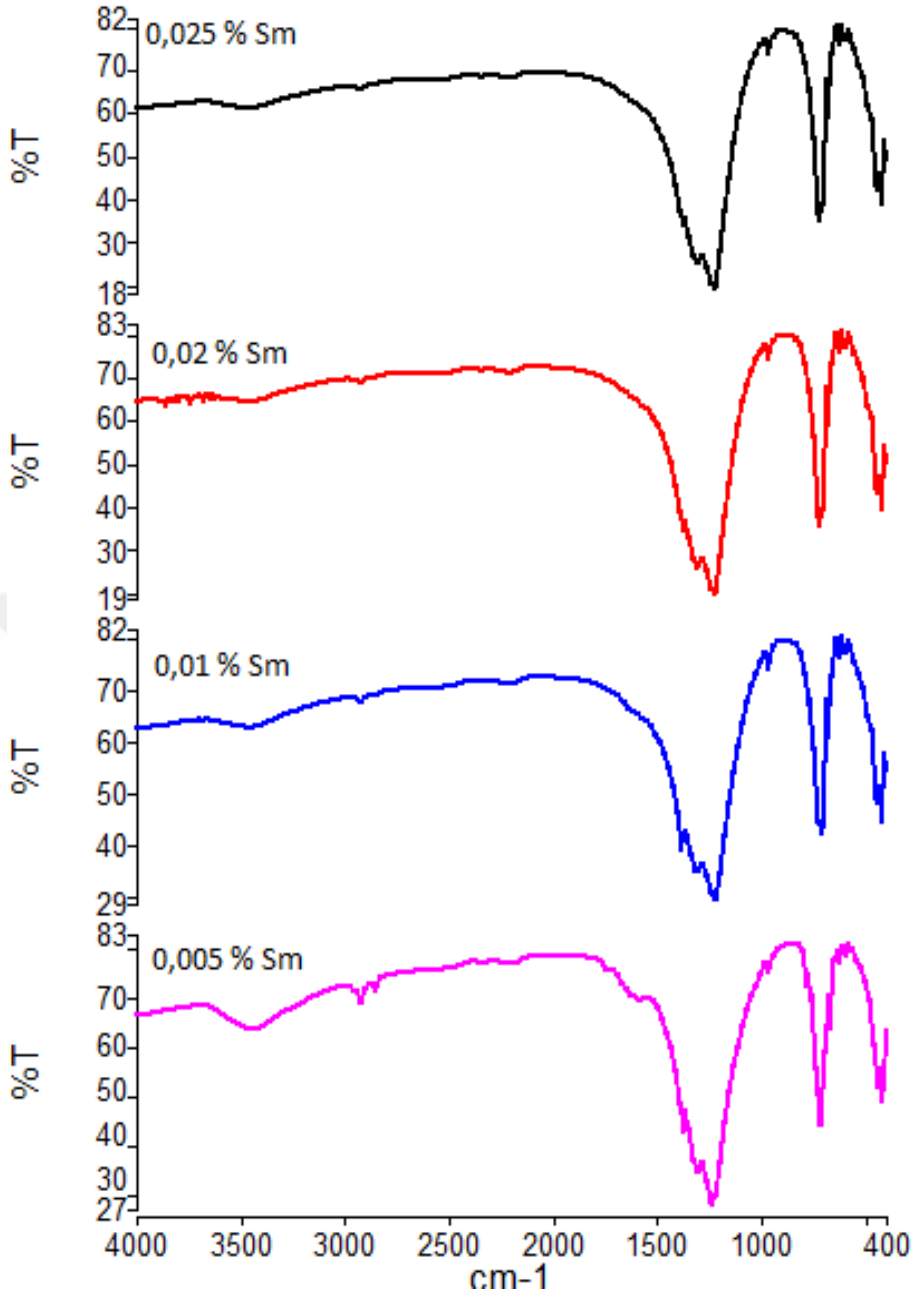

Figure 4.21. FT-IR Spectra of one hour at heating 900 °C Sm doped $Zn_3B_2O_6$ at different concentrations

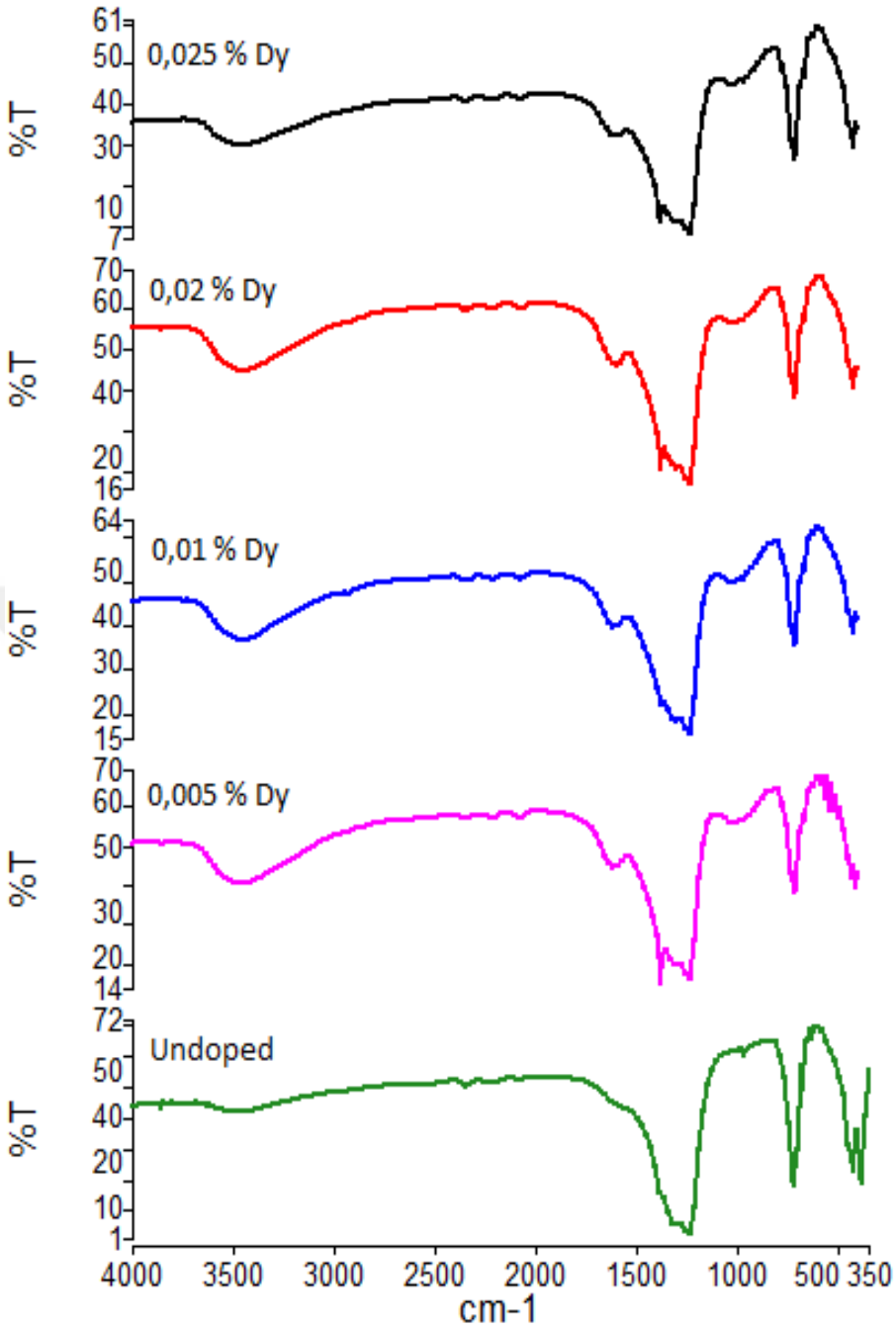

Figure 4.22. FT-IR Spectra of Synthesis Un doped and Dy doped $Zn_3B_2O_6$ at different concentrations

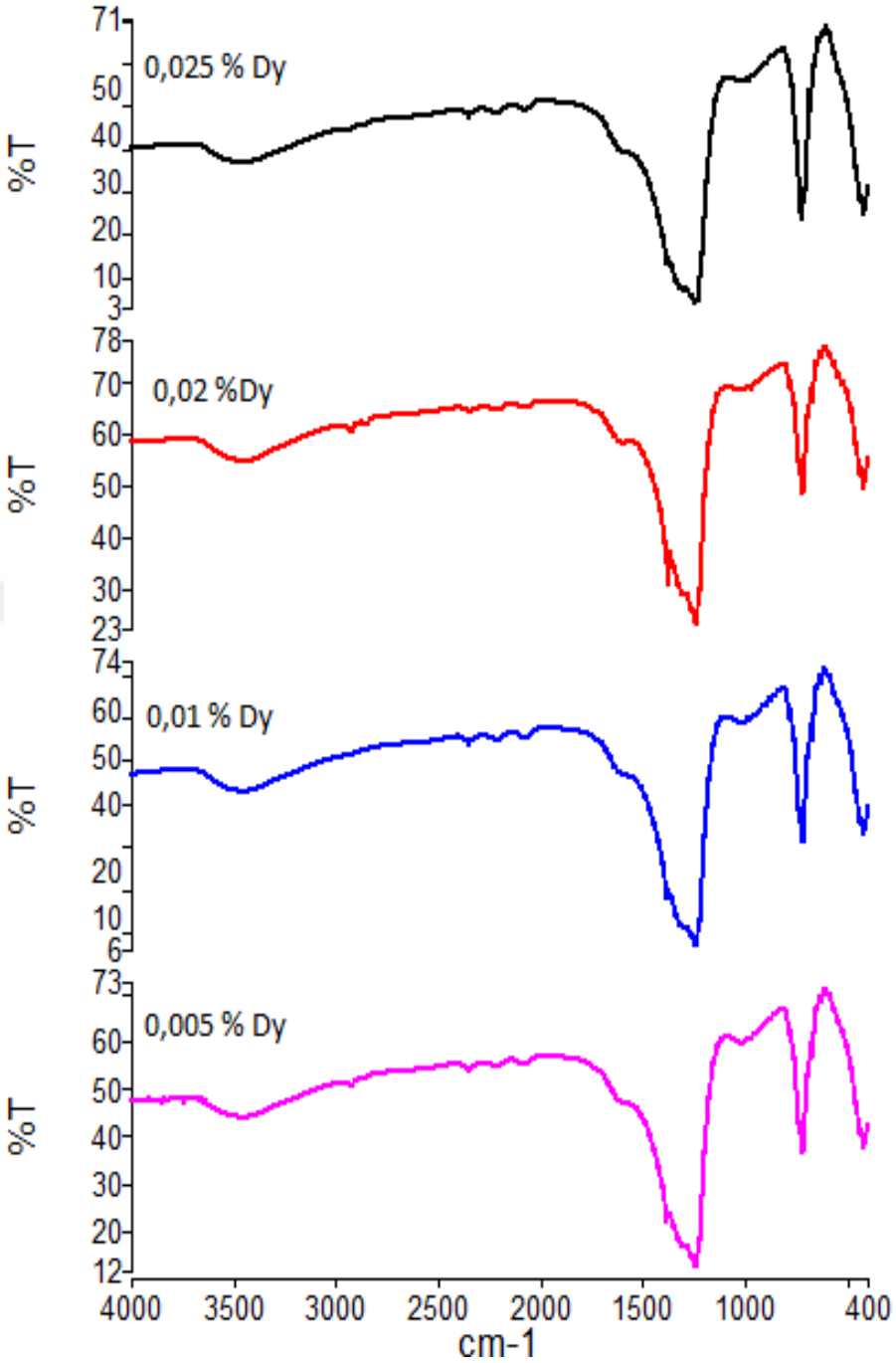

Figure 4.23. FT-IR Spectra of one hour at heating 400 ^{o}C Dy doped $Zn_3B_2O_6$ at different concentrations

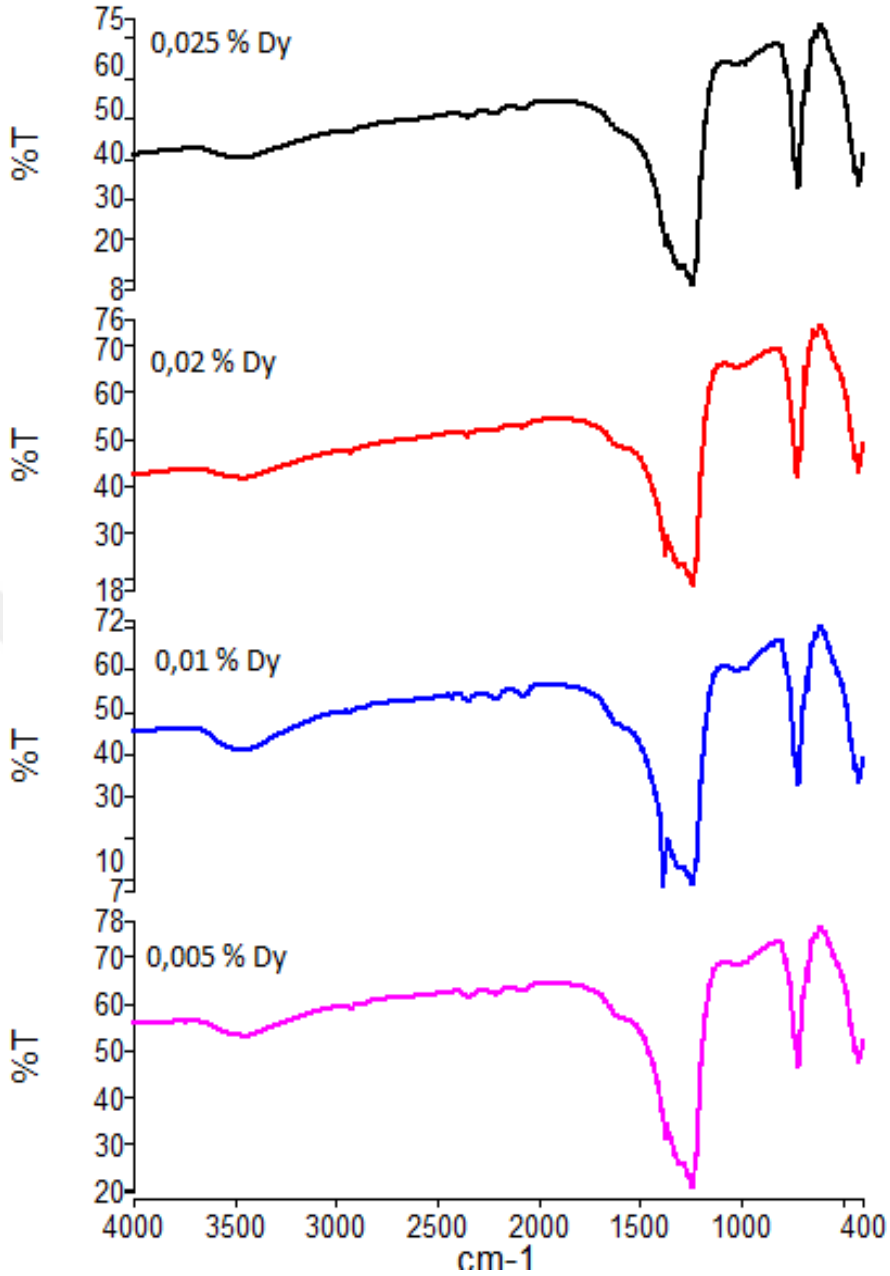

Figure 4.24. FT-IR Spectra of one hour at heating 500 °C Dy doped $Zn_3B_2O_6$ at different concentrations

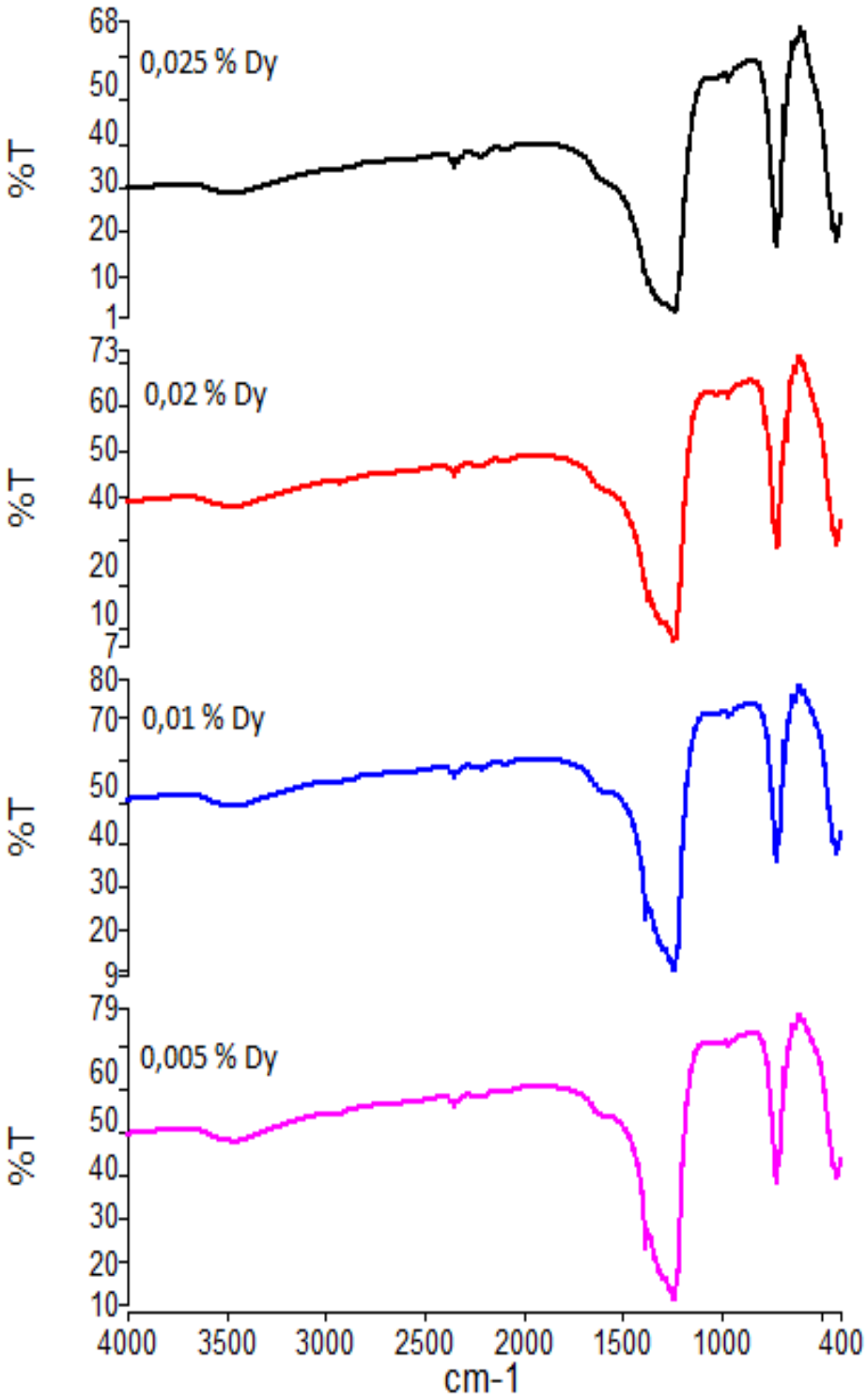

Figure 4.25. FT-IR Spectra of one hour at heating 600 °C Dy doped $Zn_3B_2O_6$ at different concentrations

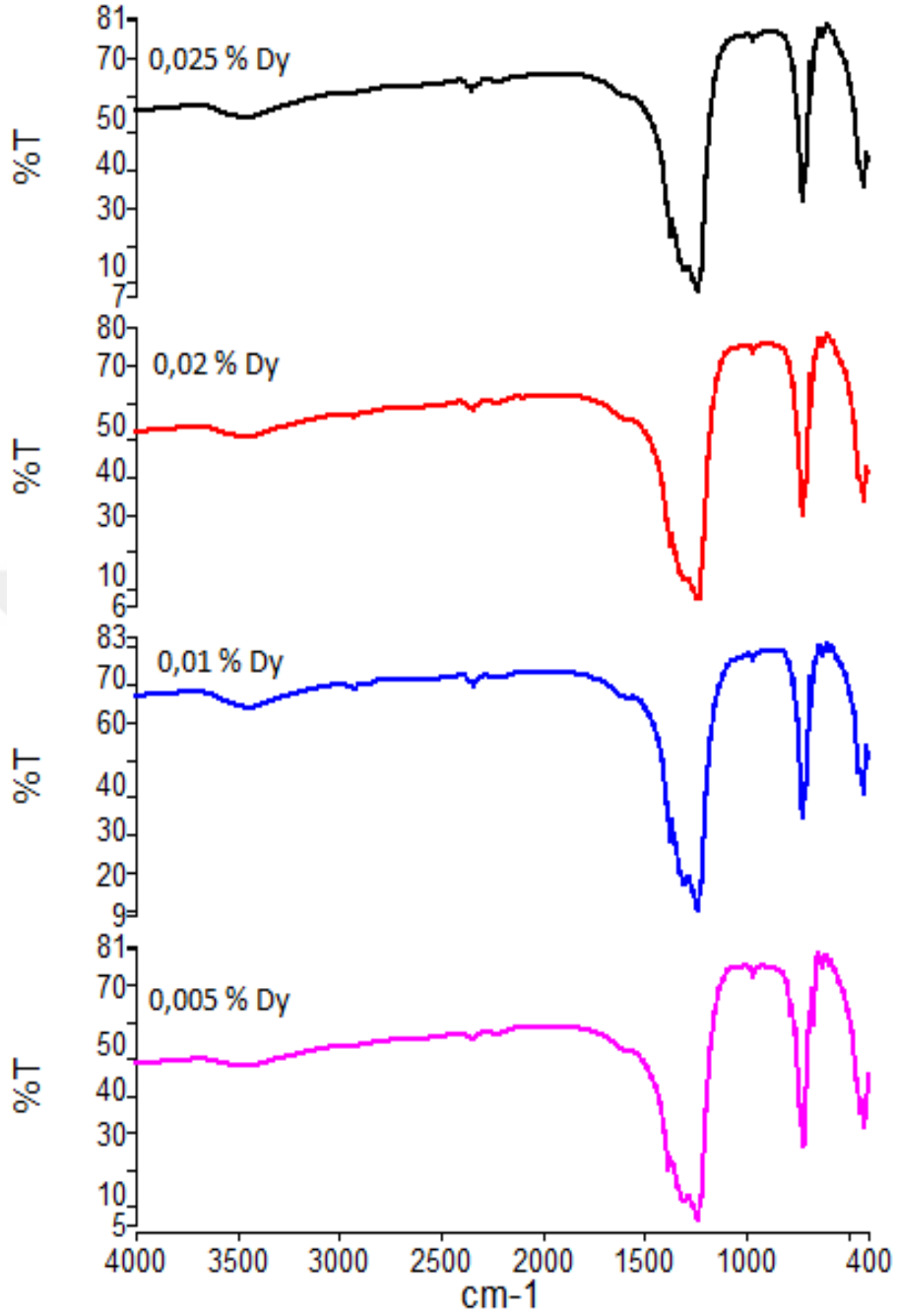

Figure 4.26. FT-IR Spectra of one hour at heating 700 °C Dy doped $Zn_3B_2O_6$ at different concentrations

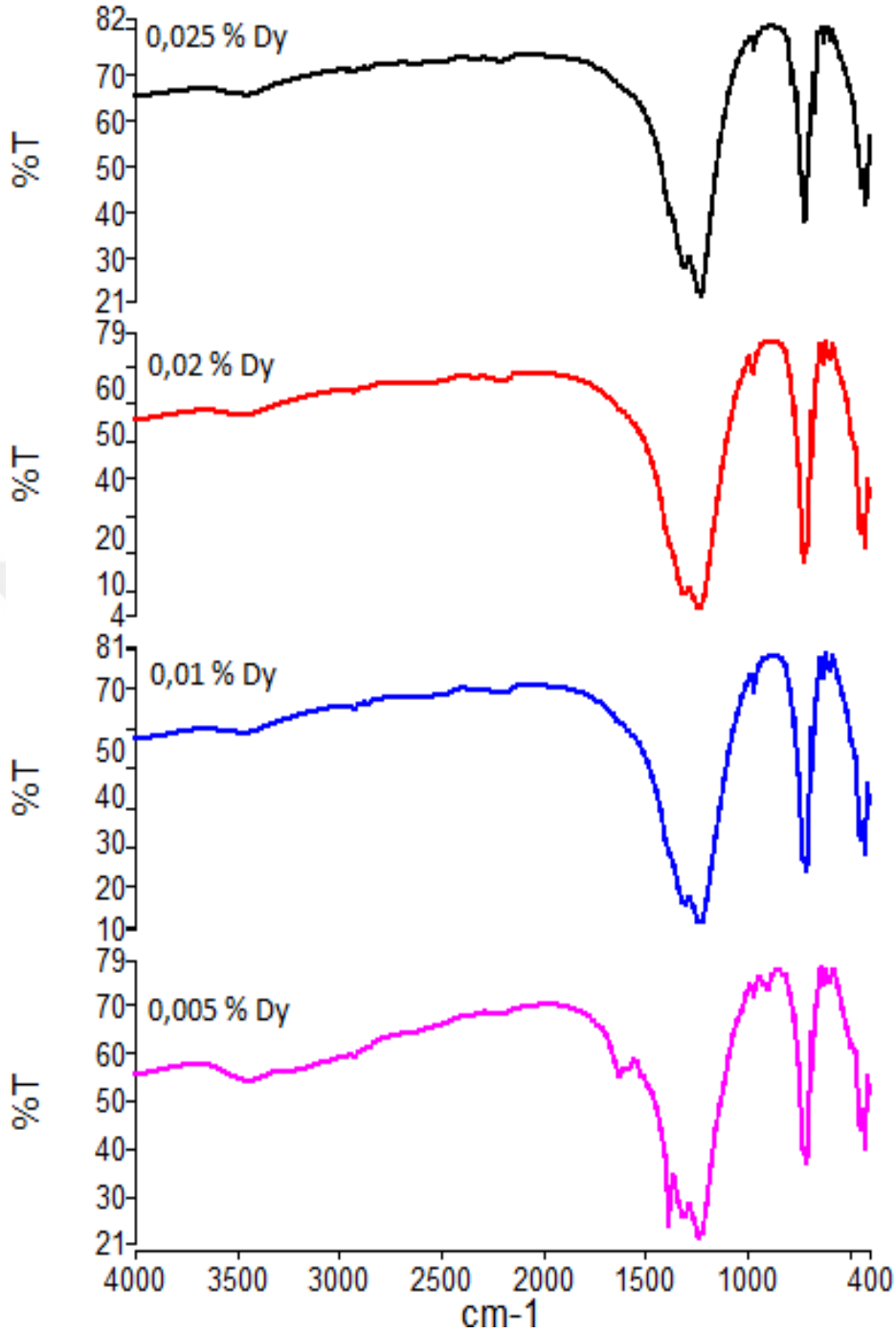

Figure 4.27. FT-IR Spectra of one hour at heating 800 ºC Dy doped $Zn_3B_2O_6$ at different concentrations

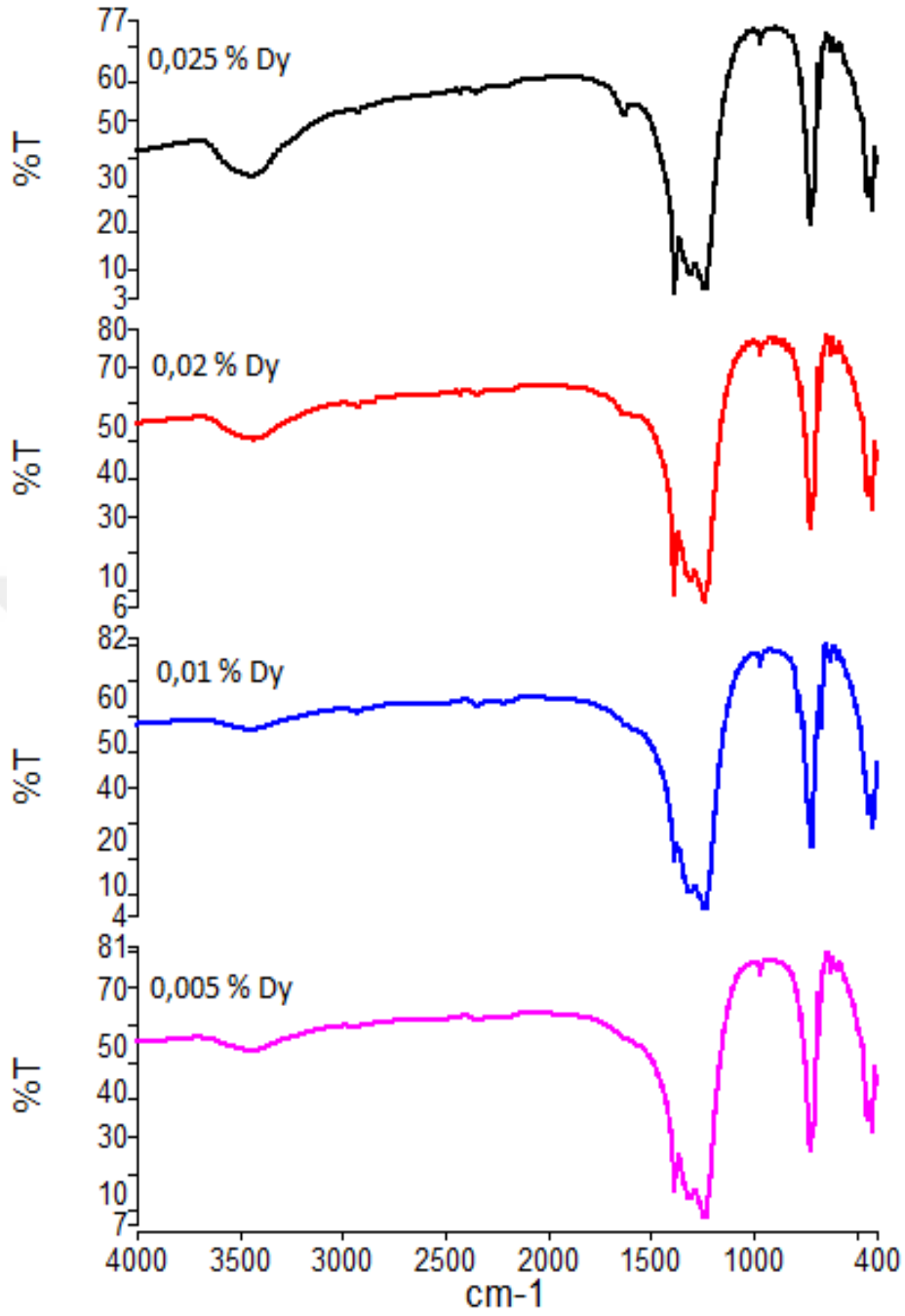

Figure 4.28. FT-IR Spectra of one hour at heating 900 ºC Dy doped $Zn_3B_2O_6$ at different concentrations

In the FTIR spectrum, BO_3 group is triangular, the vibrations are in the area of ν3 = 1100–1400 cm−1 which assigned to B–O asymmetric stretch, the band 33 at ν2 = 700–900 cm−1 is contributed to out-of-plane bend, where the one at ν1 = 900–1000 cm−1 belongs to the B–O symmetric stretch. The band at around 600 cm−1 is appointed to stretching vibration of Zn–O.In the figure 4.1-figure 4.28 shown $Zn_3B_2O_6$ different dopes at 400 ºC 500 ºC 600 ºC 700 ºC and 800 °C and 900 ºC

4.3. X-Ray Diffraction (XRD) Studies

The synthesis of zinc orthoborate, $Zn_3B_2O_6$ with glycine and different lanthanide elements (Eu^{3+}, Dy^{3+}, Sm^{3+} and Tb^{3+}) in different concentrations were carried out. The structural properties of the synthesized and heated compounds were examined with XRD technique. First of all, undoped zinc borate was synthesized and its XRD patterns was shown in Figure 4.27.

Figure 4.28 to figure 4.36 shown one hour heating 400°C and 900 °C $Zn_3B_2O_6$ Tb,Eu,Sm and Dy doped at different concentrations.

The synthesized zinc borates were done by comparing International Center for Diffraction Data (ICDD) cards with PXRD patterns for the characteristic reflections. The X-ray powder diffraction patterns of the synthesis zinc borates are like to that of ß- $Zn_3B_2O_6$ zinc borate formation given in the ICDD card No 74-1099.(50)

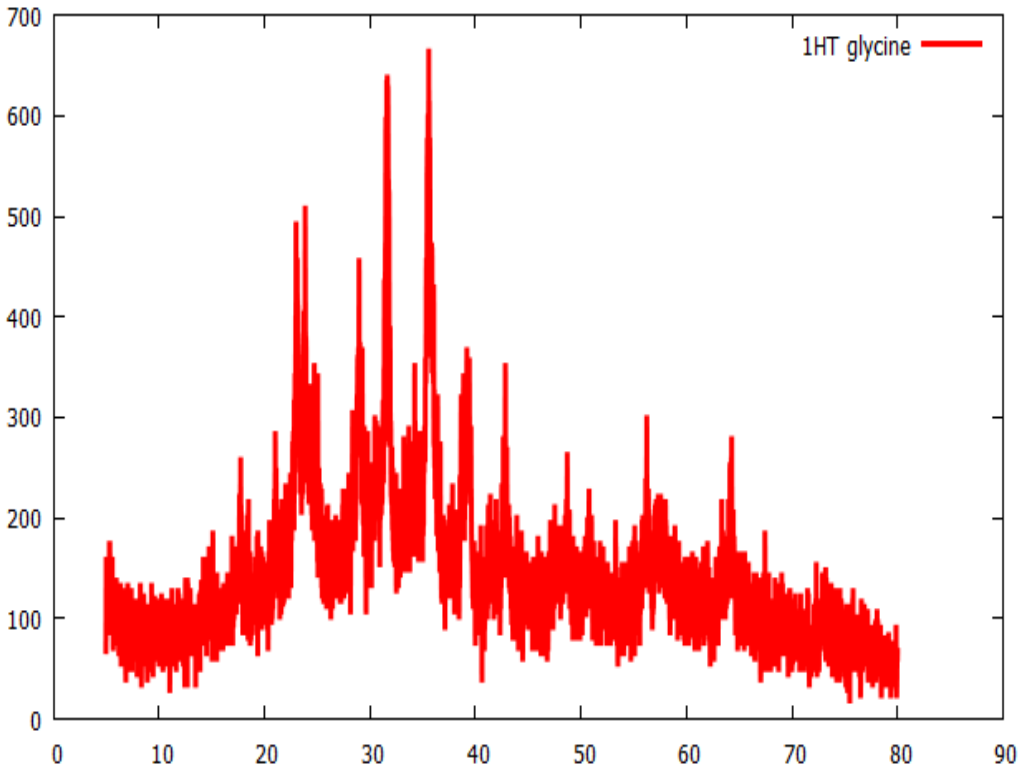

Figure 4.29. XRD Patterns of Synthesis of Zinc Orthoborate

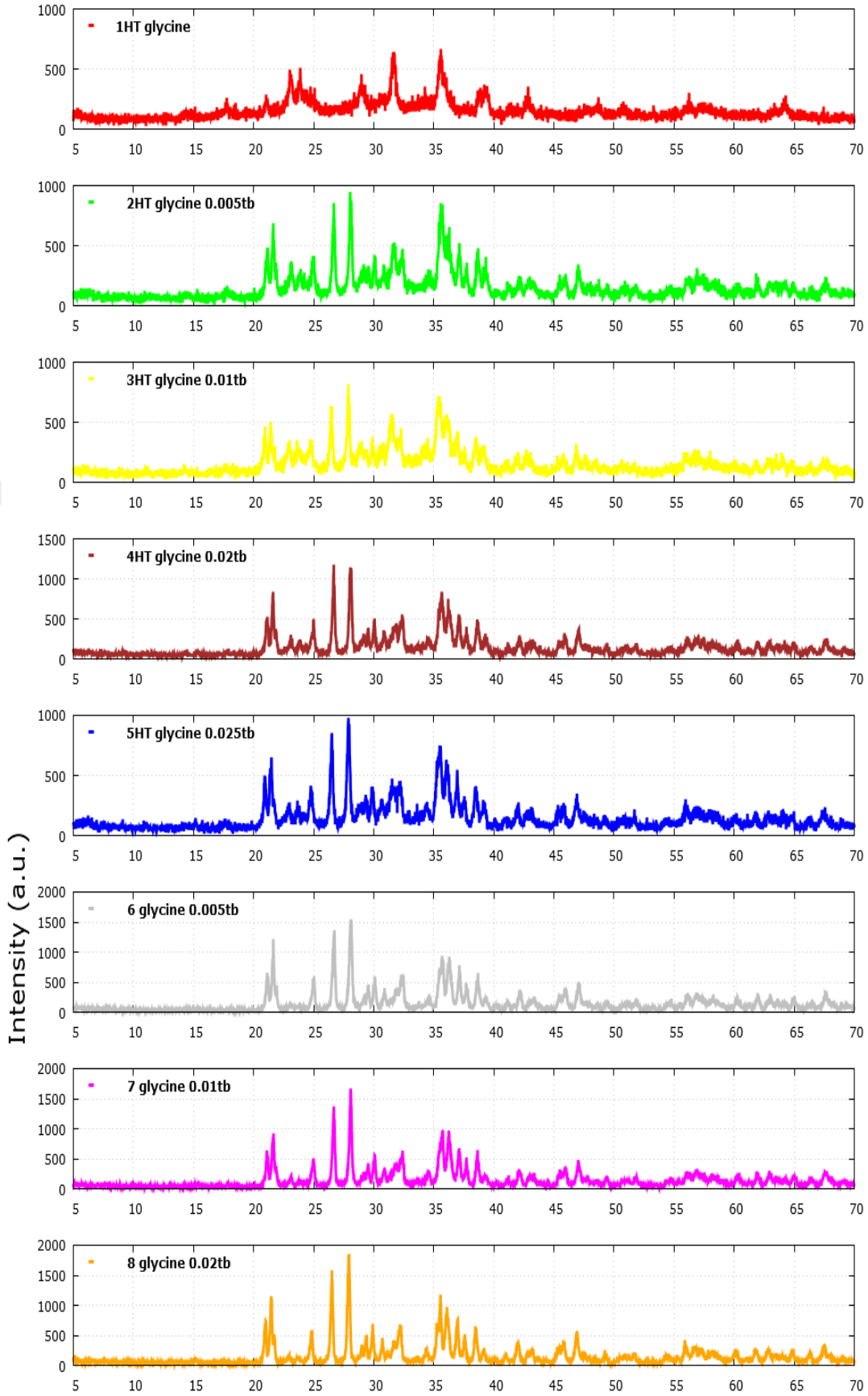

Figure 4.30. XRD Patterns of Synthesis different concentrations Tb doped $Zn_3B_2O_6$

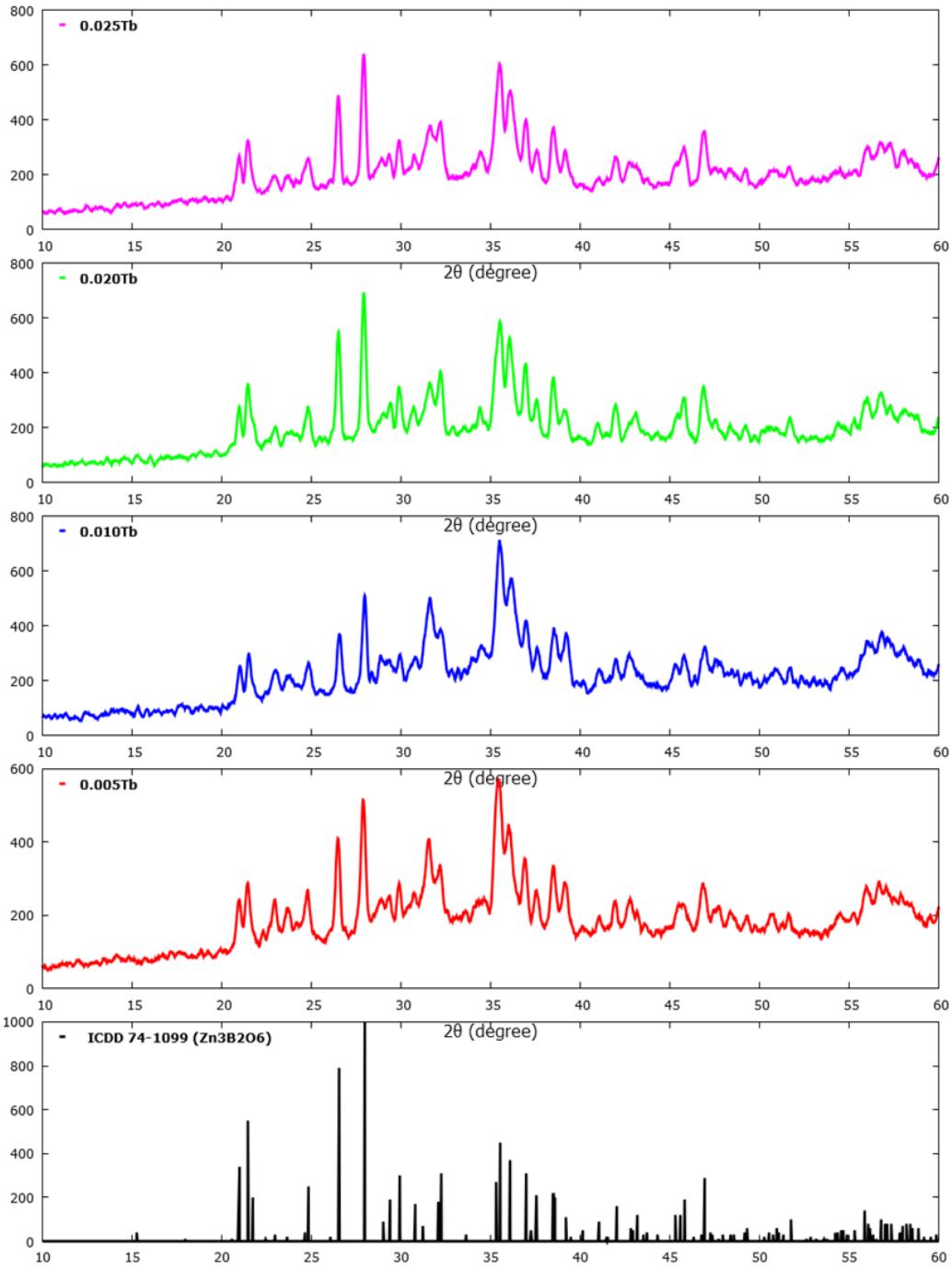

Figure 4.31. XRD Patterns of Tb doped $Zn_3B_2O_6$ at 400°C

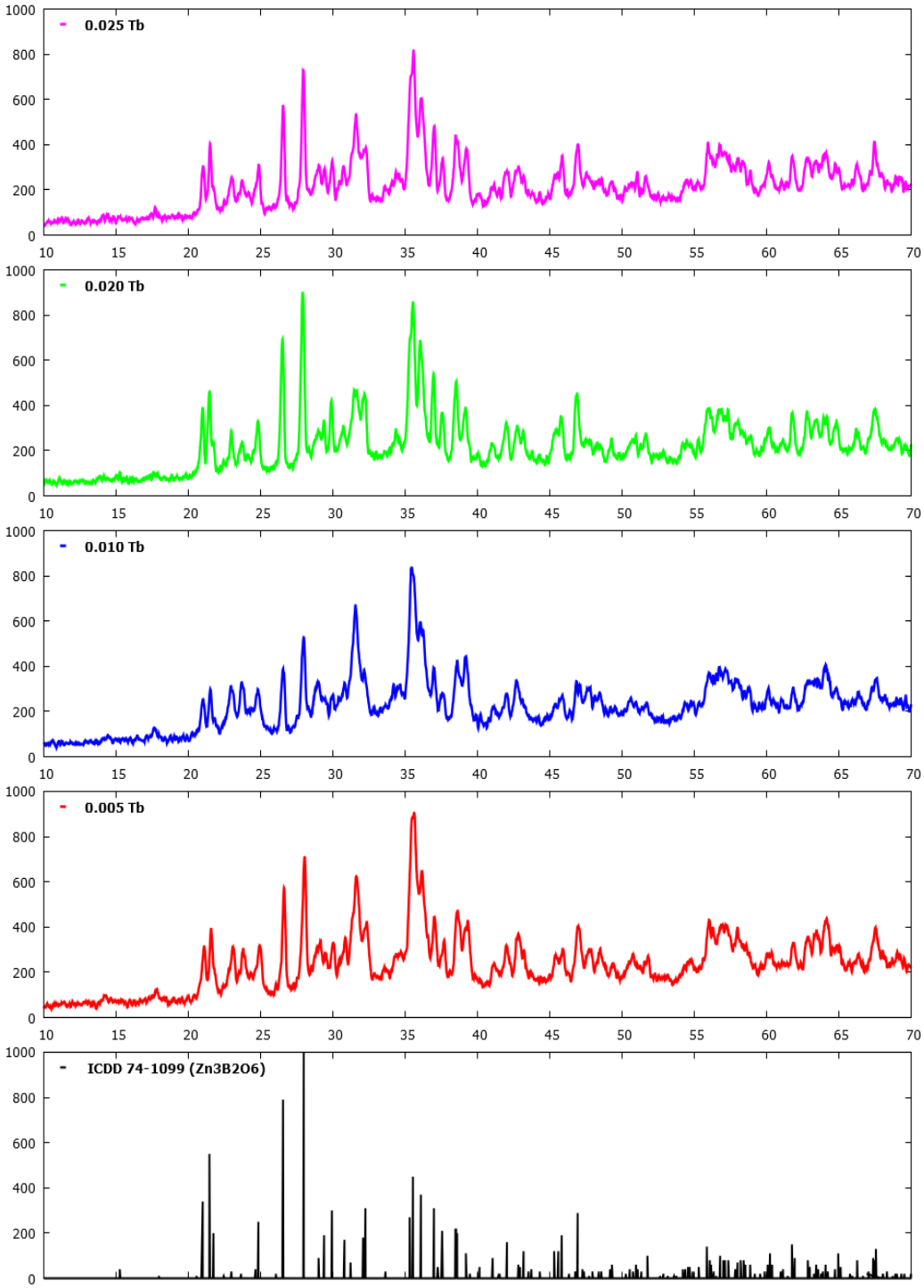

Figure 4.32. XRD Patterns of Tb doped $Zn_3B_2O_6$ at 600°C

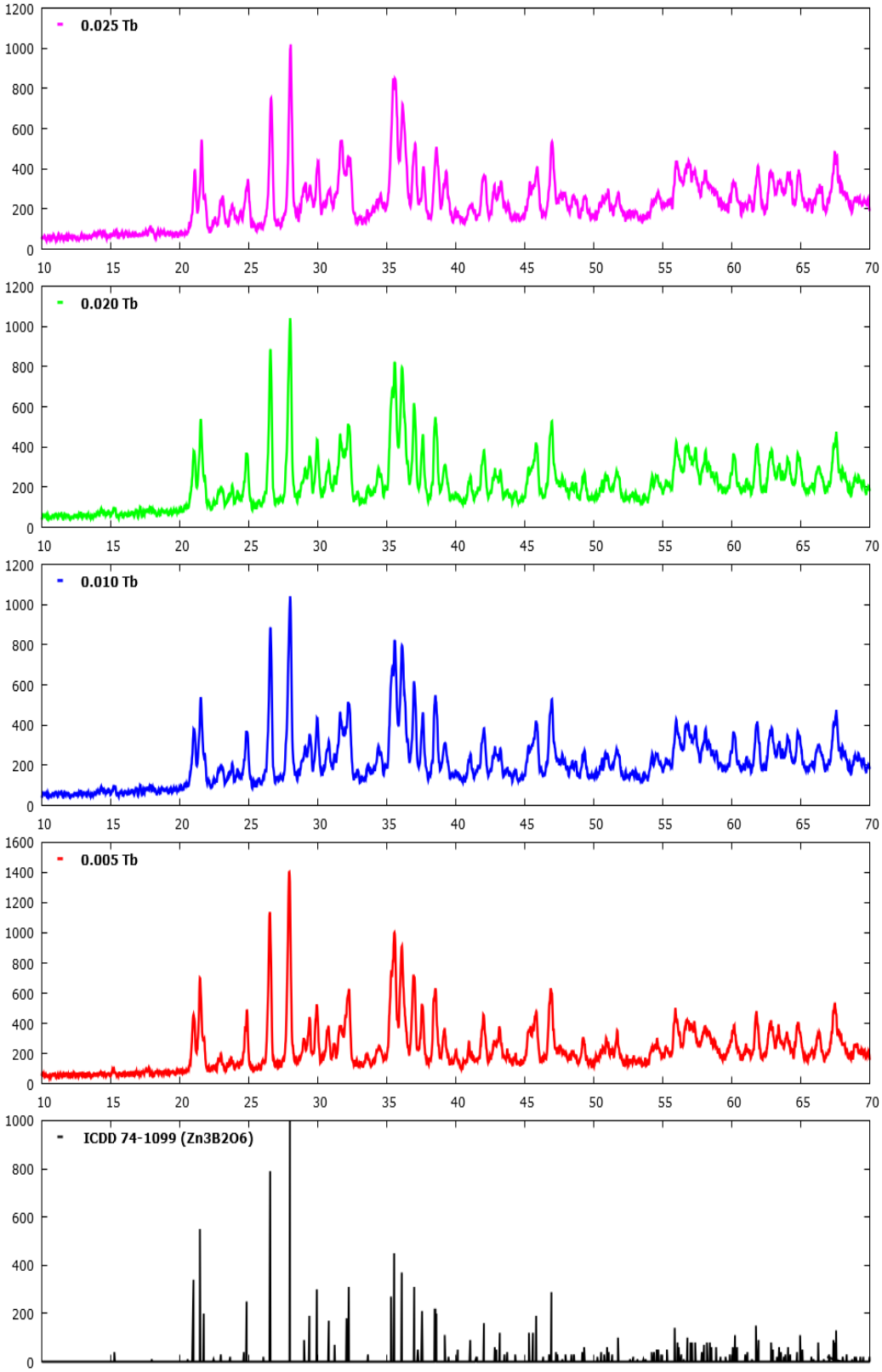

Figure 4.33. XRD Patterns of Tb doped $Zn_3B_2O_6$ at 700°C

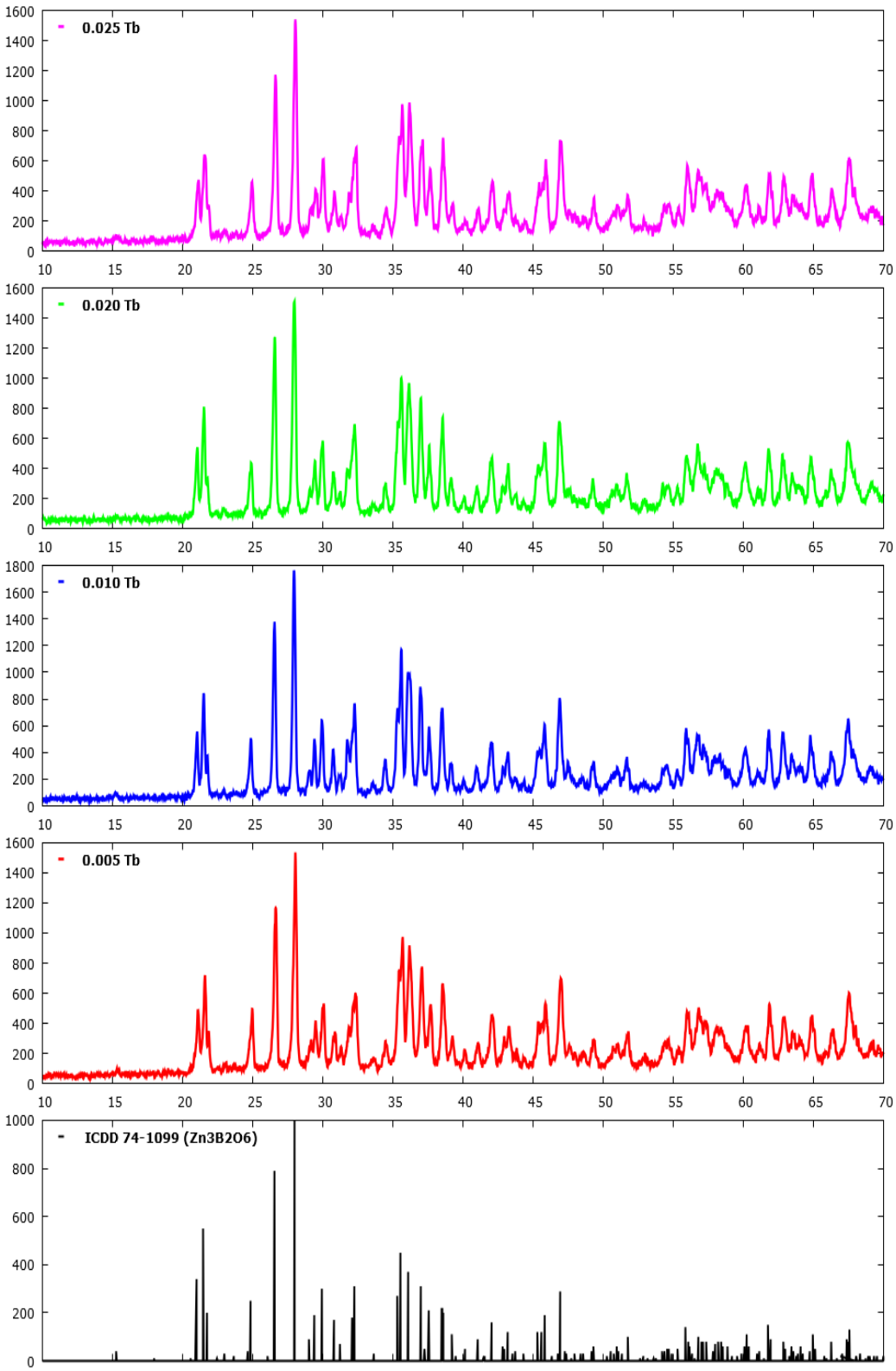

Figure 4.34. XRD Patterns of Tb doped $Zn_3B_2O_6$ at 800°C

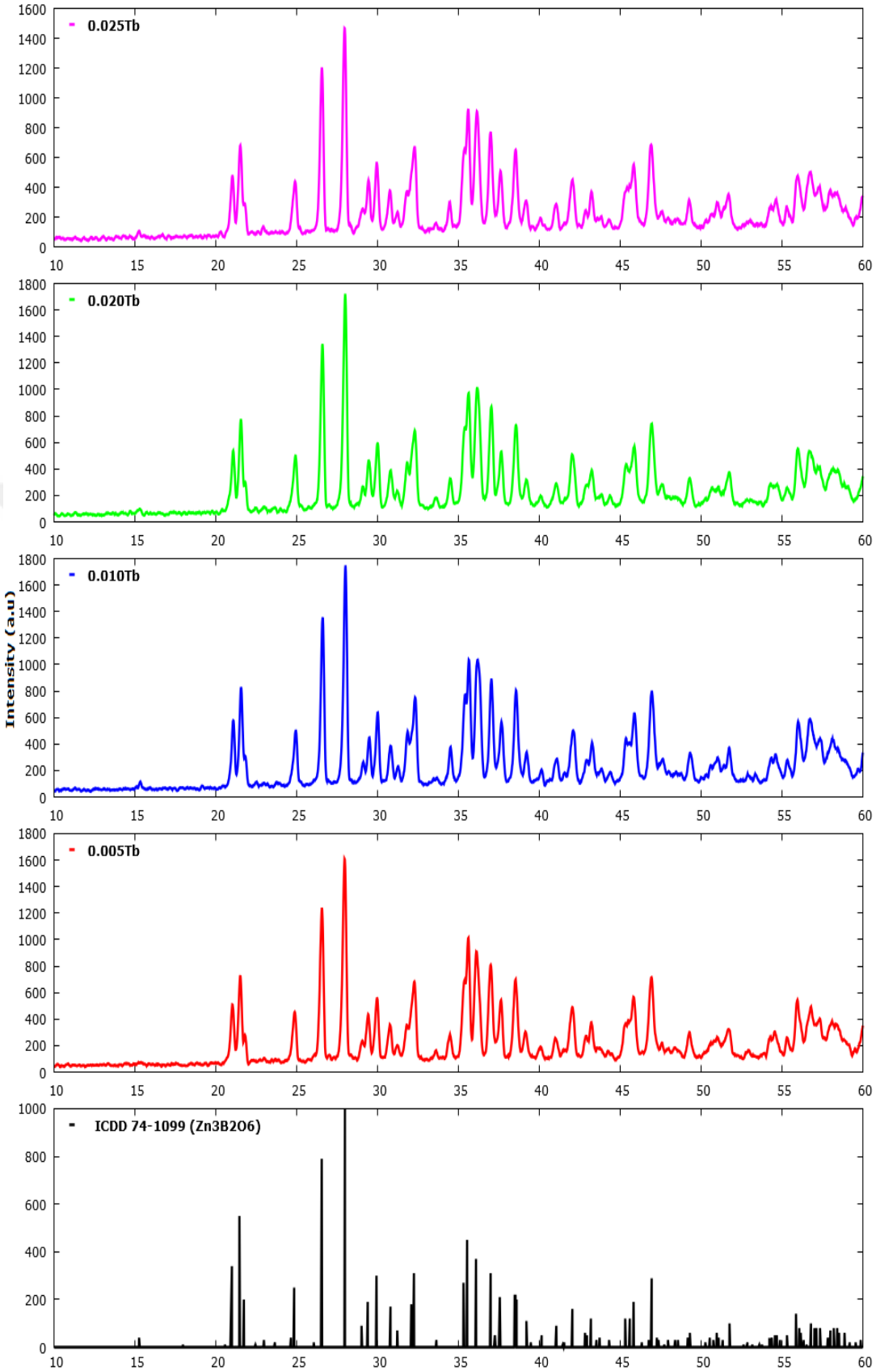

Figure 4.35. XRD Patterns of Tb doped $Zn_3B_2O_6$ at 900°C

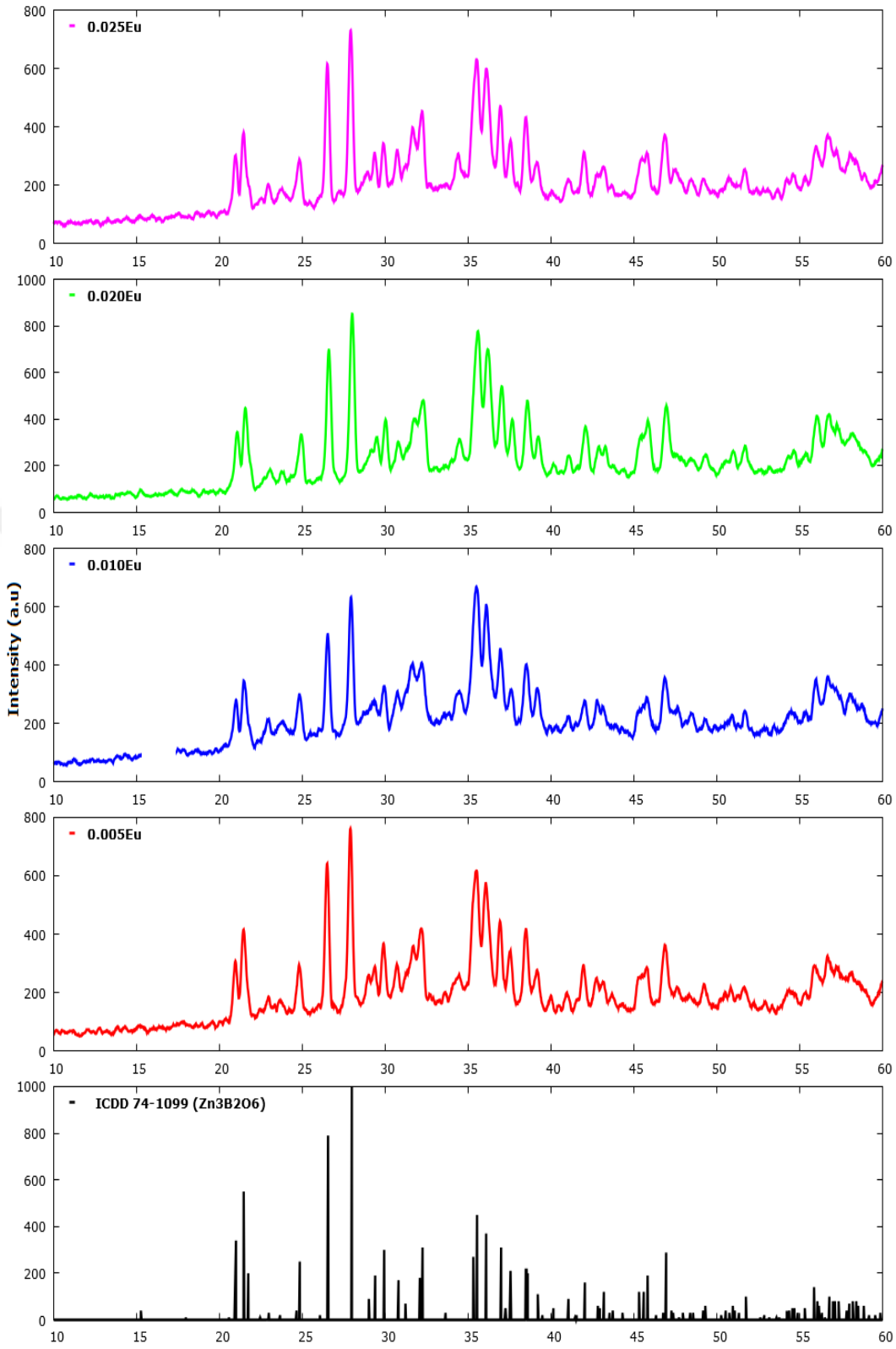

Figure 4.36. XRD Patterns of Eu doped $Zn_3B_2O_6$ at 400°C

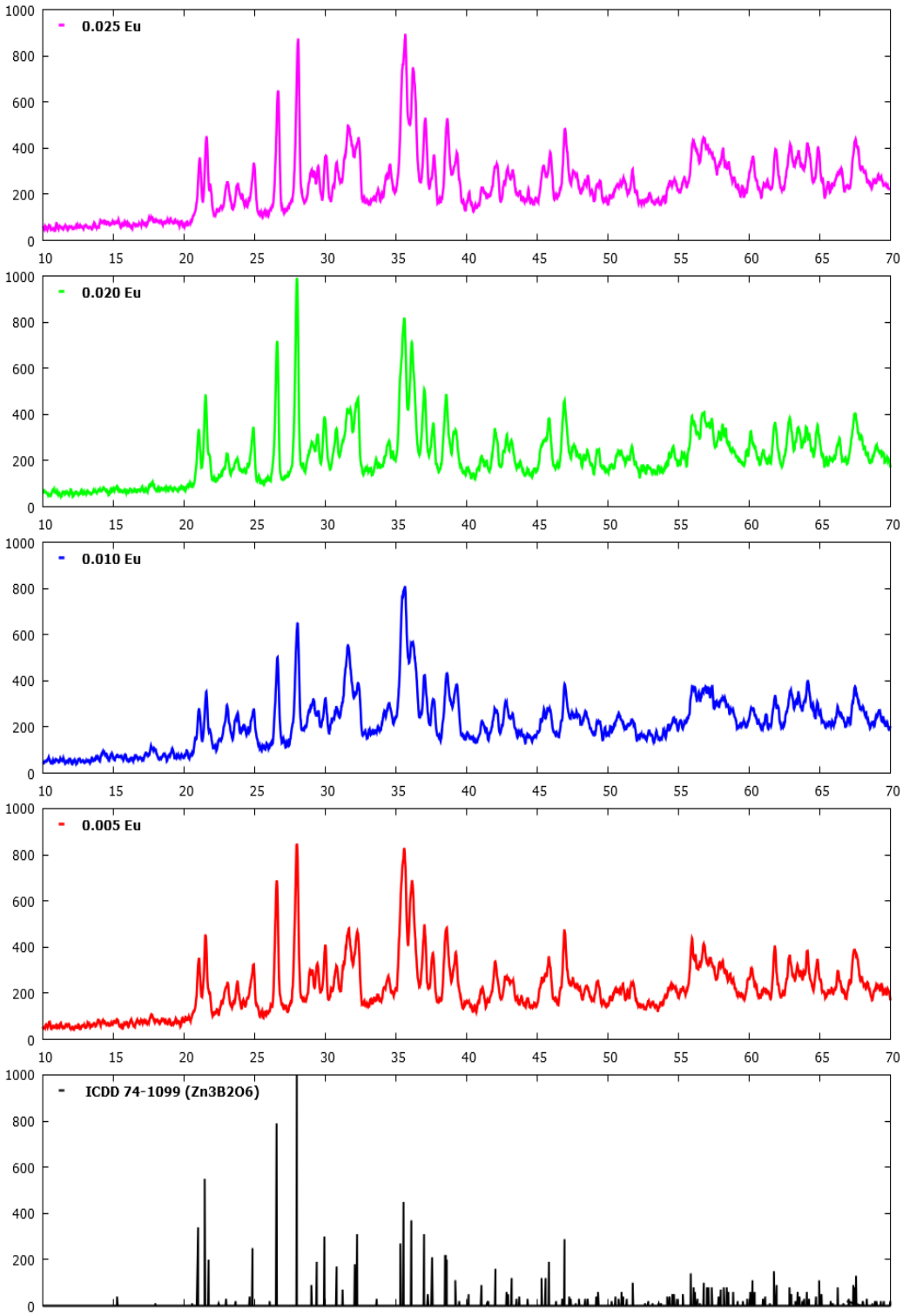

Figure 4.37. XRD Patterns of Eu doped $Zn_3B_2O_6$ at 600°C

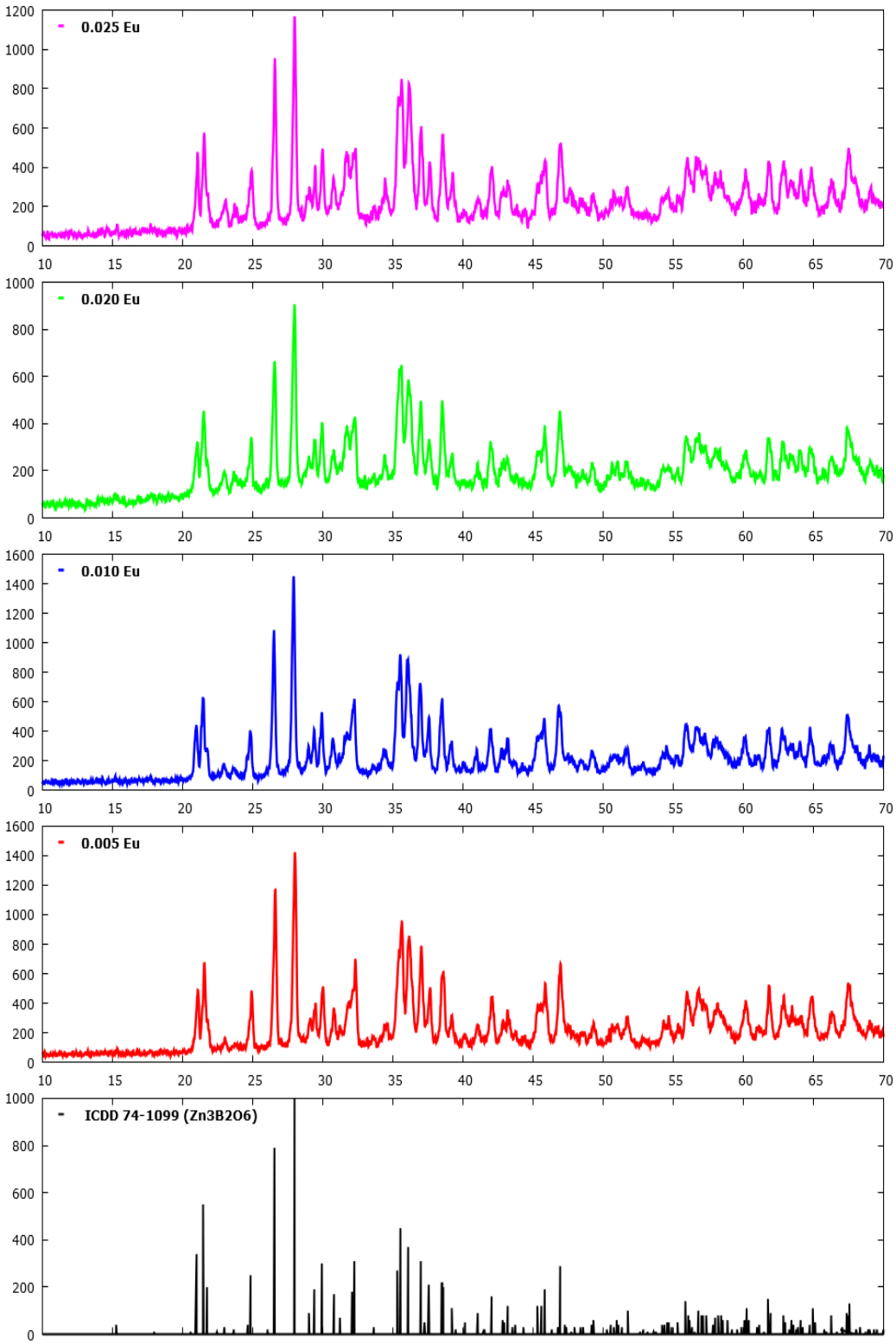

Figure 4.38. XRD Patterns of Eu doped $Zn_3B_2O_6$ at 700°C

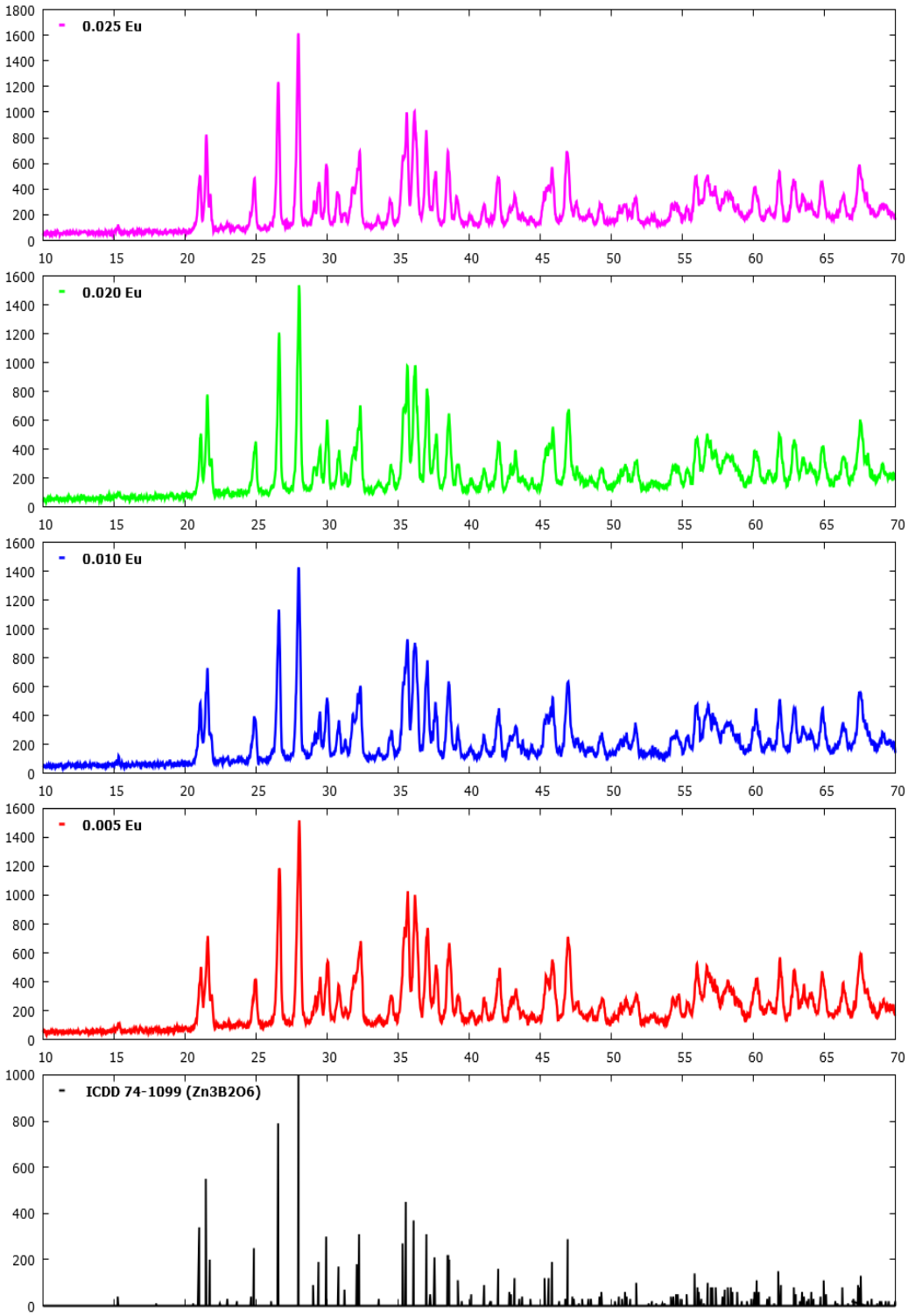

Figure 4.39. XRD Patterns of Eu doped $Zn_3B_2O_6$ at 800°C

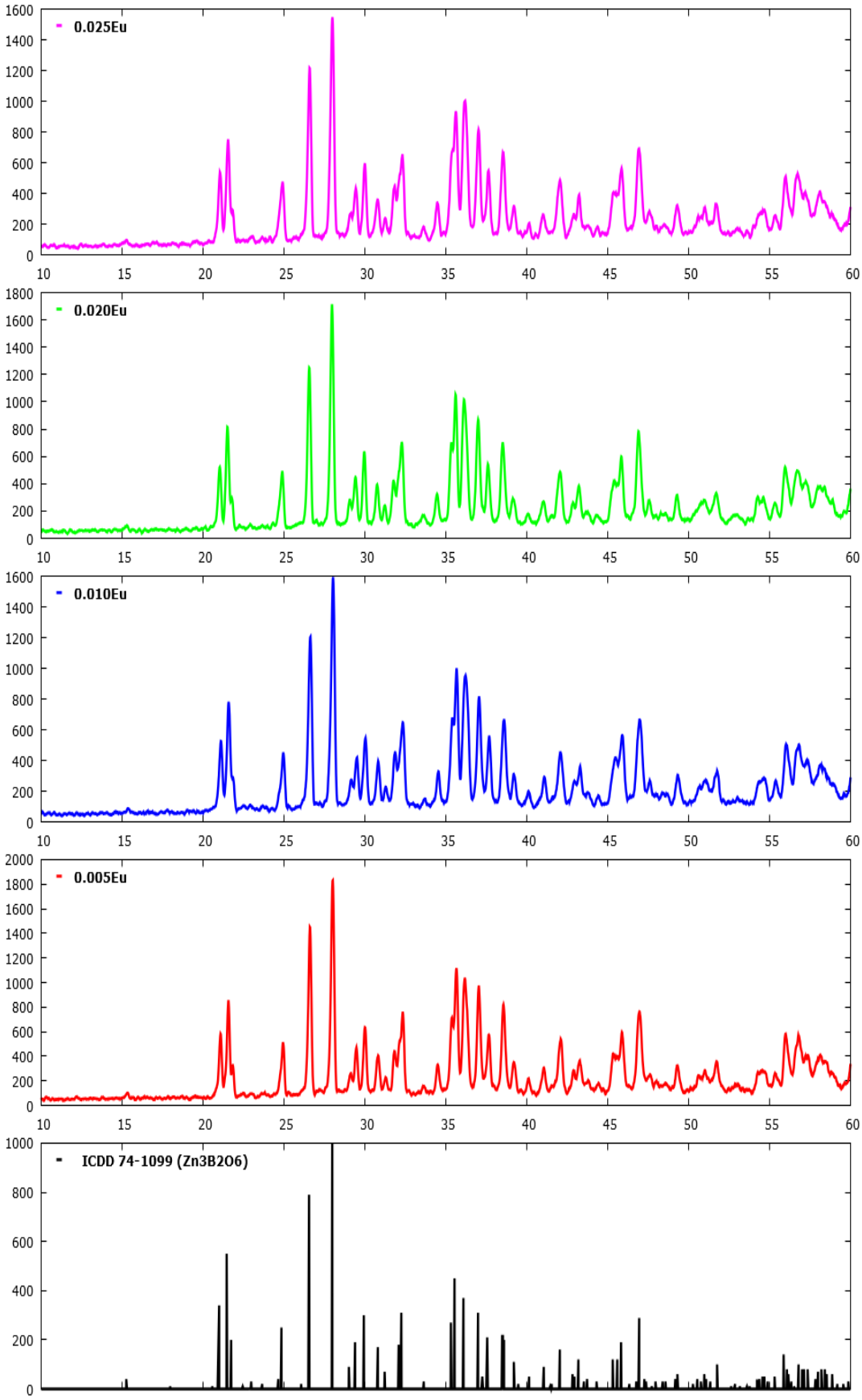

Figure 4.40. XRD Patterns of Eu doped $Zn_3B_2O_6$ at 900°C

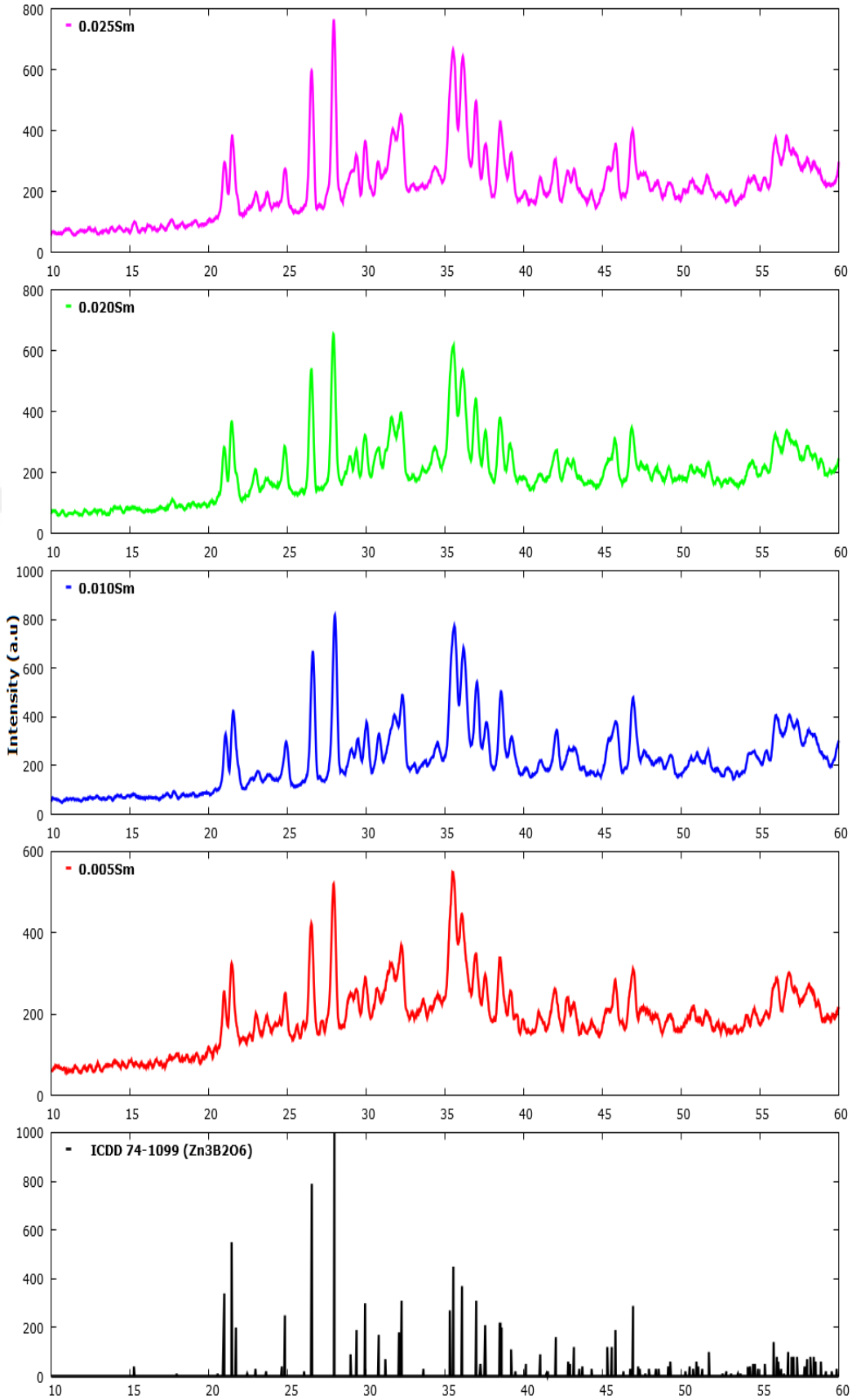

Figure 4.41. XRD Patterns of Sm doped $Zn_3B_2O_6$ at 400°C

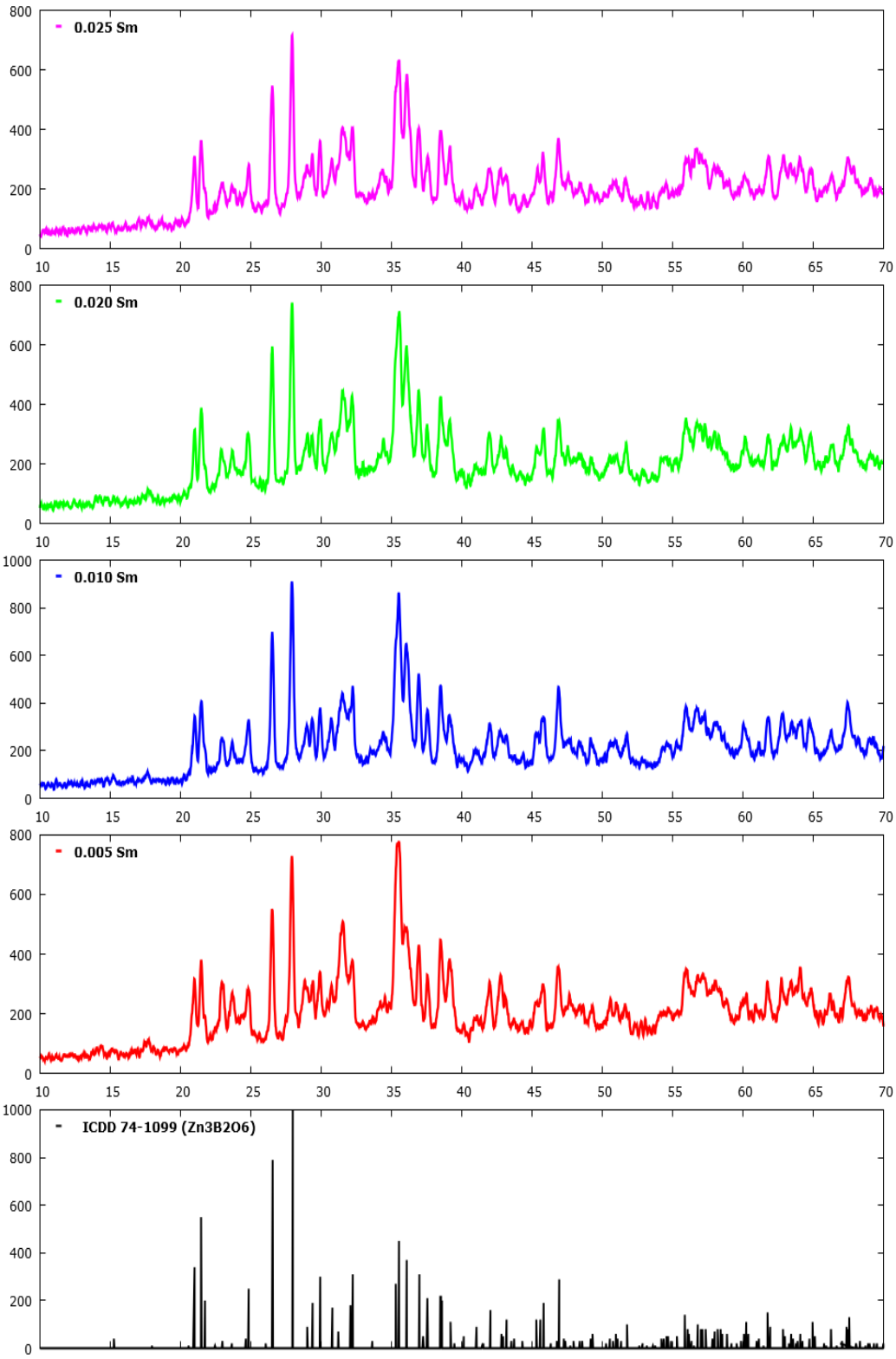

Figure 4.42. XRD Patterns of Sm doped $Zn_3B_2O_6$ at 600°C

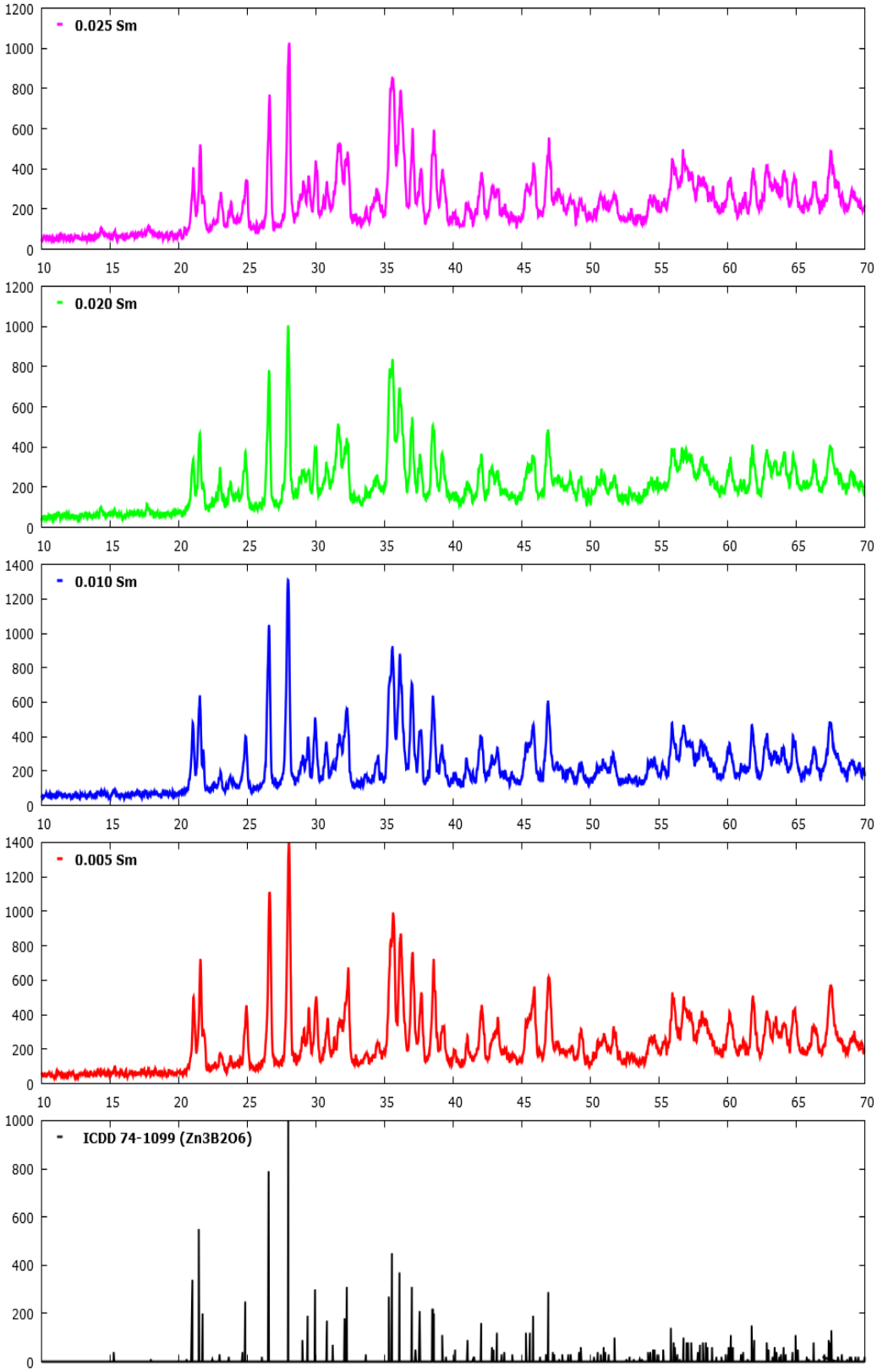

Figure 4.43. XRD Patterns of Sm doped $Zn_3B_2O_6$ at 700°C

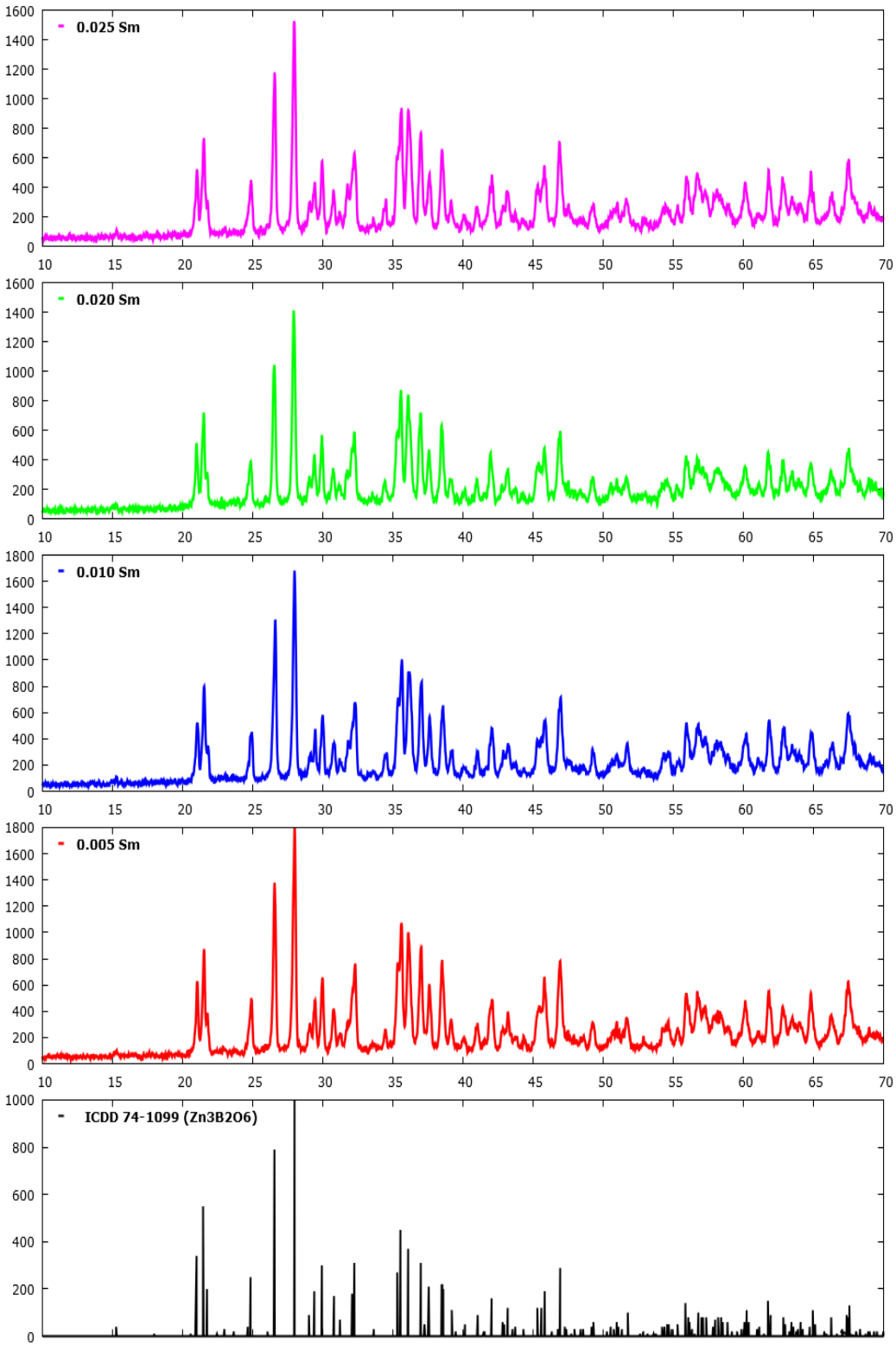

Figure 4.44. XRD Patterns of Sm doped $Zn_3B_2O_6$ at 800°C

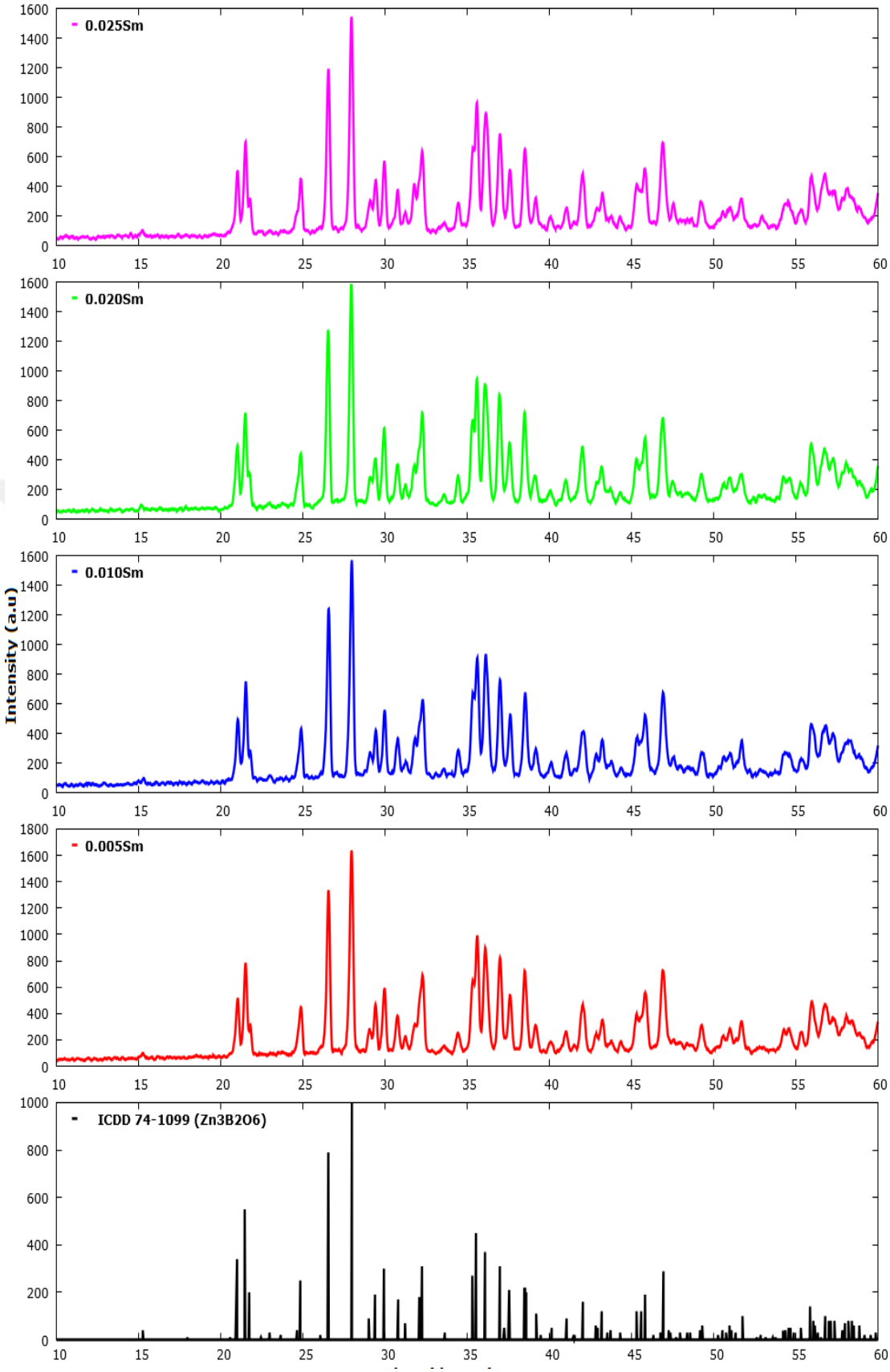

Figure 4.45. XRD Patterns of Sm doped $Zn_3B_2O_6$ at 900°C

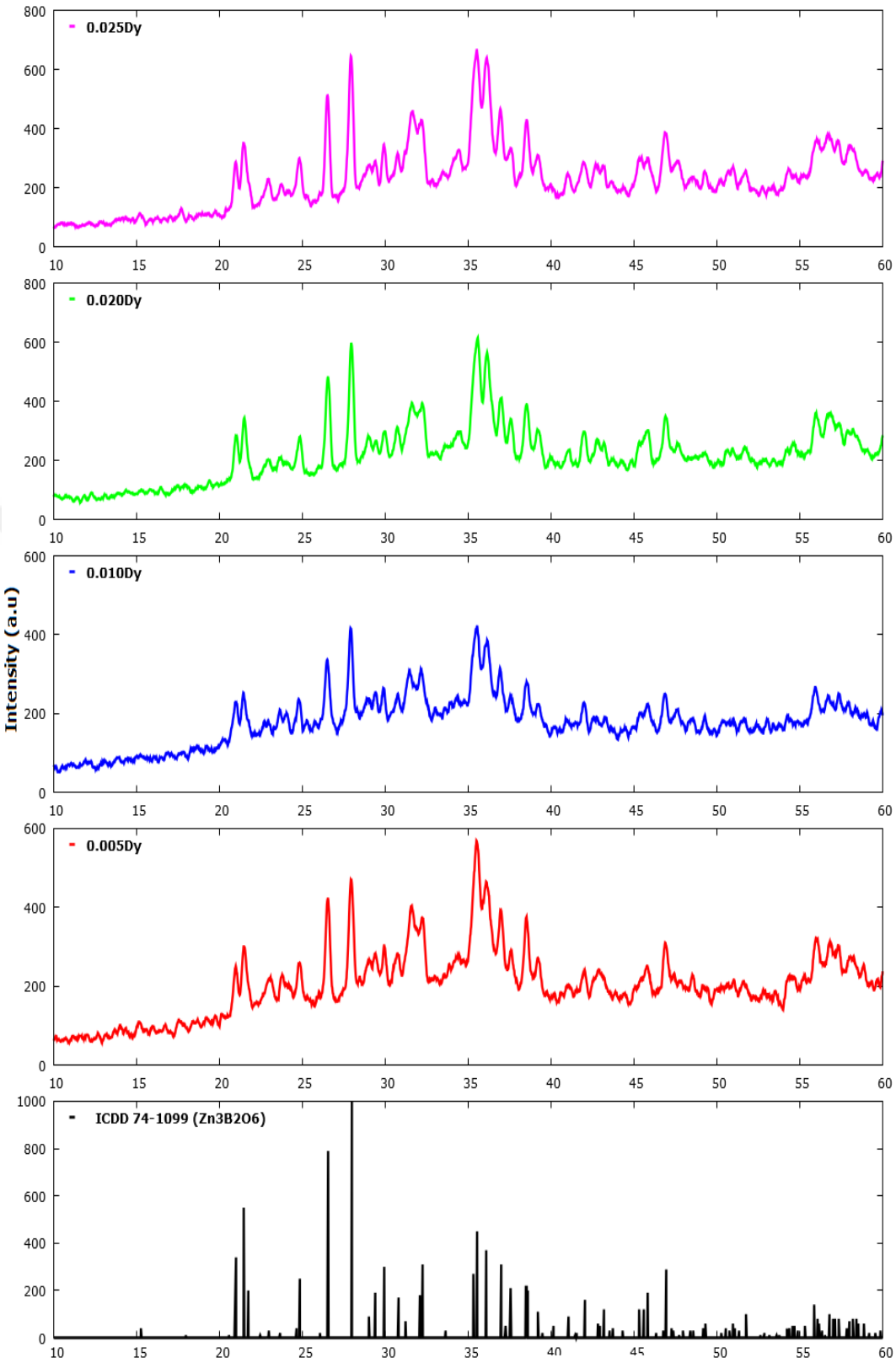

Figure 4.46. XRD Patterns of Dy doped $Zn_3B_2O_6$ at 400°C

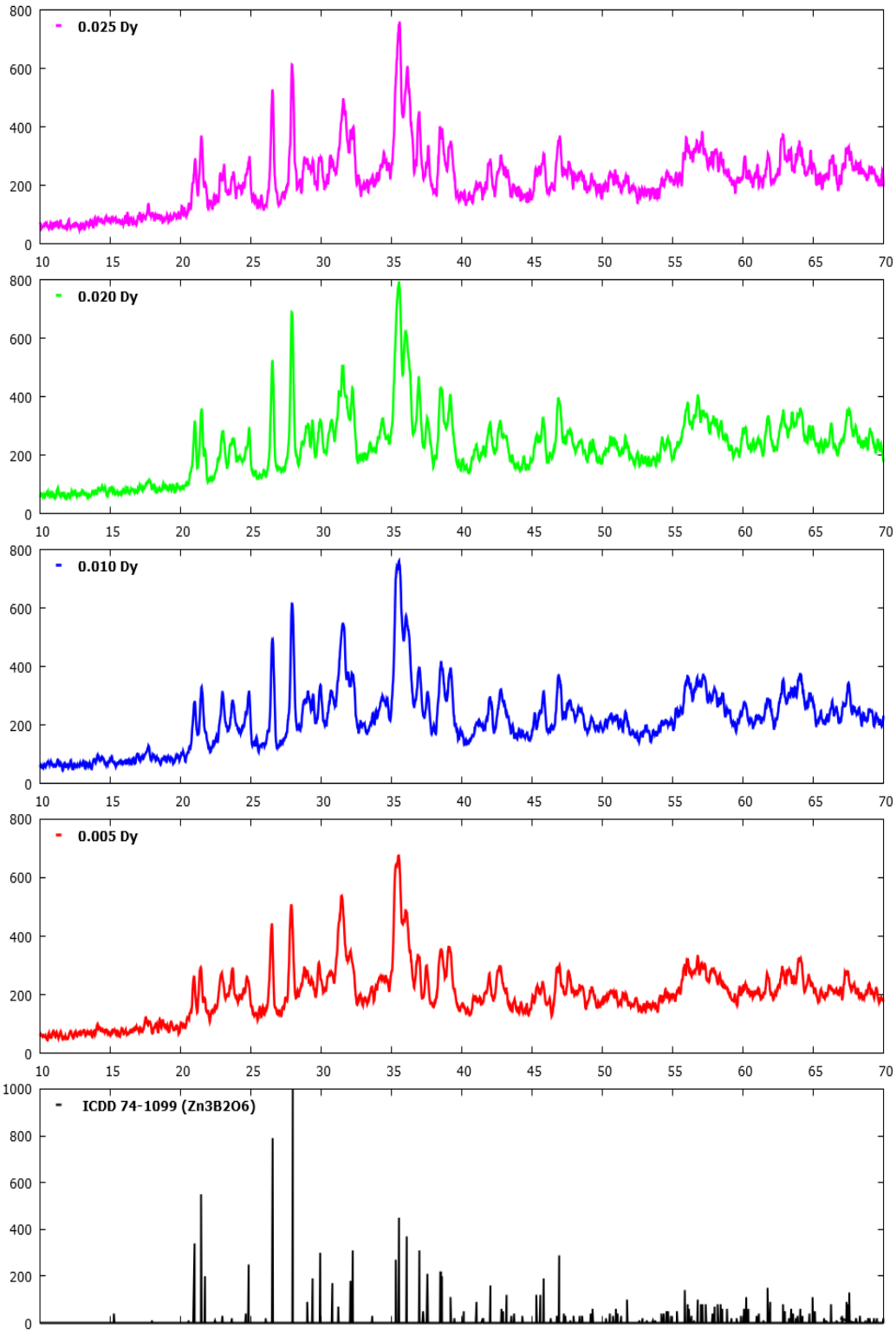

Figure 4.47. XRD Patterns of Dy doped $Zn_3B_2O_6$ at 600°C

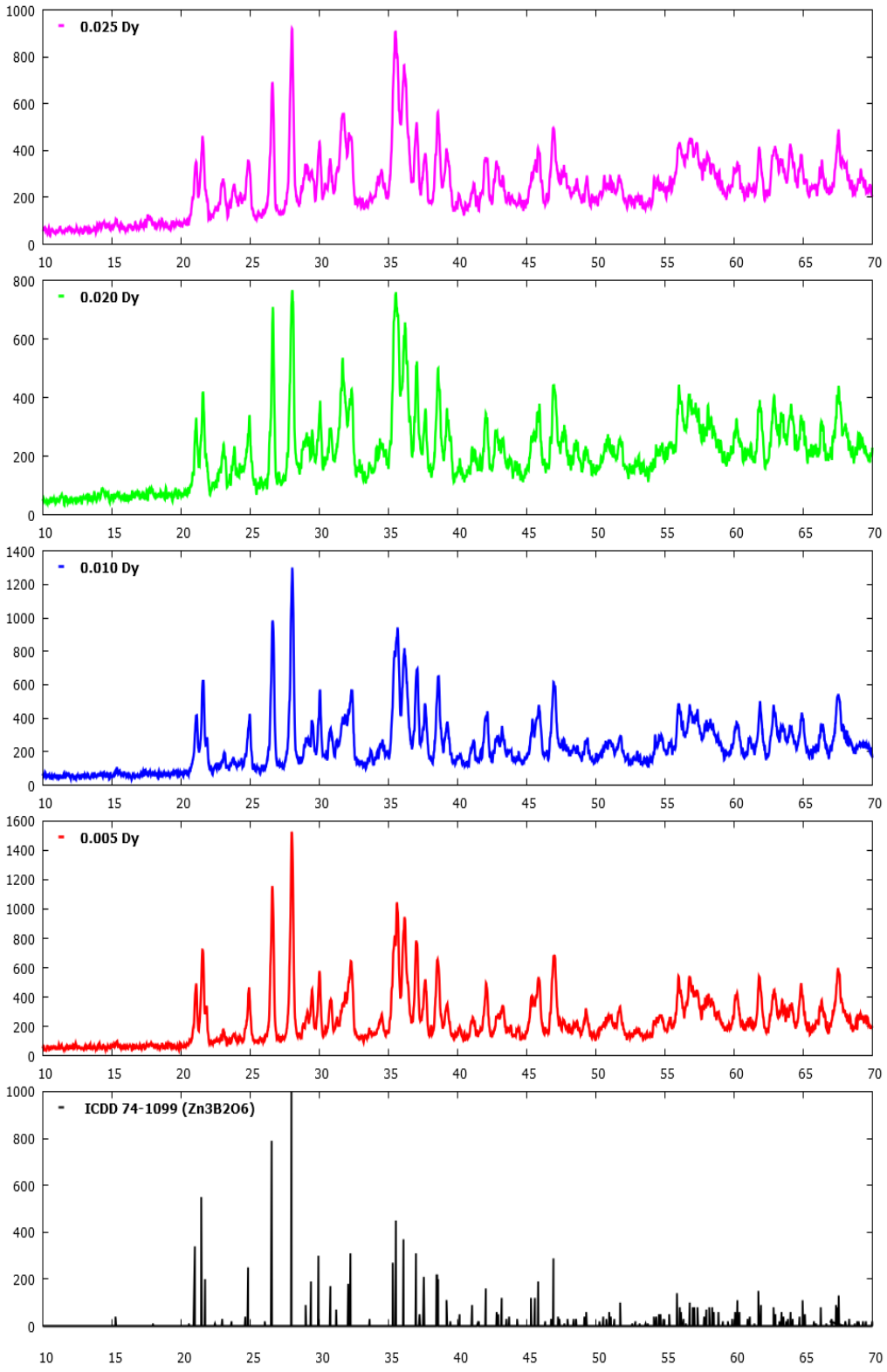

Figure 4.48. XRD Patterns of Dy doped $Zn_3B_2O_6$ at 700°C

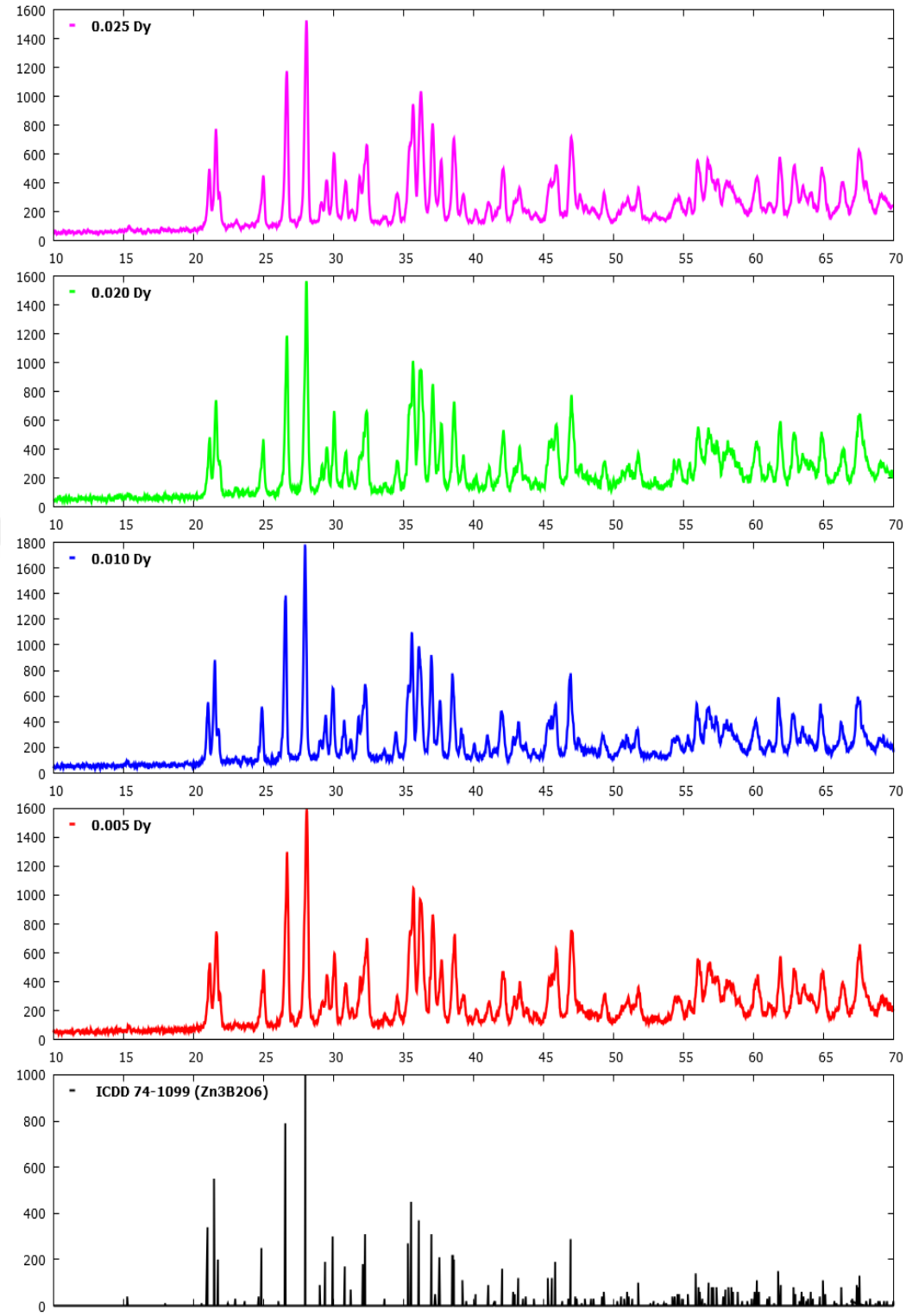

Figure 4.49. XRD Patterns of Dy doped $Zn_3B_2O_6$ at 800°C

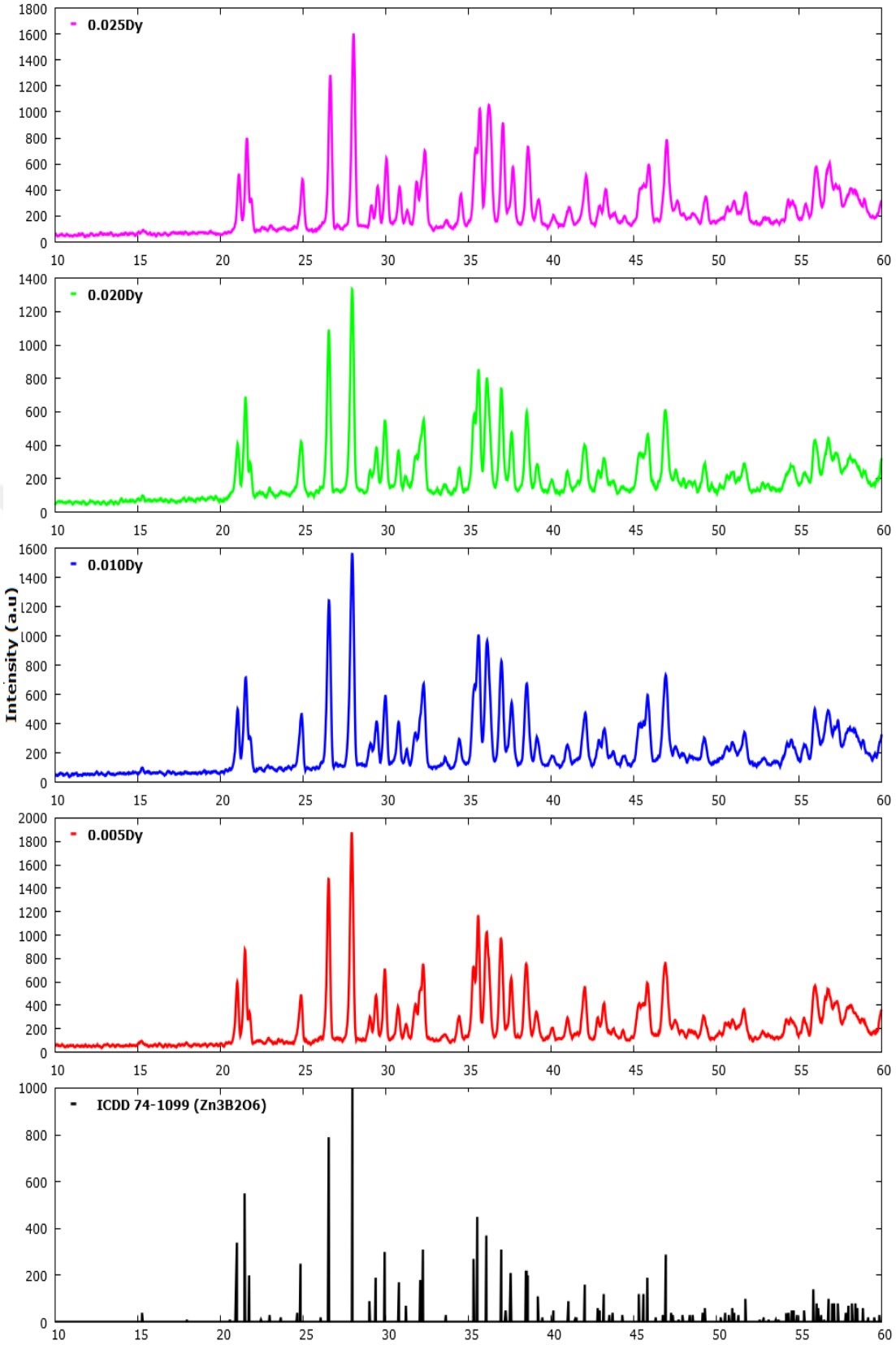

Figure 4.50. XRD Patterns of Dy doped $Zn_3B_2O_6$ at 900°C

Previously, it was reported that zinc borate was formed in alpha and beta form when synthesizing zinc borates with different fuels.In that study,it was also observed that only beta form of zinc borate was synthesized with glycine as a fuel at low and high temperatures (51)

Monocilinic crystal structure of zinc borate presence and the single sharp lines at around 2θ=~26º and 28º

The crystallites sizes determiden by using Debye Scherrer's equaition.(52)

$$D = K\lambda / \beta cos\ \theta$$

The calculated crystallites from Table 4.1 to Table 4.4 are lower at lower grades and higher at higher grades.

Table 4.1 Crystallite size of Eu doped $Zn_3B_2O_6$ at different concentration and different temperatures

Concentration	At 400C	At 900C
0,005	5,05 nm	27,75 nm
0,010	3,89 nm	26,66 nm
0,020	8,71 nm	21,49 nm
0,025	8,89nm	24,68 nm

Table 4.2 Crystallite size of Dy doped $Zn_3B_2O_6$ at different concentration and different temperatures

Concentration	At 400C	At 900c
0,005	3,96	21,11
0,010	5,00	23,63
0,020	8,33	20,06
0,025	7,73	20,57

Table 4.3 Crystallite size of Sm doped $Zn_3B_2O_6$ at different concentration and different temperatures

Concentration	At 400C	At 900C
0,005	4,31	23,77
0,010	8,55	20,45
0,020	8,64	20,73
0,025	4,39	24,86

Table 4.4 Crystallite size of Tb doped $Zn_3B_2O_6$ Tb doped at different concentration and different temperatures

Concentrations	At 400C	At 900C
0,005	4,41	24,71
0,010	5,41	23,33
0,020	3,72	24,75
0,025	4,16	20,02

4.4. The UV-Visible Spectroscopy Studies

The optical characteristics of undoped Zn3B2O6 were also determined by using UV-VIS Spectrophotometer in the range of wavelength 900-200 nm. The UV-Visible spectra of Tb3+ ion doped Zn3B2O6 are shown in Figure 4.37. Because of the increasing in the wavelength with increasing the concentration.

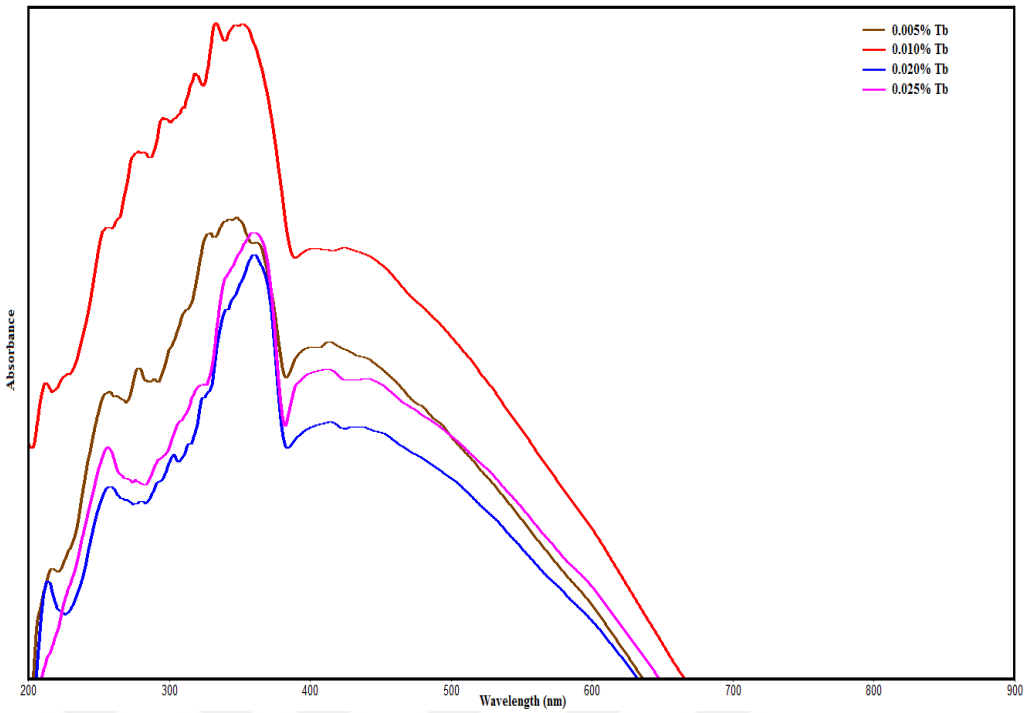

Figure 4.51. Uv-Vis Spectra of Synthesis Tb Doped $Zn_3B_2O_6$ (Absorbance)

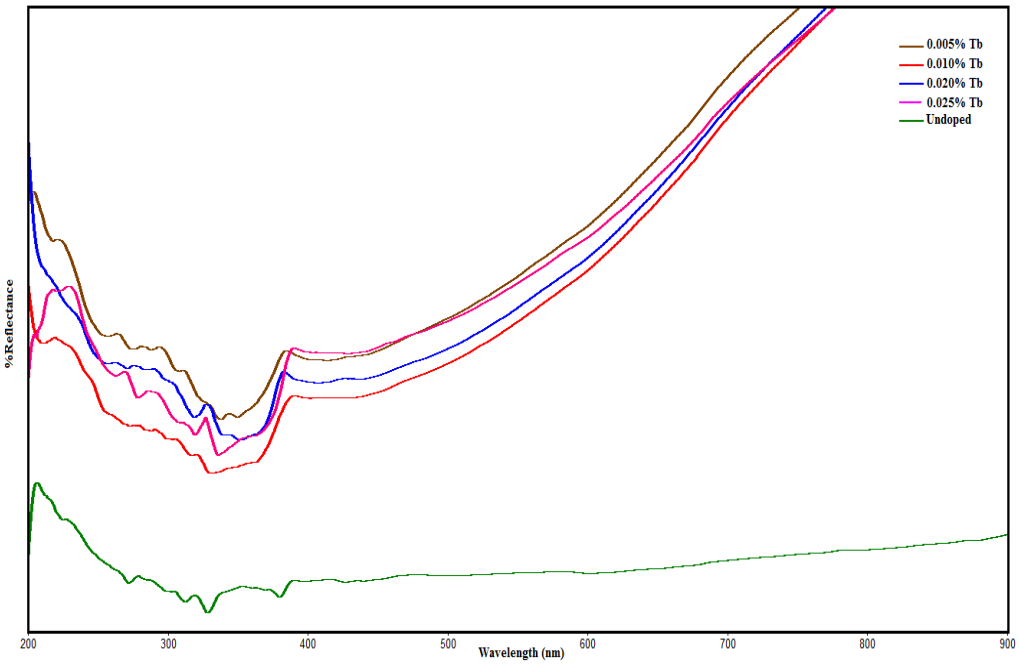

Figure 4.52. Synthesis Tb Doped $Zn_3B_2O_6$ Glycine (Reflectance)

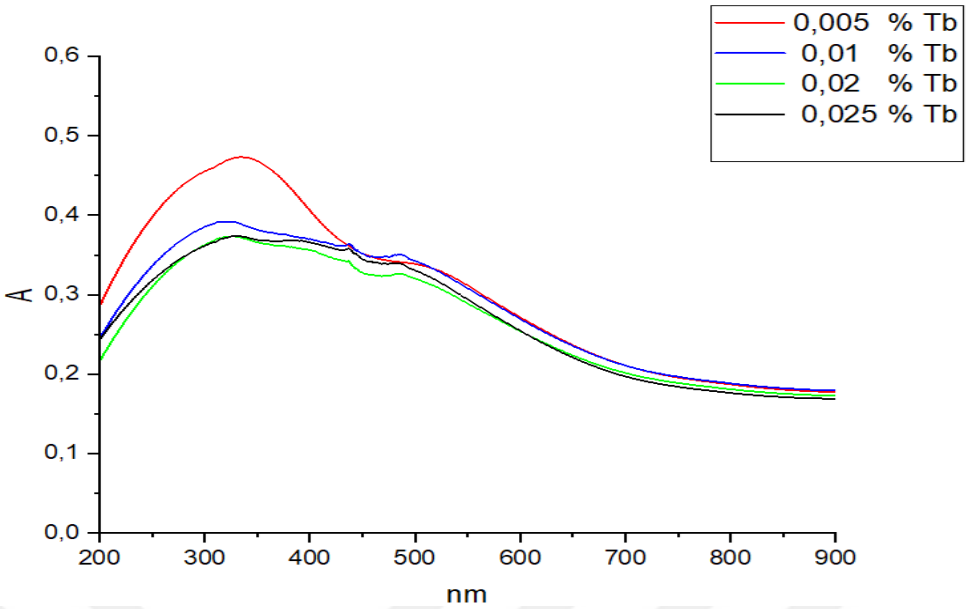

Figure 4.53. Uv-Vis Spectra of one hour at heating 600 °C Tb doped $Zn_3B_2O_6$ at different concentrations)

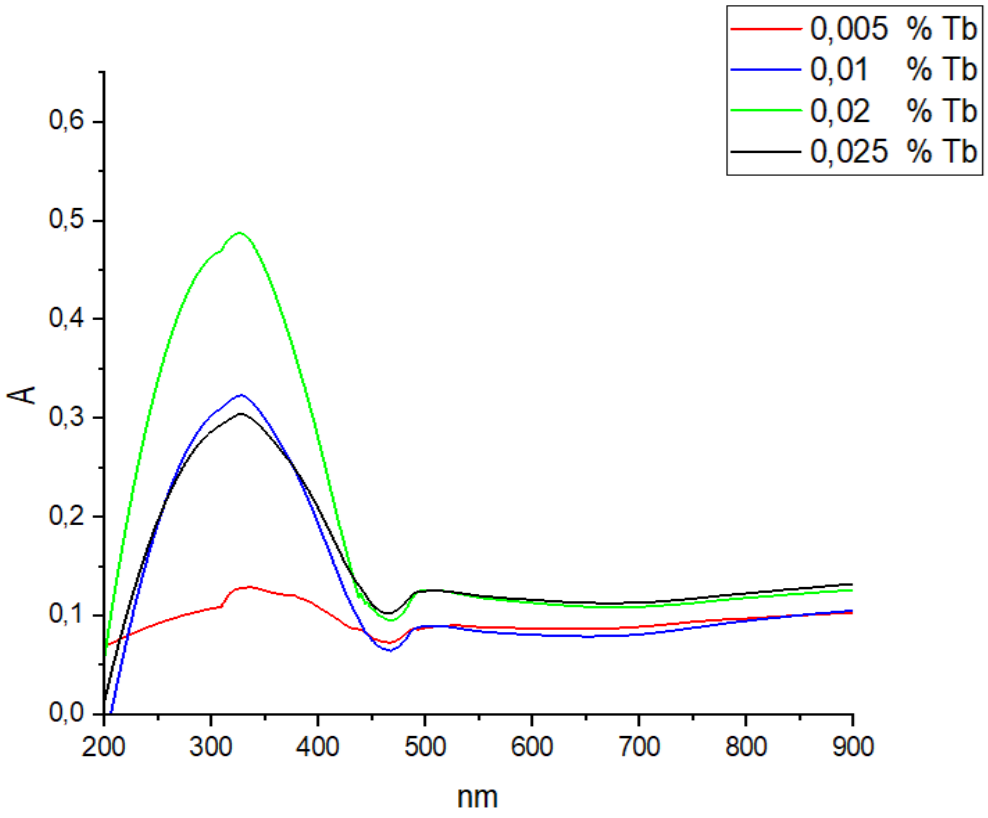

Figure 4.54. Uv-Vis Spectra of of one hour at heating 700 °C Tb doped $Zn_3B_2O_6$ at different concentrations

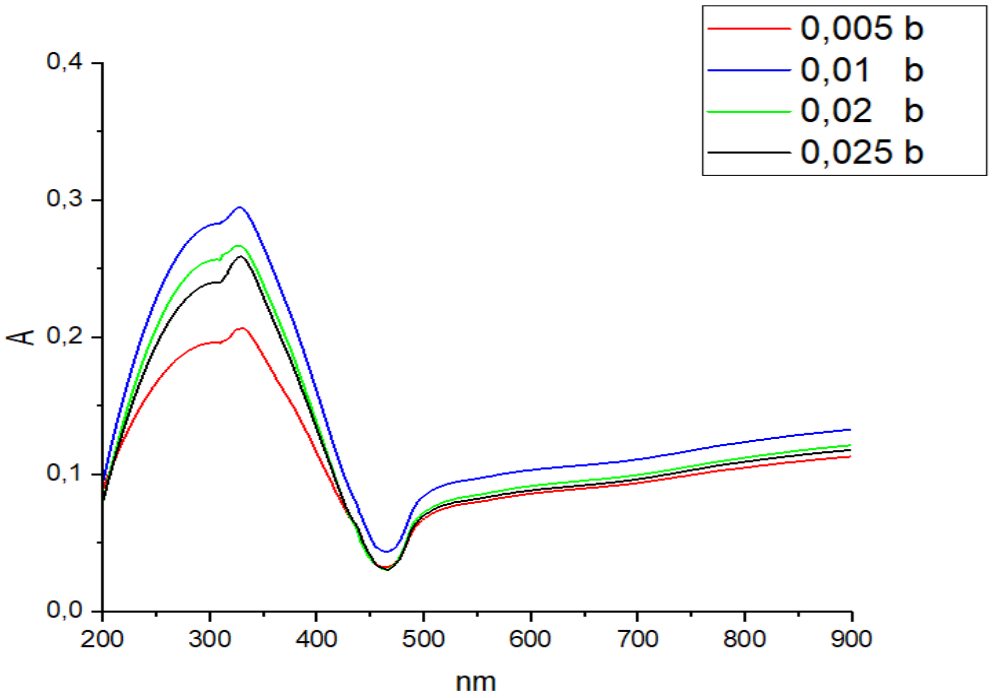

Figure 4.55. Uv-Vis Spectra of of one hour at heating 800 °C Tb doped $Zn_3B_2O_6$ at different concentrations

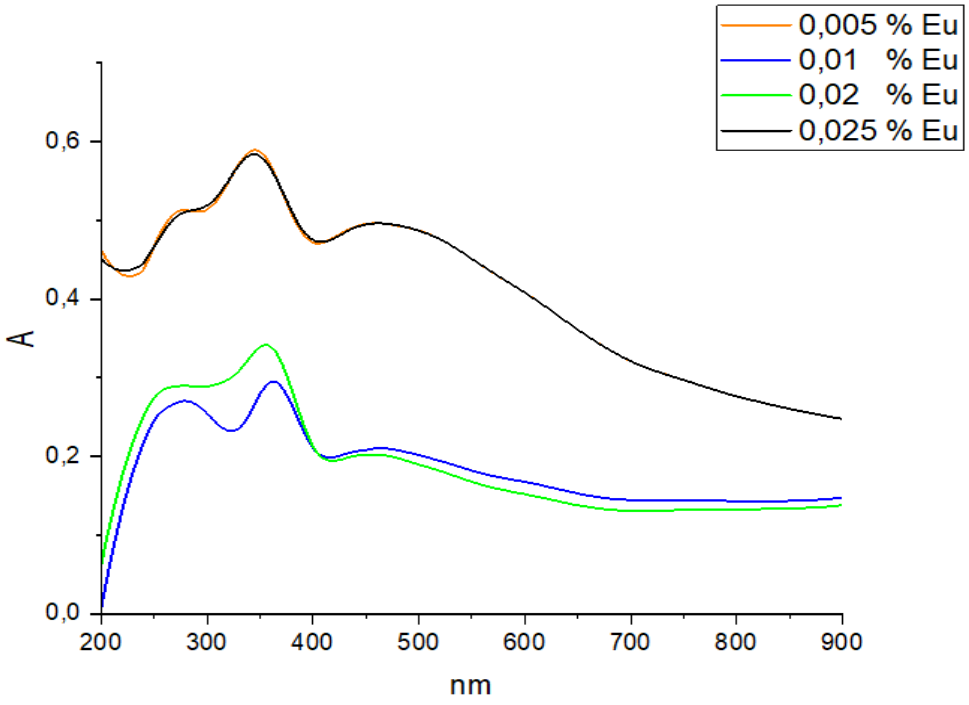

Figure 4.56. Uv-Vis Spectra of of one hour at heating 600 °C Eu doped $Zn_3B_2O_6$ at different concentrations

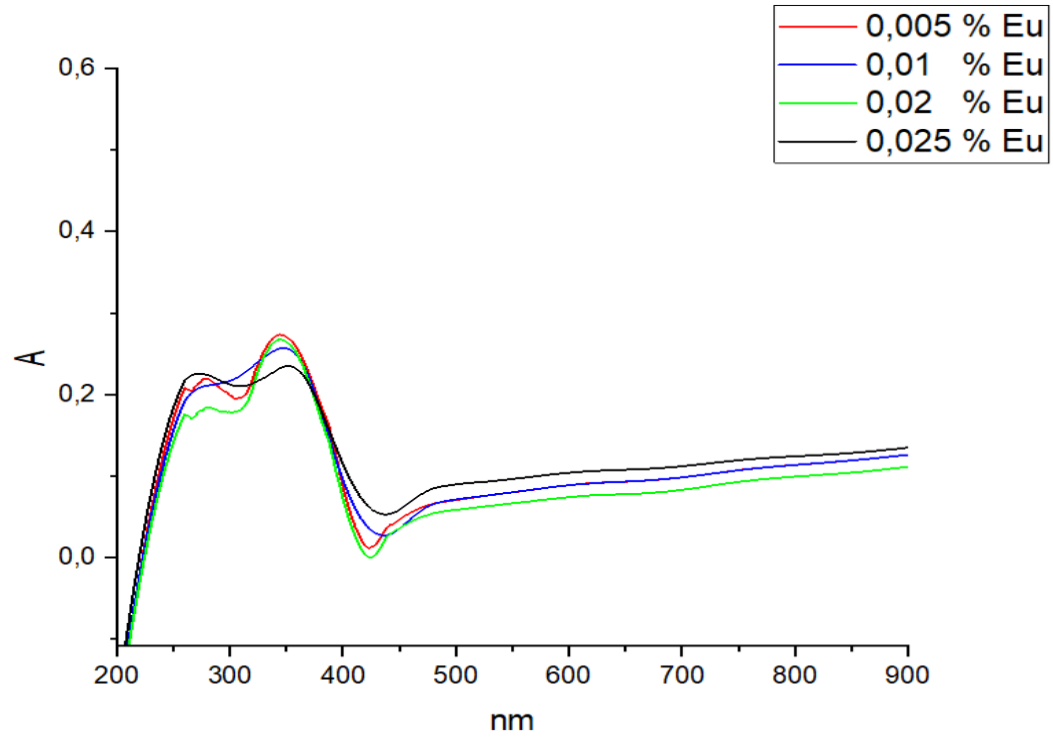

Figure 4.57. Uv-Vis Spectra of of one hour at heating 700 °C Eu doped $Zn_3B_2O_6$ at different concentrations

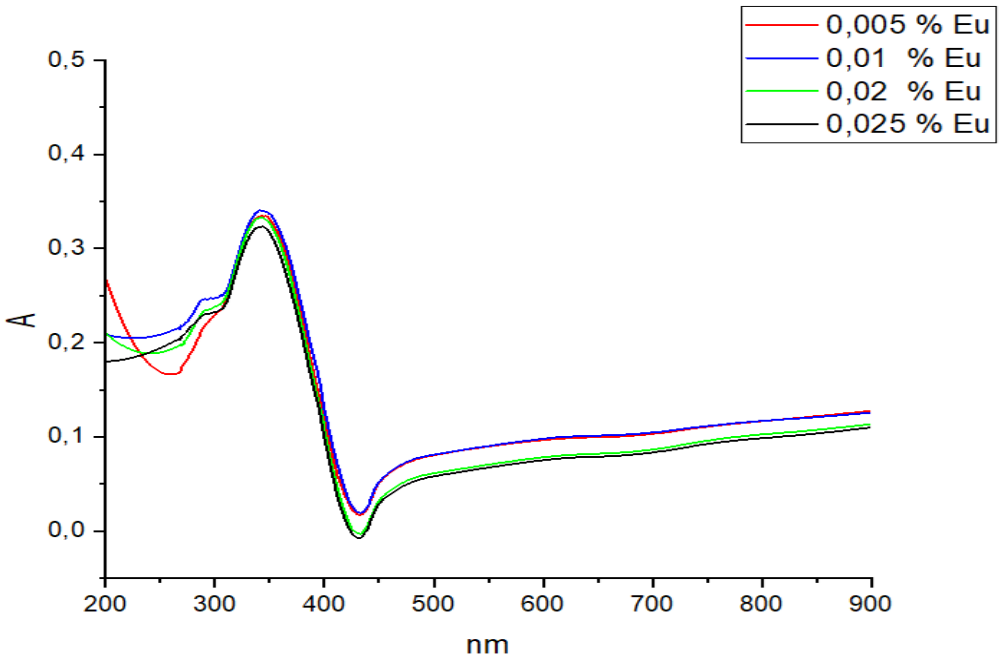

Figure 4.58. Uv-Vis Spectra of of one hour at heating 800 °C Eu doped $Zn_3B_2O_6$ at different concentrations

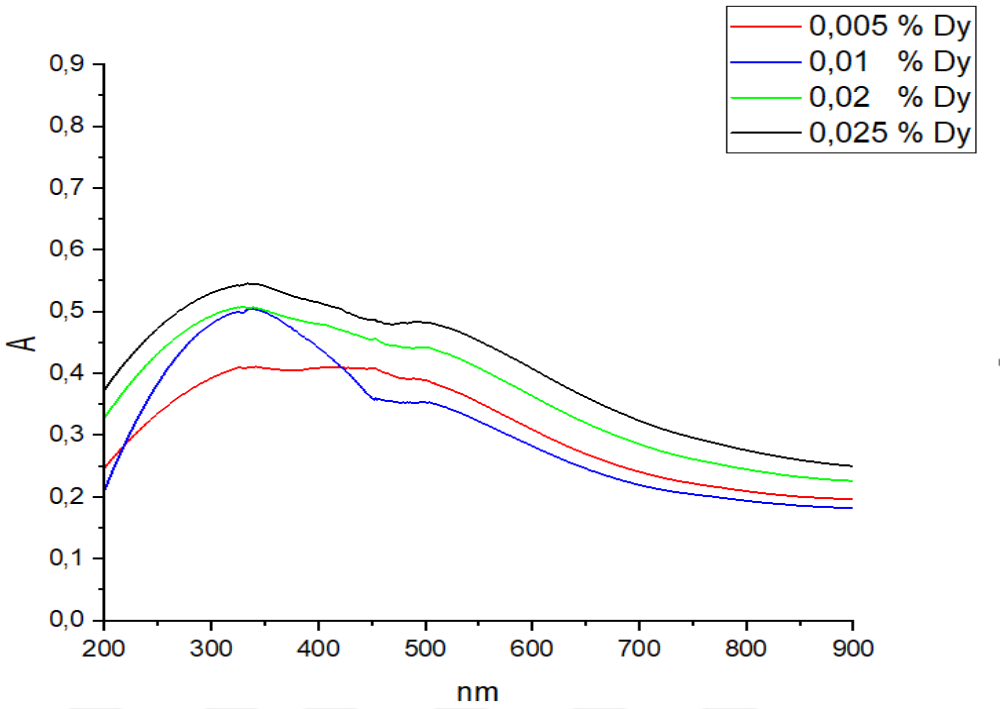

Figure 4.59. Uv-Vis Spectra of of one hour at heating 600 °C Dy doped $Zn_3B_2O_6$ at different concentrations

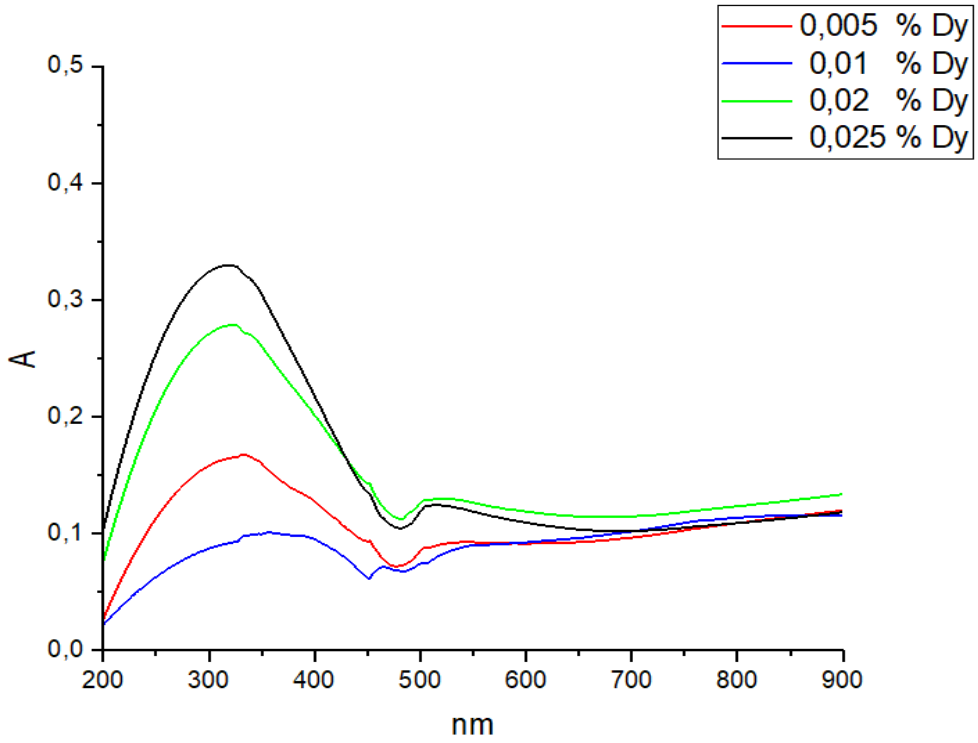

Figure 4.60. Uv-Vis Spectra of of one hour at heating 700 °C Dy doped $Zn_3B_2O_6$ at different concentrations

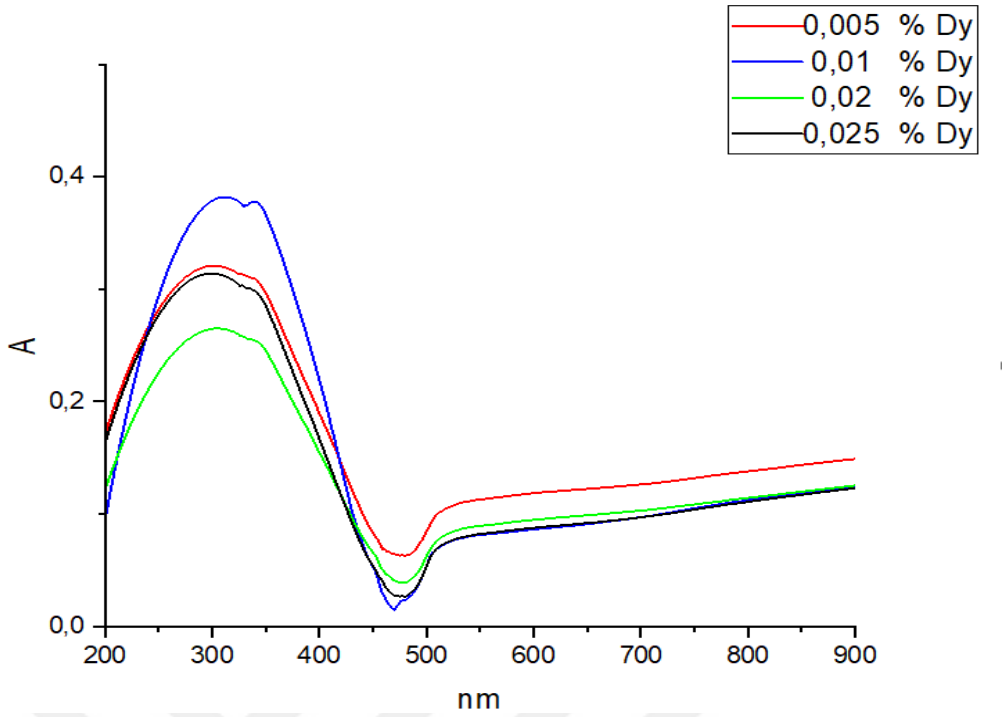

Figure 4.61. Uv-Vis Spectra of of one hour at heating 800 °C Dy doped $Zn_3B_2O_6$ at different concentrations

In this study, the Tauc plot method was used to calculate the gap energy. This method was discovered by Tauc in 1968, and as studies on thin layers increased, this method began to be used more and more.(53,54)

$$(\alpha hv)\ 1/m = B(hv - Eg)$$

where h = Planck's constant (4.135 × 10-15 eV.s),

v = frequency (s-1),

B = a comparative constant,

Eg = energy gap (eV)

The optical band gap energy were determined by using UV-VIS absorbance value by taking the intercept of the curve in the x-axis of Tauc plot. (56) It can be seen that the band gap energies found were between 5,14 eV and 5,40 eV.This change varies depending on the concentration of the lanthanide ion and temperature.

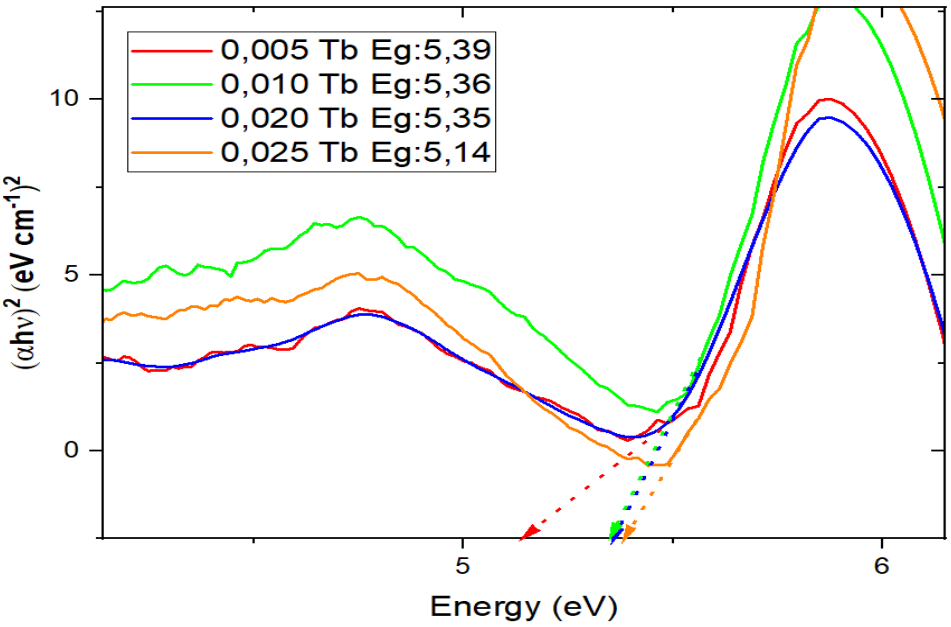

Figure 4.62. Optical Band Gap Energy Tb doped $Zn_3B_2O_6$ at different concentrations at 800 °C

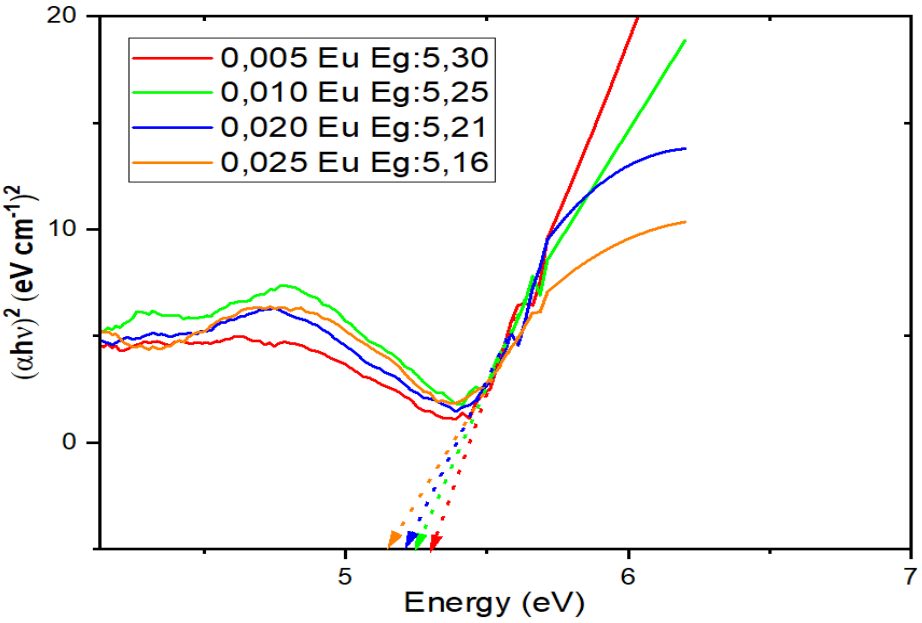

Figure 4.63. Optical Band Gap Energy Eu doped $Zn_3B_2O_6$ at different concentrations at 800 °C

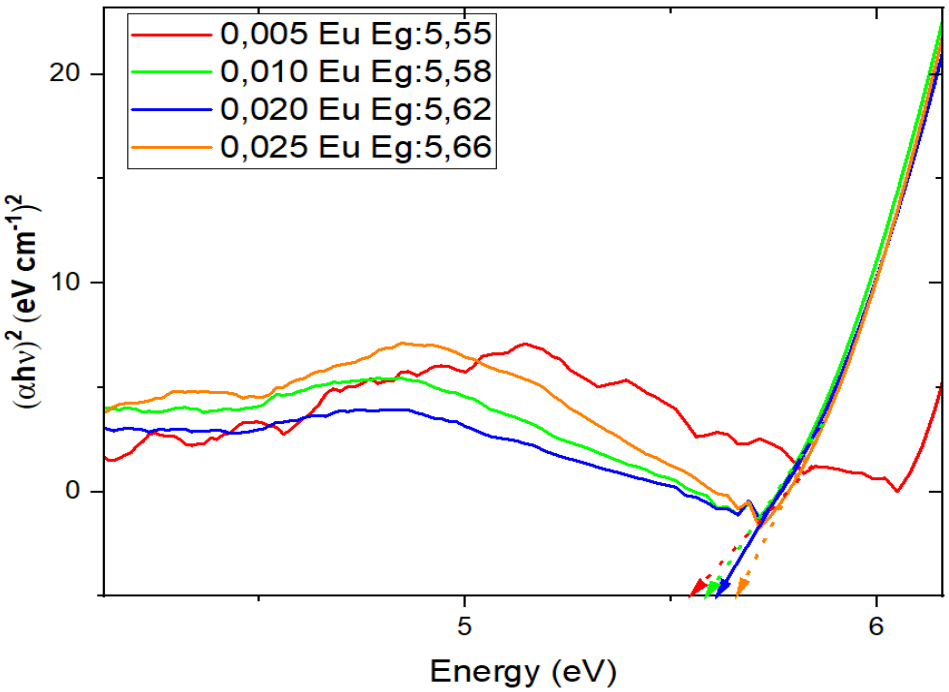

Figure 4.64. Optical Band Gap Energy Eu doped $Zn_3B_2O_6$ at different concentrations at 700 °C

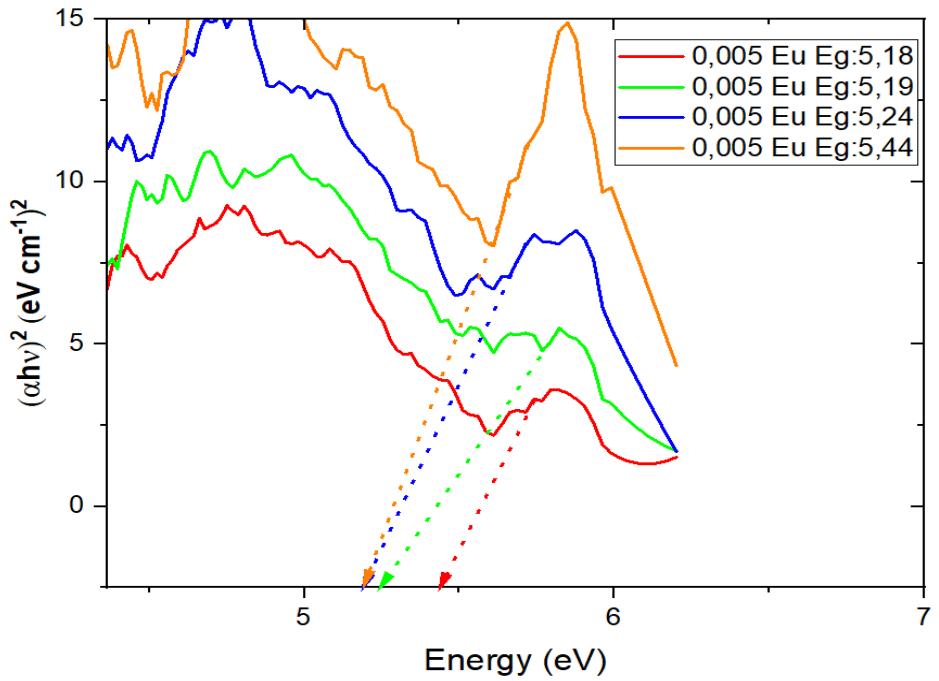

Figure 4.65. Optical Band Gap Energy Eu doped $Zn_3B_2O_6$ at different concentrations at 700 °C

5. CONCLUSIONS AND RECOMMENDATIONS

In this study, the undoped and lanthanide elements doped zinc orthoborates have been successfully synthesized by solution combustion method with glycine fuel. The synthesis of zinc orthoborates were obtained at a low synthesis temperature and low annealing time. The combustion process was carried out directly on the hot plate and the evaporation of gas was observed. The fluffy light brown powder products were obtained and there was no significant change of this color of the products on the change on dopant concentrations.

The formation of β form of zinc orthoborates was observed in the analysis of XRD. The crystal structure was determined as monoclinic form at higher temperatures, ≥700°C.

The FT-IR analysis of lanthanide ion doped zinc orthoborates were also done in the range of 4000-400 cm^{-1}. The bending vibrations of BO_3 were detected between 695-720 cm^{-1}, symmetric stretching of BO_3 vibrations were identified around 1010 and 1065 cm^{-1}. Furthermore, the bands at 1220 and 1245 cm^{-1} were assigned to the asymmetric stretching of BO_3 vibrations.

The optical properties of the obtained products were also investigated and the UV-VIS spectra was examined between 200 and 900 nm. The absorption bands were observed in the ultraviolet region in the range of 200-400 nm and the absence of any peak in the visible reagion, >400 nm, was observed which confirmed the complete substitution of dopants materials into the Zn^{2+} site.

The optical band gap energies were determined between 5,14 and 5,40. depended on the concentration of the lanthanide ion and temperature.

6. REFERENCES

1. Boron Chemistry: An Overview Heather DeFrancesco, Joshua Dudley, and Adiel Coca* Chemistry Department, Southern Connecticut State University, 501 Crescent St., New Haven, Connecticut 06515, United States

2. Boron: a Hunt for Superhard Polymorphs A. R. Oganova,b and V. L. Solozhenkoc a Department of Geosciences, Department of Physics and Astronomy, and New York Center for Computational Sciences, Stony Brook University, Stony Brook, New York 11794-2100, USA

3. Krebs, R. E. The History and Use of Our Earth's Chemical Elements: A Reference Guide, 2nd ed.; Greenwood Press: Westport, CT, 2006; p 176.

4. Fundamental Studies on the Ion-Exchange Separation of Boron Isotopes Kakihana Hidetake

5. 1 , Kotaka Masahiro 1 , Satoh Shohei 1 , Nomura Masao 1 , Okamoto Makoto 1
6. Garrett, Donald E. (1998). Borates: handbook of deposits, processing, properties, and use. Academic Press. pp. 102, 385–386. ISBN 978-0-12-276060-0.)

7. Boron and borates ROBERT B. KISTLER AND CAHlT HELVACI https://www.researchgate.net/publication/308557859_Boron_and_borates

8. doi:10.1006/jcis.2001.8138

9. An Introduction to Boron: History, Sources, Uses, and Chemistry William G. Woods Office of Environmental Health and Safety, University of California, Riverside, California

10. Borate deposits: An overview and future forecast with regard to mineral deposits Cahit Helvacı* Dokuz Eylül Üniversitesi, Jeoloji Mühendisliği Bölümü, 35160 Buca/İzmir, Turkey, ORCID ID orcid.org/0000-0002-8659-1141

11. Greenwood and Earnshaw, 1997) (Helvaci, 2005)

12. Chemistry of elements N.N Greenwood and Earnshaw (p 136)

13. Shorrocks VM. Boron Deficiency-Its Prevention and Cure. London: Borax Consolidated
14. Eltepe HE, Balköse D, Ülkü S. Effect of Temperature and Time on Zinc Borate Species Formed from Zinc Oxide and Boric Acid in Aqueous Medium. Industrial & Engineering Chemistry Research. 2007; 46(8):2367–2371.

15. Improvedsynthesisoffinezincborateparticlesusingseedcrystals Deniz Gu¨ rhan a, GayeO¨ . C- akal b, I˙nci Erog˘lu a, SaimO¨ zkar c,

16. Effect of Temperature and Time on Zinc Borate Species Formed from Zinc Oxide and Boric Acid in Aqueous Medium H. Emre Eltepe,† Devrim Balko1se,*,‡ and Semra U2 lku1‡

17. Liu, X., Zhu, W., Cui, X., Liu, T., Zhang, Q., 2012, Facile thermal conversion route synthesis, characterization, and optical properties of rod-like micron nickel borate. Powder Technology, 222, 160–166.

18. Chen X, Xue H, Chang X, Zhang L , Zhao Y, Zuo J et al. Syntheses and crystal structures of the α- and ß-forms of zinc orthoborate, $Zn_3B_2O_6$. Alloys and Compounds. 2006; 425(1-2):96-100.

19. Syntheses and crystal structures of the - and -forms of zinc orthoborate, Zn3B2O6 Xuean Chena,∗, Haiping Xuea, Xinan Changa, Li Zhang a, Yinghua Zhaoa,Jianlong Zuoa, Hegui Zanga, Weiqiang Xiao b

20. Rare earth elements FRANCES WALL Head of Camborne School of Mines and Associate Professor of Applied Mineralogy, Camborne School of Mines, University of Exeter, Penryn, UK

21. Rare Earth Elements Stephen B. Castor and James B. Hedrick

22. Effect of Al3+ on the photoluminescence properties of Ce3+-doped Zn3(BO3)2 nanoparticles Wen Guo Zoua,b, Meng Kai Lqa, *, Feng Gua , Shu Fen Wanga , Guang Jun Zhoua , Zhi Liang Xiua , Hong Yan Xq

23. T.r. Bolu Abant İzzet Baysal Unıversıty Instıtute of Graduate Studıes Department of Chemistry the Influence of Synthesıs Condıtıons on the Crystal Structure of Some Nanosızed Zınc Orthoborate Materıals Muhammed ÖZTÜRK Academıc Supervısor Prof. Dr. Ayşe MORKAN Bolu, Ocak – 2023

24. Bobkova NM, Khotko SA. Structure Of Zinc-Borate Low Melting Glasses Derived From IR Spectroscopy Data. Journal of App. Spectroscopy. 2005; 72(6): 853–857

25. Peng R, Li Y, Su H , Lu Y, Yu C, Yu G, et al. A detailed study of the substitution mechanism for improved zinc-borate: High-performance and its crystal structure variation. Journal of Materials Research and Technology 2021;12:1360-1367.

26. Briggs M. Boron Oxides, Boric Acid, and Borates. Kirk-Othmer Encyclopedia of Chemical Technology. 2001; 4: 241-294

27. Briggs M. Boron Oxides, Boric Acid, and Borates. Kirk-Othmer Encyclopedia of Chemical Technology. 2001; 4: 241-294

28. Rao CNR, Biswas K (2015) "Essentials of inorganic materials synthesis".

29. Chen S, Zhang D and Sun G (2014) "In situ synthesis of porous ceramics with a framework structure of magnesium borate whiskers",Mater.Lett.121:206-208.

30. Structural Characterization and Chemistry of the Industrially Important Zinc Borate, Zn[B3O4(OH)3] David M. Schubert,* Fazlul Alam, Mandana Z. Visi, and Carolyn B. Knobler† U.S. Borax Inc., 26877 Tourney Road, Valencia, California 91355 Received August 13, 2002. Revised Manuscript Received November 28, 2002

31. Effect of zinc borate on the thermal degradation of ammonium polyphosphate F. Samyn, S. Bourbigot ∗, S. Duquesne, R. Delobel Laboratoire Proc´ed´es d'Elaboration des Revˆetements Fonctionnels (PERF), LSPES – UMR 8008, Ecole Nationale Sup´erieure de Chimie de Lille (ENSCL), Avenue Dimitri Mendele¨ıev – B ˆat. C7, BP 90108, 59652 Villeneuve d'Ascq Cedex, France Received 17 November 2006; received in revised form 9 February 2007; accepted 9 February 2007 Available online 16 February 2007

32. S. Bourbigot, F. Carpentier, M. Le Bras, C. Fernandez, Polym. Addit., chapitre 14 (2001)

33. P.C. Burns, Can. Mineral. 33 (1995)

34. M. Bettinelli, A. Speghini, M. Ferrari, M. Montagna, J. Non-Cryst. Solids 201 (1996)

35. J.M.F. Van Djik, F.H. Schuurmans, J. Chem. Phys. 78 (1983)

36. Spectroscopic and dielectric studies of Sm3+ ions in lithium zinc borate glasses Sunil Thomas a , Sk. Nayab Rasool b , M. Rathaiah c , V. Venkatramu c , Cyriac Joseph a ,

N.V. Unnikrishnan a, ∗

37. J.L. Piguet, J.E. Shelby, J. Am. Ceram. Soc. 68 (1985) 450

38. Judd–Ofelt parameters and radiative properties of Sm3+ ions doped zinc bismuth borate glasses A. Agarwal a , I. Pal a , S. Sanghi a,*, M.P. Aggarwal b

39. J.L. Adam, A.D. Docq, J. Lucas, J. Solid State Chem. 75 (1988)

40. C.K. Jorgensen, Prog. Inorg. Chem. 4 (1962)

41. Luminescence studies of Dy3þ doped bismuth zinc borate glasses B. Shanmugavelu, V.V. Ravi Kanth Kumar

42. Vijayakumar, R., Venkataiah, G., & Marimuthu, K. (2015). White light simulation and luminescence studies on Dy 3+ doped Zinc borophosphate glasses. Physica B: Condensed Matter, 457, 287–295.

43. Spectroscopic and photoluminescence characteristics of Dy3þ ions in lead containing sodium fluoroborate glasses for laser materials C. Madhukar Reddy a , G.R. Dillip a , B. Deva Prasad Raju b,n

44. E. Culea, L. Pop, S. Simon, Mater. Sci. Eng. B 112 (2004) 59

45. M. Tanaka, Y. Masumoto, Very weak temperature quenching in orange luminescence of ZnS:Mn2+ nanocrystals in polymer, Chem. Phys. Lett. 324 (2000)

46. J. Dexpert-Ghys, R. Mauricot, M.D. Faucher, Spectroscopy of Eu3+ ions in monazite type lanthanide orthophosphates LnPO4, Ln = La or Eu, J. Lumin. 69 (1996) 203–215

47. Synthesis, thermoluminescence and dosimetric properties of La-doped zinc borates Nil Kucuk a,n , Ilker Kucuk a , Merve Cakir a , Sule Kaya Keles b

48. L. Juan, Z. Chunxiang, T. Qiang, H. Jingquan, Z. Yanli, S. Qiang, W. Shubin, J. Rare Earths 26 (2008)

49. Structural analysis and luminescence studies of Ce3+: Dy3+ co-doped calcium zinc gadolinium borate glasses using EXAFS R. Rajaramakrishnaa , Y. Ruangtaweepa,∗ , S. Sattayapornb , P. Kidkhunthodb , S. Kothanc , J. Kaewkhaoa,

50. Vijaya Kumar, M.V., Jamalaiah, B.C., Rama Gopal, K., Reddy, R.R., 2012. Optical absorption and fluorescence studies of Dy 3 -doped lead telluroborate glasses. J. Lumin

51. Lattice Parameter Determinations with an XRay Spectrogoniometer by the DebyeScherrer Method and the Effect of Specimen Condition Henry M. Otte

52. Comparative study of crystallite size using Williamson-Hall and DebyeScherrer plots for ZnO nanoparticles To cite this article: S Mustapha et al 2019 Adv. Nat. Sci: Nanosci. Nanotechnol. 10 045013

53. Tauc Plot Software: Calculating energy gap values of organic materials based on Ultraviolet-Visible absorbance spectrum To cite this article: Albert Zicko Johannes et al 2020 IOP Conf. Ser.: Mater. Sci. Eng. 823 012030

54. Tauc, J.; Grigorovici, R.; Vancu, A. Optical Properties And Electronic Structure of Amorphous Germanium. Phys. Status Solidi B 1966, 15, 627−637

55. Evaluation of the Tauc method for optical absorption edge determination: ZnO thin films as a model system Brian D. Viezbicke, Shane Patel, Benjamin E. Davis, and Dunbar P. Birnie III*